Genetic and morphological characterization of skeletal evolution in giant mice from Gough Island

By

Michelle D. Parmenter

A dissertation submitted in partial fulfillment of
the requirements for the degree of

Doctor of Philosophy

(Genetics)

at the

UNIVERSITY OF WISCONSIN-MADISON

2017

Date of final oral examination: 06/05/2017

The dissertation is approved by the following members of the Final Oral Committee:

Bret A. Payseur, Professor, Genetics
John Doebley, Professor, Genetics
Karl Broman, Professor, Biostatistics
Nicole Perna, Professor, Genetics
John Orrock, Professor, Zoology

Table of Contents

Table of Contents i
Table of Figures and Tables ii
Acknowledgements iii
Abstract vi
Chapter 1 Introduction 1
Chapter 2 Genetics of Skeletal Evolution in Unusually Large Mice from Gough Island 18
Chapter 3 Genetics and Functional Morphology of Mandibular Evolution in Giant Mice from Gough Island 55
Chapter 4 Conclusions and Future Directions 97
References 107
Appendix A Supplementary Material for Chapter 2 130
Appendix B Supplementary Material from Chapter 3 164

Table of Figures and Tables

Chapter 2 Genetics of Skeletal Evolution in Unusually Large Mice from Gough Island 18

Figure 2.1 X-ray image of mouse skeleton and locations of phenotypes. 44

Figure 2.2 Phenotypic distributions of skeletal traits..... 46

Figure 2.3 Genomic intervals of QTL for skeletal measurements..... 48

Figure 2.4 Standardized additive and dominance effects 50

Table 2.1 Shape evolution in GI mice..... 52

Table 2.2 Tests of pleiotropy *vs.* close linkage..... 53

Chapter 3 Genetics and Functional Morphology of Mandibular Evolution in Giant Mice from Gough Island 55

Figure 3.1 Diagram of mouse mandible and location of landmarks..... 87

Figure 3.2 Locations of highly diverged Euclidean distances 88

Figure 3.3 CVA of mandible shape 89

Figure 3.4 Maximum bite force and maximum passive jaw gape 90

Figure 3.5 Chromosomal locations of QTL for mandible traits 91

Figure 3.6 Centroid size QTL 92

Table 3.1 ANOVA table for centroid size 93

Table 3.2 Mahalanobis distances and Procrustes distances from CVA..... 94

Table 3.3 Estimates of jaw performance..... 95

Acknowledgements

I first wanted to recognize my advisor, Bret Payseur, for his guidance and mentorship throughout my time as his graduate student. His intellectual insights were a massive asset to my research. His careful and thoughtful approach to science is nothing short of inspiring and has fundamentally changed how I approach science and critical thinking. His genuine interest in mentorship was not only beneficial to my time in graduate school; it has inspired me to provide the same quality of mentorship to others. I would also like to thank each of the members of my dissertation committee for their support and critical feedback throughout the development of my projects, experiments, and ideas. I would like to thank Nicole Perna, who as Chair of the J. F. Crow Institute for the Study of Evolution provided opportunities and constant support of my interest in scientific outreach.

I have been extremely fortunate to collaborate with some of the leading experts in their respective scientific fields. I would like to thank Karl Broman for his intellectual insights, contributions, and mentorship in statistical approaches. His collaborations were instrumental to the development and analysis of my research. I would also like to thank Christopher Vinyard, who has done an incredible amount of collaborative work on these projects, including data collection, training, and providing valuable knowledge and mentorship in functional morphology and biomechanics. I want to thank Peter Ryan and Richard Cuthbert for their efforts in capturing and obtaining mice from the island. The Gough Island mouse research program would not have been possible without their efforts.

I would like to thank my current and past labmates for their conversations, both scientific and non-scientific, providing a fun and engaging lab environment. Your constant encouragement and support has greatly benefited my experience in graduate school. I am especially grateful for

Melissa Gray, who laid the foundation of the Gough Island mouse research and led the efforts of generating the Gough x WSB cross. I would also like to thank Mark Nolte, who has dedicated a huge amount of time and effort towards running the Gough mouse colony and keeping the Gough inbred lines flourishing.

I would like to acknowledge the large number of undergraduates who have been instrumental to my research. They have all shown great dedication towards these projects and the lab, including the incredible team efforts in order to maintain the Gough Island mouse colony. I would especially like to thank Irene Ford and Caley Hogan for putting a tremendous amount of energy towards generating animals and collecting X-Ray images for Chapter 2, Oren Feldman-Schultz for his assistance in data collection for Chapter 2, and Jake Nelson for his large contributions towards Chapter 3. Without the combined efforts of every student, this work wouldn't have been obtainable.

The work I presented here would not be possible without the financial support from: the National Institutes of Health (NIH) Genetics training grant, the National Science Foundation Graduate Research Fellowship Program (NSF-GRFP) Predoctoral Fellowship, the UW-Madison Graduate School Dissertation Completion Fellowship, and NIH funding for the Gough Island mouse project (R01GM100426A).

I want to thank all of the friends I have made during my almost six years in Madison, particularly my classmates. I had never lived anywhere outside of Oregon, and they quickly became my Wisconsin family. The mutual support we provided one another though late night study sessions, coffee breaks, and much-needed trips to the library were essential to my success here. I especially wanted to acknowledge Kaitlin Dickinson, whose constant encouragement, advice, and kindness has kept me thinking positively throughout graduate school. Her incredible

kindness is a rare trait that I will always cherish in our friendship for years to come. I also wanted to acknowledge Martin Bontrager, who has been a voice of reason and perspective for me, both inside and outside of graduate school, reminding me that success will come regardless of the rough road to get there.

And lastly I would like to thank my fiancé, Robert Phetteplace, for his undying support and selflessness throughout my time in graduate school. After I decided to attend graduate school in Wisconsin, without hesitation he picked up his life and left his family to move to Madison with me so I could accomplish my goals. I am forever grateful for that. He was a source of stability and calm during particularly challenging moments in graduate school, including while I was giving Prelim B, finishing manuscripts, and defending my thesis. There are no words to express just how thankful I am to have him by my side. We have made a life here in Madison, and I am excited to see where the future takes us.

Abstract

Understanding the genetic basis of morphological evolution in nature is an area of study that still eludes evolutionary biologists. Islands are natural laboratories with distinct differences in habitat from the mainland, facilitating repeated cases of rapid morphological evolution of colonizing populations. Many examples of evolution on islands involve the vertebrate skeleton, particularly in the house mouse *Mus musculus domesticus*. Although the genetic basis of skeletal variation has been studied in laboratory strains of house mice, the genetic determinants of skeletal evolution in nature remain poorly understood. This thesis investigates skeletal evolution in a population of giant house mice from Gough Island. Focusing on an island population from the same subspecies as the laboratory mouse allows for the identification of genetic loci associated with skeletal evolution using quantitative genetic techniques. Through quantitative trait locus (QTL) mapping, it was discovered that pronounced changes in the size of the Gough Island mouse skeleton evolved through a few genetic loci acting in pleiotropy with global effects on growth. Gough Island mice exhibit an elongation of the skull, prompting the characterization of mandible morphology and jaw performance in Gough Island mice. Geometric morphometric and quantitative genetic techniques were used to investigate the genetic basis and functional morphology of mandibular evolution in Gough Island mice. Size and shape changes of the Gough Island mouse mandible are pronounced. This includes the expansion and narrowing of the mandible, along with the widening of the condyle. The size and shape dimensions are controlled by distinct sets of loci. Regions of the mandible also show differences in their genetic architectures, suggesting that aspects of the evolution of mandible morphology in Gough Island mice are modular. This work highlights the importance of utilizing island populations in order to obtain a better understanding of complex trait evolution in a natural context.

Chapter 1

Introduction

Evolution on Islands

Islands have been captivating biologists for hundreds of years. Charles Darwin's voyage on the HMS Beagle took him to the Falkland Islands, where he first observed large differences between island and mainland fossil forms (King, Stokes, and Fitz-Roy 1836). This observation inspired him to begin his comparative studies between flora and fauna populations during his voyage, most famously on the finches of the Galapagos Islands (Lack 1947). This helped spark the development of his theory of evolution and adaptation through natural selection (Darwin 1859). Alfred Russell Wallace, who independently conceived the theory of evolution by natural selection and was also inspired by islands, studied differences in biota across the Malay Archipelago (Wallace 1880).Ever since the time of Darwin and Wallace, islands have played critical role in the development of evolutionary theory.

Islands provide an important source of evidence for evolution. Islands are microcosms with definable boundaries, often referred to as "natural laboratories," providing an ideal setting for studying spatial and temporal patterns of adaptive radiation and diversification (MacArthur and Wilson 1967; Diamond 1975). Their geographic isolation from other landmasses reduces the influences from neighboring environments (Losos and Ricklefs 2009). Islands are younger than mainland landmasses and have reduced species diversity, resulting in relatively simple biotas, an observation that impressed nearly all naturalists visiting islands (Hooker 1867; Williamson 1984). These unique features of islands allow adaptation and evolution to be more easily observable. Additionally, the ancestral mainland source can sometimes be identified, which allows for direct comparisons.

The island environment is distinct from the mainland. Newly colonizing populations face significant shifts in environmental conditions, resource availability, and predation risk (Grant

1998; Losos and Ricklefs 2009). The weather on islands is often more harsh than mainland areas due to increased exposure to the oceanic climate (Whittaker and Fernández-Palacios 2007). Islands at high latitudes usually exhibit cold temperatures, which can affect an organism's ability to regulate body temperature (Chown and Smith 1993). Many islands also exhibit distinct seasonal fluctuations, which can affect breeding, survival, and other life history traits of island organisms (Whittaker and Fernández-Palacios 2007; Berry and Bronson 1992). Islands harbor unique flora and fauna, resulting in a shift in available food sources distinct from the mainland (Losos and Ricklefs 2009). The decrease in biodiversity on islands likely reduces the abundance of predators and competitors (van der Geer et al. 2011).

The striking differences between island and mainland areas can facilitate rapid evolution (Mayr 1954; MacArthur and Wilson 1967; Pergams and Ashley 2001). A landmark study by Virginie Millien in 2006 using fossil record data to compare the rates of evolutionary change between island and mainland populations of mammals confirmed that island species undergo accelerated evolutionary changes over relatively short timescales (Millien 2006). The fossil record has also provided evidence that morphological changes occur rapidly after species become isolated on islands (Raia and Meiri 2006).

The facilitation of rapid differentiation could be due to multiple factors. The isolated nature of islands often results in a bottleneck in the numbers of colonizing individuals, leading to founder effects (Mayr 1954; Allendorf 1986). This, along with the reduction in migration, which limits the introduction of new genetic material, leads to the reduction in genetic diversity in island populations and may play a role in differentiation of island populations (Mayr 1954). The unique island environment can also generate new or shifting selective pressures for colonizing populations. Changes from a mainland to an island ecology allows for organismal changes often

not permitted on the mainland, commonly resulting in unusual island forms distinct from those found elsewhere (Gillespie and Clague 2009). In the late 1800's, Charles Forsyth Major was one of the first to thoroughly compare fossils among islands and mainland areas, identifying unique morphologies of extinct elephant and hippo species on Mediterranean islands (Major 1902). Insular populations often display systematic differences in morphology, population density, life history, and behavior (Adler and Levins 1994; Herrel et al. 2008). This phenomenon was coined the "island rule" (Valen 1973), and has been argued to be due to adaptations to an island environment (Berry 1985; Adler and Levins 1994; Renaud and Auffray 2010; Lyras, van der Geer, and Rook 2010; Raia and Meiri 2011).

One of the most common changes that populations experience on islands is a shift in body size, and has been viewed as the canonical feature of the island rule (Foster 1964; Sondaar 1977; Case 1978; Lawlor 1982; Lomolino 1985; Lomolino et al. 2012). In 1964, Foster published the first comprehensive review on differences in body size evolution among taxonomic groups of mammals, including dwarfism in insular carnivores and artiodactyls and gigantism in rodents (Foster 1964). Although originally described as a rule without exceptions, researchers began questioning the validity and generality of the island rule based on their observations that body size trends in certain species or taxonomic groups do not fit the predictions of the island rule, including lagomorphs and certain families of rodents (Lawlor 1982; Lomolino 1985; Meiri, Dayan, and Simberloff 2005; Meiri, Dayan, and Simberloff 2004; Meiri, Cooper, and Purvis 2008; Raia and Meiri 2011; Lomolino et al. 2012; Palombo 2009).

Refinements to the island rule followed shortly after, mostly in the context of body size (Adler and Levins 1994; Lawlor 1982). It was argued that the rule is less about taxonomic membership and more likely a gradual trend from gigantism in smaller species of insular

mammals to dwarfism in larger species (Heaney 1978; Lomolino 1985). The reduction in interspecific competitors and predators on species-poor islands are predicted to select for larger individuals (Heaney 1978; Lomolino 1985), and limited resources, including food availability, select for smaller individuals of larger species since they are better able to survive and reproduce with less food (Hessey R, Allee, and Schmidt 1951; Lawlor 1982). To best explain the island rule, the relative importance of these factors for mammals of a particular body size should be considered (Lomolino 1985). The led to the term "island syndrome" being preferred by some, as it a more general descriptor of all differences related to island evolution (Adler and Levins 1994).

House mouse as a model for island evolution

The house mouse (*Mus musculus*) has become the most widely dispersed and common wild mammal species (Bonhomme and Searle 2012; Babiker and Tautz 2015). This is due to their commensal relationship with humans, and their large distribution is associated with human expansion and the spread of agriculture thousands of years ago (Bonhomme and Searle 2012). House mice have been successful at colonizing a wide variety of new habitats due to their ability to adapt both physiologically and genetically (Berry and Jakobson 1975a; Bonhomme and Searle 2012). House mice began colonizing islands around the world relatively recently along with human exploration of the oceans and islands by ship (Bonner 1984; Chapuis, Boussès, and Barnaud 1994). This has provided fodder for studying patterns of insular evolution (Pergams and Ashley 2001).

Rodents are among the most well studied organisms in terms of differences between island and mainland populations (Adler and Levins 1994). Largely due to the tremendous efforts

by RJ Berry, differences between island and mainland populations of house mice have been characterized (Berry, Peters, and Aarde 1978; Berry 1970). This includes mouse populations on islands across the globe, including those in the North Atlantic (Berry 1964; Berry, Jakobson, and Peters 1978; Davis 1983; Berry et al. 1991; Lister and Hall 2014), South Atlantic (Rowe-Rowe and Crafford 1992; Russell 2012; Gray et al. 2015), Sub-Antarctic (Berry and Peters 1975; Berry, Peters, and Aarde 1978; Berry, Bonner, and Peters 1979), the Mediterranean (Renaud and Auffray 2010; Boell and Tautz 2011), Southern Indian Ocean (Boell and Tautz 2011) and Hawaii (Berry et al. 1981; Boell and Tautz 2011). These comparisons have provided the field with a tremendously rich resource in which to study the evolution of the house mouse in an island context.

Island populations of house mice systematically exhibit characteristics of the island syndrome (Adler and Levins 1994). This includes increases in body size (Foster 1964; Valen 1973; Lomolino 1985; Meiri et al. 2008), higher and more stable population densities (Gliwicz 1980), reduced dispersal (Tamarin 1978), reduced reproductive output (Stamps and Buechner 1985), and reduced aggression (Stamps and Buechner 1985). The tendency towards gigantism has been documented extensively in house mice across the globe, particularly on North Atlantic islands (Berry 1964; Berry 1968; Berry and Jakobson 1974; Berry and Peters 1975), South Atlantic islands (Rowe-Rowe and Crafford 1992; Russell 2012; Gray et al. 2015), and Sub-Antarctic islands (Berry and Peters 1975; Berry, Peters, and Aarde 1978; Berry, Bonner, and Peters 1979).

Models have been developed in efforts to explain the mechanisms of the island syndrome specifically in rodents (Adler and Levins 1994; Millien and Damuth 2004; Raia and Meiri 2006; Raia and Meiri 2011; Lomolino et al. 2006; Lomolino et al. 2013). The degree of isolation and

island area are two factors argued to affect aspects of the island syndrome in rodents (Adler and Levins 1994). An increase in island isolation is predicted to reduce dispersal, which could lead to higher densities and reduced aggression. Higher densities would also likely result in reduced reproductive output and an increase in body size. A decrease in island area is predicted to decrease biodiversity (particularly the number of predators and competitors) and increase population densities. The reduction in the pressure to evade predators and compete with competitors due to their lower abundance is a likely driver of gigantism (Corbet 1961; Foster 1964; Adler and Levins 1994). Gigantism in rodents may be related to island temperature. House mice are larger on colder islands compared to mice on equatorial islands (Berry and Jackson 1979). A larger body area likely allows for more efficient temperature regulation, and therefore may be a critical adaptation to cold temperatures (Berry and Jackson 1979). Together, these factors are not mutually exclusive and any combination of these could potentially lead to an advantage of being larger.

Body size correlates with nearly all aspects of a species' biology, especially the vertebrate skeleton (Peters 1986; Calder 1996; Schmidt-Nielsen 1984). The mammalian skeleton presents an ideal system in which to study the evolution of a set of correlated traits, also known as morphological integration (Olsen and Miller 1958). The evolution of correlated traits is dependent on the degree to which they are developmentally or functionally related (Lande 1980), therefore, studying skeletal divergence can reveal information on multi-trait evolution. Functional, developmental, and genetic interactions among traits are expected to produce patterns of co-variation across the skeleton (R. Lande 1980; Atchley and Hall 1991b; Lynch and Walsh 1998), which could either facilitate or constrain evolution compared to predictions for

single traits (C. P. Klingenberg 2008a; R. Lande 1980; Parsons, Márquez, and Albertson 2012; Schluter 1996).

Divergence in body size suggests correlated changes to the skeleton (Atchley, Rutledge, and Cowley 1981; Biewener 2005). One major focus in insular house mouse studies has been documenting their distinct skeletal morphologies (Berry 1964; Berry and Peters 1975; Berry, Jakobson, and Peters 1978; Berry, Peters, and Aarde 1978; Slábová and Frynta 2007). Variation in the presence and abundance of skeletal variants in the skull, humerus, pelvis, vertebrae, and the tail has been documented (Berry 1964; Berry, Jakobson, and Peters 1978). Mice from Skokholm and the Isle of May show high incidence of the interfrontal bone (a minor skeletal variant of the skull), which is rare in mice of mainland Britain (Berry 1964). The interfrontal bone varies in its presence among inbred strains of house mice, and it has been used as an indicator of changes in skull proportions, as its size has a positive correlation with the relative increase in skull width (Johnson 1976; Hanken and Hall 1993). Faroe Island mice display distinct skull traits, including a narrowing of the mesopterygoid fossa, which is not observed in mainland mice or laboratory mice of similar size (Berry, Jakobson, and Peters 1978). Some island populations exhibit a high incidence of variants within the thoracic vertebrae and cervical vertebrae (Berry 1964).

Increases in head and body measurements have been documented in both North and South Atlantic island mouse populations (Berry 1964; Berry and Peters 1975; Berry, Bonner, and Peters 1979), which suggests an enlargement of the skeleton. Many island mouse populations exhibit relatively shorter tails compared to mainland mice, except for mice from Gough Island and Tristan da Cunha Island, which have relatively longer tails than their mainland counterparts (Berry and Peters 1975). The tail is an important heat-regulating organ in mice (Harrison,

Morton, and Weiner 1959) and is important for balance and locomotion (Siegel 1970). Most studies of house mouse skeletal morphology on islands have focused on skeletal variants and body proportions, and the utilization of detailed characterizations, particularly quantitative traits, are limited (Scriven and Bauchau 1992; Pergams and Ashley 2001). More detailed characterizations of skeletal morphology of island mouse populations are needed to better understand patterns of skeletal differentiation on islands.

Mandible morphology in insular house mice populations has also been investigated (Michaux, Chevret, and Renaud 2007; Boell and Tautz 2011; Babiker and Tautz 2015). Island house mice often display an increase in mandible area compared to mainland populations (Berry, Jakobson, and Peters 1978; Davis 1983). Many island populations exhibit distinct mandibular shapes (Berry, Jakobson, and Peters 1978; Davis 1983; Scriven and Bauchau 1992; Renaud and Auffray 2010; Boell and Tautz 2011; Renaud et al. 2013; Babiker and Tautz 2015), including a narrowing of the proximal end of the mandible (ascending ramus) and a more robust distal region (alveolar region).

The mandible plays an important role in organismal function (Herring 1993). Animals use their entire jaw apparatus in behaviors related to displays and aggressive encounters, predation, and feeding (Nowak 1999). Studies have also linked morphological changes of the island mouse mandible form with changes in diet (Renaud and Auffray 2010; Babiker and Tautz 2015). Mice on the Piana islet of Corsica in the Mediterranean exhibit mandible shape changes, such as the elongation of the condyle, that may be due to food availability on the islet, which mostly is composed of tender plant material and invertebrates (Renaud and Auffray 2010). By feeding laboratory strains a soft versus hard diet, similar changes of the mandible were identified (Yamada and Kimmel 1991; Luca et al. 2003; Renaud and Auffray 2010). Mice living on the

small island of Heligoland near Germany also display an elongation of the condyle, along with a less robust angular process and an overall elongation of the mandible. It has been argued that these characteristics point towards an adaptation to a carnivorous or insectivorous diet (Babiker and Tautz 2015). Changes to mandibular morphology could have important implications to the performance and fitness of the organism. Island environments present a host of differences that could facilitate the evolution of the mandible, including shifts in predation risk and competition, food resources, and landscapes (Adler and Levins 1994; Herrel et al. 2008).

The House mouse as a quantitative genetic model of skeletal evolution

Knowledge of the genetic basis of morphological variation is essential in understanding the evolution of organismal form. Quantitative trait loci (QTL) mapping provides a way to evaluate the genetic architectures of morphological variation. The genetic basis of body size evolution has been well characterized in laboratory strains of house mice, as it has been used as a canonical complex trait in quantitative genetic studies A large number of genes are known to be involved in body size variation among laboratory strains (Reed et al. 2008) and QTL underlying body weight differences among laboratory strains have been identified (Cheverud et al. 1996; Keightley et al. 1996; Brockmann et al. 1998; Vaughn et al. 1999; Corva and Medrano 2001; Rocha et al. 2004; Kenney-Hunt et al. 2006; Shao, Reed, and Tordoff 2007; Ishikawa and Okuno 2014; Gray et al. 2015). These studies reveal the common pattern that strains with differences in body weight and growth rate are due to a large number of loci with modest effects on phenotype.

Efforts have been made to investigate the genetic basis of variation in skeletal dimensions in house mice (Cheverud, Routman, and Irschick 1997; Leamy, Routman, and Cheverud 1997; Leamy, Routman, and Cheverud 1999; Klingenberg et al. 2001b; Klingenberg 2004). Studies using knockout mouse models have found loci responsible for the proper development and form

of skeletal elements (McAlarney et al. 2001). For example, insulin-like growth factor I (IGF-I) null mice have a lower rate of skeletal growth and exhibit a shortening of the nose compared to wild-type mice (McAlarney et al. 2001). QTL have been identified for skeletal components related to size and growth differences among classical inbred strains and among strains descended from artificial selection experiments (Vaughn et al. 1999; Leamy, Routman, and Cheverud 1999; Lang et al. 2005; Kenney-Hunt et al. 2006; Kenney-Hunt et al. 2008; Norgard et al. 2008; Sanger et al. 2011; Carson et al. 2012). There is evidence of pervasive pleiotropy controlling variation of many skeletal elements (Leamy, Routman, and Cheverud 2002; Ehrich et al. 2003b; Schlosser and Wagner 2004; Wolf et al. 2005; Wolf et al. 2006; Christians and Senger 2007; Kenney-Hunt et al. 2008; Pavlicev et al. 2008; Roseman, Kenney-Hunt, and Cheverud 2009). For example, QTL associated with variation in long bone dimensions between C57BL/6J and DBA/2 strains co-localize with each other and with various correlated traits, including body weight and adipose mass (Long et al. 2005). In contrast, genetic independence has been identified between long bone lengths and organ weights using an F_2 population between LG/J and SM/J strains, which were artificially selected for divergence in body size (Kenney-Hunt et al. 2006). There is also evidence for genetic independence between early and late developing skull dimensions between LG/J and SM/J (Leamy et al. 1999; Wolf et al. 2005; Wolf et al. 2006). Together, these studies identified loci that affect skeletal morphology on both global and local scales among laboratory strains of house mice.

House mice as a model for geometric morphometrics and mandibular evolution

The house mouse mandible has long served as a model system for studying the development and evolution of complex morphological structures (Atchley and Hall 1991b;

Klingenberg and Leamy 2001; Klingenberg et al. 2001b). This is in part made possible by the development of geometric morphometrics, which provides techniques for quantifying detailed shape variation (Klingenberg 2010) based on outline contours or an arrangement of landmark points (Bookstein 1991; Dryden and Mardia 1998). Particular attention has been given to the mandible since it can be approximated to two dimensions, making it relatively simple to assess size and shape variation (Atchley and Hall 1991; Klingenberg and Navarro 2012).

The rodent mandible is composed of two parts that have different developmental origins, the ascending ramus and the alveolar region (Atchley and Hall 1991b; Klingenberg, Navarro, and Pialek 2012). A major pattern of morphological differentiation among populations of house mice is that evolutionary change differentially affects specific components of the mandible (Atchley, Plummer, and Riska 1985a; Atchley, Plummer, and Riska 1985b). Evidence for this pattern comes from both knockout studies, where inactivation of specific genes affect different parts of the mouse mandible throughout development (Francis-West et al. 1998), and studies using QTL mapping, which show that effects of loci are often localized to particular regions of the mandible (Cheverud, Routman, and Irschick 1997; Leamy, Routman, and Cheverud 1997; Mezey, Cheverud, and Wagner 2000; Klingenberg and Leamy 2001; Klingenberg et al. 2001b; Klingenberg, Mebus, and Auffray 2003; Klingenberg 2004). Together, these studies have illustrated that mandibular evolution is genetically complex.

The mandible is important for the function and performance of the jaw, including processing of food during mastication and the capturing of prey (Nowak 1999; Vaughn et al. 1999). Changes to mandibular morphology have been shown to affect aspects of jaw performance, such as the extent to which an organism can open its jaw and the maximum bite force an organism can deliver (Herring 1974; Vinyard et al. 2003; Herrel et al. 2008). These

behaviors are functionally significant to many organisms (Herring et al. 1972; Hylander 1979; Jablonski 1993; Dumont and Herrel 2003; Vinyard et al. 2003). The evolution of the performance of organismal-level functions is likely to involve heritable changes to their correlated morphologies (Lande and Arnold 1983). Therefore it is feasible that variation in the ability of the jaw to function could be due to natural selection acting on these performances and their correlated morphologies (Vinyard and Payseur 2008). Despite the likely importance the role evolution plays on aspects of jaw performance, little is known about the morphological and genetic basis that shapes organismal-level functions of the jaw. Studies investigating the consequences of mandible evolution on jaw function and performance could provide novel insights into morphological evolution.

Despite the large number of comparative studies on skeletal divergence that have been undertaken in island populations of house mice, the genetic basis underlying skeletal evolution remains to be evaluated. Although the genetic characterization of skeletal evolution in laboratory strains of house mice has been investigated, it remains an unanswered question as to whether similar genetic patterns underlie skeletal evolution in nature. Additionally, full advantage has not been taken of the house mouse as a model for studying functional morphology and biomechanical performance. We utilized a population of house mice from Gough Island in order to take advantage of the extensive resources of the house mouse model to study skeletal evolution in an island context.

House mice on Gough Island

Gough Island is a small volcanic island in the Southern Atlantic Ocean. It is one of the most remote islands in the world. South Africa is the nearest continent at over 1750 kilometers away and Tristan da Cunha is its closest island neighbor, 400 kilometers to its Northwest

(Heaney and Holdgate 1957). Due to its remoteness, there is no permanent human habitation on Gough Island. A small number of researchers occupy a meteorological station operated by the South African government on the more sheltered, east coast of the island (Heaney and Holdgate 1957). Gough Island harbors unique flora and fauna, including five different plant communities (Rowe-Rowe and Crafford 1992). Moreover, it is one of the most important islands for seabirds in the world (Wanless 2007). Gough Island is home to 23 breeding seabird species, including nearly the entire global population of Atlantic petrel and Tristan albatross (Ryan, Cooper, and Glass 2001). The only land mammal species living on the island is the house mouse (Jones, Chown, and Gaston 2003).

Mice were first reported on Gough Island by sealer George Comer in 1889 (Verill 1895). Mice likely arrived with the first sealing ships that brought the first known human visitors to the island (Verill 1895). The first dataset collected on Gough Island mice was between 1955 and 1956, where body and cranial measurements of mice were recorded at both low and high elevations (Hill 1959). More recently, it was confirmed that Gough Island mice belong to the *Mus musculus domesticus* subspecies (Gray et al. 2014). Mice likely colonized Gough Island less than 200 years ago, suggesting that any changes were likely rapid (Gray et al. 2014).

Gough Island mice are truly unique. On average, Gough Island mice exhibit twice the body mass of mainland wild house mice (Rowe-Rowe and Crafford 1992; Gray et al. 2015). They are larger than all known wild mice from any mainland or island population (Berry, Peters, and Aarde 1978), including mice from Tristan da Cunha, the closest neighboring island (Hill 1959). Gough Island mice have larger litter sizes than other wild house mice, likely due to their increased size (Berry 1968). They exhibit extremely high population densities (approximately 224 mice per hectare), some of the highest ever recorded for wild house mice (Rowe-Rowe and

Crafford 1992). Interestingly, mice on Gough Island experience low seasonal variation in numbers compared to other studied island populations (Cuthbert et al. 2016b).

The Gough Island mouse diet is also unusual. Mice on the island regularly prey upon seabird chicks, which is not a common behavior among wild house mouse populations (Jones, Chown, and Gaston 2003; Cuthbert and Hilton 2004). Stomach contents of mice at low elevation regions consist primarily of avian material during the Austral winter (Jones et al. 2003b). Winter breeding bird species, such as the Tristan albatross and Atlantic petrel, are preyed upon most (Cuthbert et al. 2013; Dilley et al. 2015). These birds have extremely low breeding success due to mouse predation on healthy chicks (Cuthbert et al. 2013; Dilley et al. 2015). In a study quantifying the level of mouse predation on nesting chicks, all monitored bird species were victim to mouse predation, with chick mortality rates as high as 87% (Dilley et al. 2015). The predation on such large prey, such as Tristan albatross chicks (up to 300 times as large as Gough Island mice), is unusual for house mice (Wanless et al. 2007). The unique environment, flora, and fauna of Gough Island, along with the unusual size, diet and behaviors of Gough Island mice, provide a rich resource for studying morphological evolution in a natural setting.

Recently, it was found that Gough Island mice achieve their extreme body size via an increased growth rate during the first 6 weeks after birth (Gray et al. 2015). A suite of genetic loci associated with their extreme body size evolution were identified, suggesting that evolution of body size on islands can be genetically complex, even when it occurs relatively rapidly (Gray et al. 2015). This work provided insights into how body size evolution occurs on islands, and lays the foundation for further investigations of morphological evolution of Gough Island mice.

Introduction of thesis chapters

This thesis utilizes the power of the house mouse model system from the perspective of quantitative genetics, geometric morphometrics, and functional morphology to characterize morphological evolution of the skeleton of an island population of mice and investigate the genetic basis of its evolution. Although laboratory strains are mostly derived from *M. m. domesticus*, they contain regions of intersubspecific origin (Yang et al. 2007). This suggests that the evolution of laboratory and natural populations could be due to different mutations, and therefore any evolutionary interpretations drawn from laboratory strains may not accurately extend to natural populations. The dynamics of artificial and natural selection may differ. Wild mice face selective pressures that are either different or absent in the laboratory, which could lead to different genetic architectures. Additionally, most biomechanical and functional studies utilize laboratory strains in order to reduce variation and environmental noise (Festing 1979), which makes it difficult to interpret data collected in laboratory strains in terms of natural populations (Bock and von Wahlert 1965). Using Gough Island mice allows for the investigation of skeletal evolution in nature while taking advantage of the extensive resources of the house mouse model.

Chapter 2 describes the results of the phenotypic characterization and genetic dissection of the divergence in skeletal morphology between Gough Island mice and a small-bodied mainland representative strain (WSB/EiJ, referred to throughout the rest of the thesis as WSB) in order to better understand how complex morphologies evolve in nature. I identified pronounced skeletal expansion and shape divergence in Gough Island mice. I used crosses between Gough Island mice and WSB and QTL mapping to identify hundreds of genotype-phenotype associations that localize to a small number of chromosomal locations underlying variation across the entire skeleton. This provided evidence that pleiotropy plays a large role in the

evolution of the Gough Island mouse skeleton. Further incorporation of body weight into my genetic analyses allowed us to disentangle QTL effects on skeletal size and skeletal shape.

Chapter 3 describes the detailed phenotypic, functional, and genetic characterization of mandibular evolution in Gough Island mice. Through comparisons between Gough Island mice and WSB, I used geometric morphometrics to identify pronounced size and shape divergence of the mandible. Direct biomechanical tests of jaw function reveal that Gough Island mice exhibit a relatively stronger bite, along with morphological characters that may influence jaw performance. QTL mapping reveals many loci associated with mandible size variation that localize to only two chromosomal regions, which were previously identified to underlie overall skeletal expansion (Parmenter et al. 2016, see Chapter 2). QTL localized to specific regions of the mandible were also identified, suggesting different evolutionary patterns based on known mandible regions. Incorporating adjustments for body weight reveal a unique set of QTL, providing evidence for QTL underlying variation in mandible shape that are distinct from those for mandible size. Finally, in Chapter 4, I discuss general conclusions and potential future directions.

Chapter 2

Genetics of Skeletal Evolution in Unusually Large Mice from Gough Island

This chapter was published as a peer reviewed article in Genetics.

Parmenter M. D., Gray M. M., Hogan C. A., Ford I. N., Broman K.W., Vinyard C. J., and Payseur B. A. (2016). Genetics of skeletal evolution in unusually large house mice from Gough Island. *Genetics* 204(4): 1559-1572.

Contributions were as follows: MDP, CJV, and BAP designed the study. MDP, MMG, CAH, and INF performed crosses and collected data. MDP and KWB conducted analyses. MDP and BAP wrote the manuscript.

Supplementary information from this chapter can be found in Appendix A.

Abstract

Organisms on islands often undergo rapid morphological evolution, providing a platform for understanding mechanisms of phenotypic change. Many examples of evolution on islands involve the vertebrate skeleton. Although the genetic basis of skeletal variation has been studied in laboratory strains, especially in the house mouse *Mus musculus domesticus*, the genetic determinants of skeletal evolution in natural populations remain poorly understood. We used house mice living on the remote Gough Island – the largest wild house mice on record – to understand the genetics of rapid skeletal evolution in nature. Compared to a mainland reference strain from the same subspecies (WSB/EiJ), the skeleton of Gough Island mice is considerably larger, with notable expansions of the pelvis and limbs. The Gough Island mouse skeleton also displays changes in shape, including elongations of the skull and the proximal vs. distal elements in the limbs. Quantitative trait locus (QTL) mapping in a large F_2 intercross between Gough Island mice and WSB/EiJ reveals hundreds of QTL that control skeletal dimensions measured at 5, 10, and/or 16 weeks of age. QTL exhibit modest, mostly additive effects and Gough Island alleles are associated with larger skeletal size at most QTL. The QTL with the largest effects are found on a few chromosomes and affect suites of skeletal traits. Many of these loci also co-localize with QTL for body weight. The high degree of QTL co-localization is consistent with an important contribution of pleiotropy to skeletal evolution. Our results provide a rare portrait of the genetic basis of skeletal evolution in an island population, and position the Gough Island mouse as a model system for understanding mechanisms of rapid evolution in nature.

Introduction

Populations that colonize islands face a host of new environmental conditions, including changes in resource availability, predation risk, and competition (Losos and Ricklefs 2009). These shifts can stimulate the evolution of unusual or exaggerated traits over a short time scale. Insular populations of mammals are enriched for cases of rapid morphological evolution, especially in traits related to body size (Foster 1964; Grant 1999; Pergams and Ashley 2001; Beheregaray et al. 2004; Lomolino 2005; Thomas, Meiri, and Phillimore 2009; Durst and Roth 2015). Comparing island populations with their mainland relatives is a powerful approach for understanding the genetic basis of evolutionary change.

Wild house mice offer a particularly useful system for revealing the mechanisms of rapid phenotypic evolution on islands. By virtue of their commensalism, house mice successfully colonized a diverse array of island environments (Bonhomme and Searle 2012). Insular house mice often display distinct skeletal morphologies. Presence-absence of skeletal variants in the skull, humerus, pelvis, and vertebrae (including the tail) have been documented (Berry 1964; Berry and Jakobson 1975a; Berry, Jakobson, and Peters 1978; Davis 1983; Berry 1986; Pergams and Ashley 2001; Renaud and Auffray 2010). Divergence in body size (Berry and Jakobson 1975b; Berry, Peters, and Aarde 1978; Berry, Bonner, and Peters 1979; Berry et al. 1981; Berry, Jakobson, and Peters 1987; Rowe-Rowe and Crafford 1992; Adler and Levins 1994; Jones, Chown, and Gaston 2003; Lomolino 2005; Russell 2012; Durst and Roth 2012; Durst and Roth 2015; Gray et al. 2015; Cuthbert et al. 2016) suggests evolutionary changes to the skeleton in other island populations. As the scaffold for the body plan, the skeleton enables movement, provides support for muscles, and protects internal organs (Pourquié 2009). Moreover, studying skeletal divergence can reveal the dynamics of multi-trait evolution. Functional, developmental,

and genetic interactions among traits are expected to produce patterns of co-variation across the skeleton Lande 1980; Atchley and Hall 1991a; Lynch and Walsh 1998). Depending on its structure, this "modularity" may facilitate or constrain evolution compared to predictions for single traits (Klingenberg 2008; Lande 1979; Parsons, Márquez, and Albertson 2012; Schluter 1996).

Although the genetic basis of skeletal evolution in island mice is unknown, considerable research has been dedicated to dissecting genetic differences in the skeleton in laboratory mice. Quantitative trait loci (QTL) have been identified for hundreds of skeletal components related to size and growth differences among classical inbred strains and among strains descended from artificial selection experiments (Vaughn et al. 1999; Leamy, Routman, and Cheverud 1999; Huang et al. 2004; D. H. Lang et al. 2005; Kenney-Hunt et al. 2006; Kenney-Hunt et al. 2008; E. Norgard et al. 2008; Sanger et al. 2011; Carson et al. 2012), with evidence that some QTL affect multiple traits (Leamy et al. 2002; Ehrich et al. 2003a; Schlosser and Wagner 2004; Wolf et al. 2005; Wolf et al. 2006; Christians and Senger 2007; Kenney-Hunt et al. 2008; Pavlicev et al. 2008; Roseman, Kenney-Hunt, and Cheverud 2009). QTL responsible for local skeletal shape variation also have been discovered, with a special emphasis on the mandible (Atchley, Plummer, and Riska 1985a; Atchley, Plummer, and Riska 1985b; C. P. Klingenberg and Leamy 2001; Klingenberg, Mebus, and Auffray 2003; Klingenberg 2004; Wagner, Pavlicev, and Cheverud 2007; Leamy et al. 2008; Wilmore et al. 2009). These findings from laboratory mice provide a rich comparative context for examining the genetic architecture of skeletal evolution in natural populations of house mice, which experience evolutionary dynamics distinct from those in laboratory conditions.

The largest known wild house mice in the world inhabit Gough Island, a remote volcanic island in the central South Atlantic Ocean (Rowe-Rowe and Crafford 1992). The massive evolutionary increase in body size of Gough Island mice – to become twice the weight of their mainland counterparts (Jones, Chown, and Gaston 2003; Gray et al. 2015) – suggests a substantial expansion of the skeleton. House mice likely colonized Gough Island a few hundred generations ago (Gray et al. 2014), raising the prospect that morphological evolution has been accelerated. In this study, we use Gough Island mice to understand the genetic basis of rapid skeletal evolution in nature.

Materials and Methods

Gough Island and its Mice

Gough Island is part of the United Kingdom Overseas Territory of Tristan da Cunha and is located approximately halfway between South America and South Africa in the South Atlantic Ocean (40° 19'S and 9° 55'W). Gough Island has an area of 65 km^2. Fifty mice live trapped on Gough Island in September 2009 were transferred to Charmany Instructional Facility in the School of Veterinary Medicine at the University of Wisconsin-Madison. Four mice died and two litters consisting of five pups were born during transport from the island to the facility. Upon their arrival, 46 mice (25 female and 21 male) were used to establish a breeding colony.

Female and male mice were housed separately in micro-isolator cages with a maximum of four mice per cage. Ground corn cobs (1/8th inch; Waldschmidt and Sons, Madison, WI) were used as bedding; irradiated sunflower seeds (Harlan Laboratories, Madison, WI) and nesting material were provided for enrichment. The room was temperature controlled (68-72 °F) and set on a 12-hour light/dark cycle. Water and rodent chow (Teklad Global 6% fat mouse/rat diet; Harlan Laboratories, Madison, WI) was provided *ad libitum*. Mice were mated after 8 weeks of age. Breeding individuals were given additional enrichments and were fed breeder chow (Teklad Global 19% protein/9% fat; Harlan Laboratories, Madison, WI) *ad libitum*. All mice were weaned between 3 and 4 weeks of age. Individual mice were toe-tattooed (using sterile lancets and tattoo paste) at 1 week of age and ear-punched at weaning for the purposes of identification. All mice were weighed to the nearest milligram, beginning one week after birth and ending at 16 weeks. After the Gough Island mice (subsequently abbreviated GI) arrived to the Charmany Instructional Facility, we performed a random-mating common garden experiment using the wild

founders. This was done in order to determine that the large body size of the GI mice has a genetic basis and not due solely to environmental factors.

Intercross experiments

Several partially inbred lines of GI mice were created through full-sib mating for 4 filial generations, a procedure expected to reduce within-line heterozygosity by 60% (Silver 1995). To incorporate variation segregating among GI mice, two partially inbred GI lines were used for intercross experiments (denoted as cross A and B). One pair of male and female siblings from each partially inbred line was crossed with WSB/EiJ (subsequently abbreviated as WSB; Jackson Laboratories, Bar Harbor, ME) to generate four independent F_2 intercrosses (Figure S2.1). WSB was chosen because it is a wild-derived strain, has a body size typical of wild house mice, is fully inbred, belongs to the same subspecies as GI mice, has a sequenced genome (Keane et al. 2011), and is featured in the Collaborative Cross (Threadgill and Churchill 2012). A total of 1,374 F_2 mice were generated: 497 from Cross A (WSBxGI=279 and GIxWSB=218) and 877 from Cross B (WSBxGI=494 and GIxWSB=383). From this F_2 population, 827 mice were used for all skeletal phenotyping and analyses: 367 from Cross A (WSBxGI=206 and GIxWSB=161) and 460 from Cross B (WSBxGI=252 and GIxWSB=208).

Phenotyping

All mice were weighed to the nearest milligram every week, beginning one week after birth and ending at 16 weeks. Dual energy X-Ray absorptiometry (DXA) was used to measure bone morphology. Digital X-Ray images (Carestream Health DXS Pro 4000) were collected for 43 F1 and 827 F2 individuals and mice from the four parental strains of the cross. X-Ray images

were taken at three postnatal time points (5, 10, 16 weeks of age) for each animal. These time points were chosen to capture multiple episodes of growth throughout postnatal development. X-Ray imaging at 5 and 10 weeks of age was performed using live animals. When individuals reached 16 weeks of age, they were either euthanized by CO_2 asphyxiation followed by imaging, or imaging was performed live followed by euthanasia (by decapitation). Liver samples were collected from all euthanized F2 individuals and stored at -80° Celsius. For imaging of live mice, an anesthetic (50-100 mg/kg ketamine/0.5-1.0 mg/kg dexmedetomidine) was administered via intraperitoneal injection prior to X-Ray imaging to allow for placement and X-Ray exposure time. A dorsal and lateral X-Ray image was taken of each individual. Skeletal dimensions were measured from the X-Ray images using Carestream Molecular Imaging Software (Carestream Health, Inc.). Measurements were chosen to capture axes of known variation across laboratory mouse strains and across species. A total of 16 measurements were used for phenotyping, including lengths and diameters of long bones, pelvis and skull (see Figure 2.1).

Additional measurements were taken from the individual skeletal measurements to determine any changes in skeletal shape (described as non-proportional size changes), particularly of the limbs. These include forelimb to hindlimb ratios (intermembral index: (humerus length + radius length)/(femur length + tibia length) x 100), the ratio of distal and proximal elements of the hindlimb (crural index: (tibia length/femur length) x 100) and forelimb (brachial index: (radius length/humerus length) x 100), and the ratio of forelimb and hindlimb proximal elements (humerofemoral index: (humerus length/femur length) x 100). Although no data was collected on the radius, ulna length was used as a substitute for the distal element of the forelimb.

Phenotypic distributions were inspected for extreme outliers. When it was concluded that outliers reflected reduced measurement accuracy caused by improper placement of animals during X-Ray imaging or a lack of X-Ray resolution, they were removed. These included 6 data points from the F2 population (for SVL at 5,10, and 16 weeks, SL at 5 weeks, SW at 5 weeks, and SL at 10 weeks), 1 data point from the WSB population (ZL at 16 weeks), and 3 data points from the GI population (FMD at 5 weeks, MC at 5 weeks, ZL at 10 weeks).

Genotyping

All mice were genotyped using the Mega Mouse Universal Genotyping Array (MegaMUGA, Geneseek, Lincoln NE). The MegaMUGA is an Illumina array platform containing approximately 77,800 markers. Most of these markers are single nucleotide polymorphisms (SNPs), although some are structural variants and transgenic markers. The markers are densely and relatively evenly spaced at 33kb across the genome, found across all autosomes, sex chromosomes and the mitochondria. This array was designed in order to maximize the number of informative markers for the Collaborative Cross (Aylor et al. 2011; Threadgill and Churchill 2012), the diversity outbred cross (Svenson et al. 2012), and wild house mouse populations (Churchill et al. 2004; Collaborative Cross Consortium 2012). The Collaborative Cross features eight parental strains, one of which is WSB. Liver tissue from all F2s and the parents of the cross were sent to Geneseek (NeoGene Corporation, Lincoln, NE) for DNA extraction and genotyping. A total of 1,536 samples were sent, including controls and samples from mice that died before reaching 16 weeks of age.

Multiple controls were used for DNA extraction and genotyping in order to identify technical and biological errors. Liver tissue was organized into 16 (96 well) plates in such a way

to minimize array batch effects on related sets of samples. Tissue from WSB was placed in identical wells on every plate to account for plate extraction effects. The four GI parental samples were replicated four times each across the 16 plates. Replicate samples of the first well of each plate were placed in a random well and run on different arrays.

We examined the genotypes for technical, biological, and data entry errors. We omitted markers that were not informative in the crosses and those with high levels of missing data. We removed a few individuals with high levels of missing data. We also removed a small number of individuals that had large numbers of Mendelian inconsistencies or mismatched sex, which was most likely unresolved sample mix-ups. Following these initial screens, the cleaned data included the four GI parents of the crosses, 70 F1 individuals, 1,346 F2 individuals, and 33,191 markers. In all subsequent analyses, we focused on a subset of 11,833 markers that were fixed in the four GI parents and therefore segregated as in a standard F2 intercross between inbred lines. We estimated inter-marker genetic distances assuming a genotyping error rate of 0.2% and converted estimated recombination fractions to map distances with the Carter-Falconer map function (Carter and Falconer 1951).

Single-trait QTL analysis

Single-trait QTL analysis was performed using Haley-Knott regression (Haley and Knott 1992) on a 0.5 cM grid across the genome, as implemented in R/qtl (Broman and Sen 2009). Analysis was conducted separately for each of the 16 skeletal traits at 5, 10, and 16 weeks with sex, mother, and observer as additive covariates. Genome-wide significance thresholds were determined by permutation (Churchill and Doerge 1994), with adjustments for the X chromosome (Broman et al. 2006). Numbers of permutations were 47,840 and 946,400 for the

autosomes and the X chromosome, respectively. A QTL was considered significant if its maximum LOD score met a 5% genome-wide significance threshold.

Additional single-trait scans were performed on F2s using two different methods to control for effects of body size on each skeletal trait: (1) by using relative skeletal sizes as our traits and (2) by treating body weight as an additive covariate in the model. Relative skeletal size was calculated by dividing each skeletal trait by the cube root of body weight for each individual (trait/body weight$^{0.33}$) and is referred to as the shape ratio (Mosimann 1970; Jungers, Falsetti, and Wall 1995). The use of shape ratios accounts for the isometric component of body size, while maintaining allometric (size-correlated) shape and non-allometric (size-independent) shape. Alternatively, the treatment of body weight as a covariate accounts for both isometric shape and allometric shape, leaving non-allometric shape.

Genetic effects

QTL effects were measured using both additive and dominance effects. Additive effects were calculated as half the difference in genotype means between the GI and WSB homozygotes. Dominance effects were calculated as the difference between the genotypic mean of the GI/WSB heterozygote and the average genotypic mean of the GI and WSB homozygotes. In order to compare effects across traits and time points, additive effects were standardized by dividing by the phenotypic standard deviation. Dominance effects were standardized by dividing the dominance effects by the additive effects (d/a). These ratios can be broken down into broad categories defined in Kenney-Hunt *et al.* 2006. Strong overdominant QTL are defined by having d/a ratios > 2.5. A QTL is considered to be overdominant when d/a is between 1.5 and 2.5. GI is considered to be dominant to WSB when d/a is between 0.5 and 1.5. A QTL is considered

codominant when d/a is between -0.5 and 0.5. WSB is considered to be dominant to GI when d/a is between -0.5 and -1.5. A QTL is considered to be underdominant when d/a is between -1.5 and -2.5. Strong underdominant QTL are defined by having d/a ratios < -2.5.

Phenotypic correlations

Pearson product moment correlations were calculated for each pair of the 16 skeletal traits and body weight at 5, 10, and 16 weeks. Correlations of each trait with itself at different time points were also calculated. We observed significant trait correlations across the skeleton (see Results), raising the prospect that joint analysis of multiple traits could provide additional insights into genetic architecture. When traits are correlated, multi-trait mapping increases the power to detect QTL and increases the precision of estimated QTL location (Jiang and Zeng 1995; Knott and Haley 2000).

To form trait sets for multi-trait mapping, we fit the phenotypic correlations to models we developed (see Table S2.6) based on well-established knowledge of mouse developmental and functional processes, including temporal patterning of the prenatal skeleton (Shubin, Tabin, and Carroll 1997; Wellik and Capecchi 2003), germ layer and cell type origins (Jiang et al. 2002; Morriss-Kay; Jeong et al. 2004; Gross and Hanken 2008; Yoshida et al. 2008), orthogonal patterning of skeletal axes (Wellik and Capecchi 2003; Carapuço et al. 2005), and effects of mechanical load on limb elements (Rauch 2005). Each model was composed of non-overlapping sets of skeletal traits partitioned into hypothesized modules. The best-fitting model was selected using MINT (Márquez 2008), which calculates a goodness of fit statistic γ^* that measures the similarity between expected and observed covariance matrices. Models were ranked based on their γ^* value, and support for rankings was measured by jackknifing.

Joint mapping of multiple skeletal traits

In light of the correlations between skeletal dimensions across F2s, we used two approaches to map QTL for sets of traits. First, we performed principal component analysis (PCA) on the full set of 16 measurements in the F2 population using the prcomp function in R (Mardia, Kent, and Bibby 1979; R Core Team 2016). Separate analyses were conducted for each time point (5, 10, 16 weeks). We used single-trait QTL mapping to search for QTL for each of the 16 principal components; we report results for PC1 and PC2. QTL significance thresholds were established using permutation tests (1,000 replicates and 18,736 replicates for the autosomes and the X chromosome, respectively).

We used multi-trait QTL analysis as a second method to identify loci that affect suites of traits, as implemented in R/qtlpvl (Tian and Broman 2015). Separate analyses were performed on trait sets delineated using two criteria: (1) overlapping 1.5 LOD intervals in single-trait QTL analyses (Figure 2.3 and Table S2.3), and (2) membership in the same modules of best-fitting models from MINT analyses of phenotypic correlations (Table S2.6). Multi-trait mapping used the same genotype probabilities, informative markers, and covariates used in single-trait QTL analyses. QTL significance thresholds were established using permutation tests (1,000 replicates and 18,736 replicates for the autosomes and the X chromosome, respectively).

Tests for pleiotropy

To evaluate whether each QTL associated with multiple traits reflected the action of a single pleiotropic locus or two linked loci, we conducted a statistical test for pleiotropy, as implemented in R/qtlpvl (Tian and Broman 2015; Tian et al. 2016.).The test was performed

separately on two datasets: (1) QTL for skeletal traits from single-trait analyses and QTL for body weight from Gray *et al.* 2015 that have overlapping 1.5 LOD intervals, and (2) QTL for traits within each module of the most supported models from MINT analyses. In this framework, the null hypothesis (H_0) is that one QTL controls all traits (pleiotropy) and the alternative hypothesis (H_1) is that two linked QTL control the traits (linkage), with each trait affected by one of the two QTL. Multiple-trait QTL mapping was first performed under a single-QTL model, H_0. Then a two-dimensional scan over the chromosome was performed, with a two-QTL model, H_1, with each trait being affected by one or the other QTL. This involved an approximation in which, rather than consider all possible allocations of the traits to the two QTL, the traits were sorted based on their estimated QTL location, when considered individually, and then each possible cutpoint of this list was considered. Each possible cutpoint split the traits into two groups affected by the two different QTL. The test statistic LOD_{2v1} was calculated by subtracting the LOD score of H_1 (maximizing over both QTL positions and the split of the traits into two groups) from the LOD score of H_0 (maximizing over QTL position). A p-value for the test of H_0 was calculated by a parametric bootstrap, with a large p-value indicating that the data are consistent with pleiotropy (H_0).

Results

Phenotypic variation

GI mice have larger skeletons than WSB mice across postnatal development, with all but one trait (height of the cranial vault at 16 weeks) showing significant expansions at all three time points (t-test; maximum P-value=0.005; Figure 2.2 and Table S2.1). GI and WSB mice were raised in the same environment on a common diet; as a result, most differences should be genetic in origin. Averaging across traits, the GI skeleton is 14-15% (5, 10 weeks of age) and 12% (at 16 weeks of age) larger than the WSB skeleton. Tibia midshaft diameter (TMD) shows the greatest proportional differences between GI and WSB (24% larger in female GI mice at 5 weeks of age and 22% larger in male GI mice at 10 weeks of age). Substantial divergence is also seen in the humerus and pelvis in females and in the humerus, pelvis, and femur in males (>17% larger in GI averaged across 5, 10, and 16 weeks of age).

Some of the skeletal differences between GI and WSB mice represent changes in shape. The width and depth of the skull show the smallest difference between GI and WSB, exhibiting only a 3-6% increase in GI mice, whereas the skull is 12-15% longer in GI mice. Both humerus and femur lengths show proportionally greater expansion in GI than their respective diameters late in postnatal development (Figure 2.2). Ratios of hindlimb to forelimb lengths (intermembral indices) and humerus to femur lengths (humerofemoral indices) are similar in GI and WSB mice. In contrast, brachial and crural indices are smaller in GI mice, indicating disproportionate expansion of proximal vs. distal limb elements relative to WSB (Table 2.1).

The majority of the skeleton increases in size across postnatal development in both GI and WSB mice (Table S2.2). More skeletal elements show significant increases in size between 5 and 10 weeks than between 10 and 16 weeks of age. In house mice, males are typically larger

than females (Snell 1941). Although body weight and growth rate are sexually dimorphic in GI mice (Gray et al. 2015), not all GI skeletal elements show statistically significant differences in size between the sexes (see Figure 2.2). However, for all traits there are at least some small differences in the means between the sexes, with male averages exceeding female averages.

The trait means of the F1 population from the GI and WSB intercross are closer to the GI means than the WSB means (data not shown). The trait means of the F2 population from the GI and WSB intercross are intermediate compared to the parents (Figure 2.2). All 16 skeletal traits follow normal and continuous distributions (Figure S2.2). All but two skeletal traits (height of the cranial vault at 5-10 weeks, metatarsal and calcaneus length at 10-16 weeks) in the F2 population show significant increases in size over postnatal development (t-test; maximum P-value=0.016).

Single-trait QTL mapping

A total of 208 QTL are identified across 16 skeletal traits and three time points (Figure 2.3 and Table S2.3). Multiple QTL are detected for all traits, with the exception of humerus midshaft diameter (HMD) and proximal tibia width (PTW) at 5 weeks of age. Nineteen of the 20 chromosomes contain at least one significant QTL for at least one time point. A large proportion of QTL for different traits co-localize, based on overlapping confidence intervals. Over half of all QTL are found on chromosomes 4, 7, 10, and 15, and span the entire skeleton, from skull to hindlimb. These highly co-localizing QTL are potentially pleiotropic and may act as global regulators of growth.

Effects of some QTL are restricted to specific regions of the skeleton (Figure 2.3), including the skull, femur, and other hindlimb elements. Numbers of QTL are similar across the

three time points (69, 73, and 66 QTL at 5, 10, and 16 weeks of age, respectively). Although QTL on chromosomes 4, 7, 10, 11, and 15 are often found across all three time points, other QTL are mostly or entirely restricted to one time point. QTL on chromosomes 2, 5, 6, 13, 18, and X for hindlimb diameters (PTW, HMD, FMD) are not identified at early time points, suggesting these loci contribute to variation in size occurring later in postnatal development. In contrast, QTL on chromosome 16 (contributing to variation in skull widths and hindlimb lengths) disappear with age, suggesting these loci confer early growth differences between the two strains. There is a relative paucity of QTL for limb diameter traits, likely due in part to low repeatability. Because these traits are very small (< 1mm), they are more difficult to measure. Consistent with this idea, we observed higher standard deviations for limb diameter traits compared to longer measurements (data not shown).

Standardized additive and dominance effects for all QTL are illustrated in Figure 2.4. Additive effects are small to moderate, ranging from 9% to 23% of the mean phenotypic differences between GI and WSB mice. The largest additive effect is 0.48 mm for skull width (SW; chromosome 10 QTL at 10 weeks). Average values across traits of the standardized additive effect are also small: 0.23, 0.23, and 0.29 mm at 5, 10, and 16 weeks of age, respectively. The GI allele is associated with skeletal expansion at most QTL (93%); exceptions are primarily QTL for widths and diameters.

Inspection of standardized dominance values (d/a) reveals that the majority (63%) of QTL are codominant (d/a between -0.5 and 0.5). No QTL exhibit strong overdominance. The largest d/a ratio is 1.9 for the diameter of the tibia (TMD) QTL on chromosome 6 at 16 weeks of age; this is the only case of GI overdominance (d/a between 1.5 and 2.5). The GI allele is at least partially dominant (d/a between 0.5 and 1.5) at 6% of QTL. In contrast, WSB dominance (d/a

between -0.5 and -1.5) is seen at 27% of the QTL. Only five QTL show values consistent with underdominance (d/a between -1.5 and -2.5) or strong underdominance (d/a < -2.5) of WSB alleles. The lowest d/a ratio (-3.2) is for the sacral vertebrae length (SVL) QTL on chromosome 15 at 16 weeks of age.

Accounting for body weight has disparate effects across QTL (Table S2.4). Many QTL are no longer significant, including loci on chromosomes 7, 10, 11, and 15. Some QTL are maintained, most of which map to chromosomes 4 and 14 and underlie pelvic and hindlimb traits. New QTL are identified in both weight-adjusted scans; many of these QTL also map to chromosome 14 and contribute to pelvic and hindlimb dimensions. Results depend on the method used to account for weight. QTL for skull and hindlimb traits on chromosome 7 are both maintained and acquired when shape ratios (trait/body weight$^{0.33}$) are used, but not when body weight is used as a covariate. QTL for skull and hindlimb traits on chromosomes 3 and 10 are maintained and acquired when body weight is used as a covariate, but not when shape ratios are used. Although there are some differences in results across the 5, 10, and 16 week time points, the overall patterns in the weight-adjusted scans remain similar, both in the traits involved and the chromosomal positions of QTL.

As a preliminary examination of epistasis, we tested for interactions among all pairs of single-trait QTL identified for each skeletal trait using the add.int function in R/QTL (Broman and Sen 2009). Out of the 430 tested QTL pairs, only 20 (5%) show a statistically significant interaction at the uncorrected $P<0.05$ threshold, consistent with what we would expect based on chance alone.

Phenotypic correlations

Most pairs of skeletal traits are positively correlated in the F2s (Figure 2.5). High correlations are observed between measurements of the skull, pelvis, and hindlimb (absolute average Pearson's *r* value = 0.54, 0.69, 0.62 at 5, 10, and 16 weeks, respectively; maximum P-value = $2.2e^{-16}$). Humerus length (HL) shows the most divergent pattern: weaker than average correlations with many traits and strong negative correlations with a few traits (absolute average Pearson's *r* value across time points = 0.19; maximum P-value = $2.2e^{-16}$). Body weight is also highly correlated with all skeletal traits. Although correlation patterns are similar across the three time points, there are notable differences. The correlation between humerus length (HL) and the mid-shaft diameter of the humerus (HMD) changes during development, starting at 5 weeks as a positive correlation and ending at 16 weeks as a negative correlation (5 weeks: Pearson's *r* = 0.11; P-value = 0.001; 10 weeks: Pearson's *r* = -0.004; P-value = 0.875; 16 weeks: Pearson's *r* = -0.08; P-value = 0.012). The correlation between the midshaft diameter of the femur (FMD) with both the midshaft diameter of the humerus (HMD) and ulna length (UL) increases during development. Intra-trait correlations across pairs of time points are high and positive (Table S2.5). The earliest and latest time points (5 and 16 weeks) show a lower correlation compared to the correlations among consecutive time points.

Analyses of phenotypic correlations using MINT reveal evidence for modularity (non-random trait groupings) across the skeleton (Table S2.6). Overall, the null hypothesis of independence among traits fits the data poorly. Modules based on developmental timing (H_1) show the best fit at 5 and 10 weeks of age. In contrast, modules that separate the skeleton into axial and appendicular components (H_3) receive the most support at 16 weeks. Limb-specific analyses also support modularity. For models H_0-H_5, the limb length versus diameter model (H_4) fits best for all three time points.

Principal component analyses

Principal components 1 and 2 collectively explain more than half of F2 skeletal variation at each age. (Figure S2.3A). Four QTL (on chromosomes 4, 7, 10, and 15) contribute to PC1 at all three time points. Two lines of evidence suggest that these loci are involved in global size expansion. First, they overlap with the QTL that affect the largest number of traits. Second, PC1 scores are highly positively correlated with body weight (Pearson's $r = 0.78$; $P < 0.0001$), whereas PC2 scores are weakly correlated with body weight ($r = -0.10$; $P = 0.003$). A single QTL (on chromosome 4) contributes to PC2 across time points (Figure S2.3B). This locus overlaps with QTL that are maintained in analyses adjusted for body weight, suggesting that it contributes to the evolution of shape.

Multiple-trait QTL mapping

Multi-trait QTL mapping identifies QTL that are not found in single-trait mapping or principal component mapping, including loci that affect the skull, pelvis, and limb lengths (Table S2.7). Overall, LOD scores are higher and confidence intervals are narrower than in single-trait scans. Otherwise, multi-trait and single-trait analyses reveal similar genetic properties in terms of QTL co-localization across traits and temporal variation in QTL activity (Table S2.7 and Table S2.8).

Pleiotropy vs. linkage

All but one of the co-localizing skeletal QTL from single-trait analyses and body weight QTL from Gray *et al.* (2015) are consistent with pleiotropic models at 5 and 10 weeks of age

(Table 2.2). Although additional QTL fit linkage models at 16 weeks, most QTL support pleiotropic models at this age as well. These results again suggest that co-localizing QTL are global regulators of growth rather than contributors to specific skeletal elements. Results for skeletal modules from multi-trait mapping are similar (Table S2.9). For whole-skeleton modules, pleiotropy is rejected for only 16 and 10 percent of QTL at 5 and 10 weeks of age, respectively (maximum $P \leq 0.03$). Support for linkage is greater at 16 weeks of age (30%; maximum $P \leq 0.03$). Limb-specific modules exhibit similar patterns (Table S2.9). These results raise the prospect that the majority of detected QTL control more than one trait within a given module. In cases where pleiotropy is rejected, it is possible to infer which traits are affected by each of the two linked QTL. For example, for the QTL on chromosome 4 for the hindlimb module at 5 weeks, a partitioning of limb length and diameter elements is inferred (Table S2.9).

Discussion

We uncovered pronounced skeletal evolution in GI mice. The entire GI skeleton expanded. Heterogeneity in the degree of expansion gave rise to anatomically local patterns of divergence, including a relatively longer and narrower skull and an elongation of proximal vs. distal elements of the limbs. Our genetic portrait of skeletal evolution in GI mice adds to a growing list of studies that reveal the genetic basis of rapid evolution in novel environments (Shapiro et al. 2004; Cresko et al. 2004; Colosimo et al. 2005; Hoekstra et al. 2006; Abzhanov et al. 2006; Pool and Aquadro 2007; Gray et al. 2015). We found QTL underlying global skeletal divergence. Over half of all QTL are located on only four chromosomes and contribute to variation in traits spanning the entire skeleton. In addition, we found QTL responsible for changes to specific elements.

The extensive co-localization of QTL for many traits raises the intriguing prospect that a modest number of genetic changes were responsible for the expansion of the GI mouse skeleton. Skeletal QTL on chromosomes 1, 4, 6, 7, 8, 9, 10, 11, 15 and 16 co-localize with all but one of the QTL for body weight and growth rate discovered in the same cross (Gray et al. 2015), and co-localized loci show evidence of pleiotropy. This genetic architecture could facilitate morphological evolution across the body (Cheverud 1984; Roff 1997), with natural selection to increase body size generating correlated expansions of the skeleton. For example, pleiotropy has been hypothesized to enable rapid phenotypic divergence among dog breeds (Chase et al. 2002). At the same time, our inference of pleiotropy should be viewed with caution. The power to distinguish pleiotropy from linkage is constrained by mapping resolution, which is relatively low in an F2 intercross.

By incorporating body weight into our genetic analyses, we were able to disentangle QTL effects on skeletal shape from QTL effects on overall body size. Skeletal QTL on chromosomes 7, 10, and 15, largely disappear after adjusting for body weight, suggesting that these loci act as global regulators of growth rather than affecting local skeletal traits. Allometric shifts in GI mice to a relatively long and narrow skull and to relatively elongated proximal limb elements are also captured by the genetic analysis using body weight as a covariate.

These alterations in skeletal size and shape may have functional consequences. The elongated skull – a feature that is atypical for house mice (Samuels 2009) – could indicate a shift toward a more specialized diet. Carnivores and insectivores sometimes exhibit an elongated rostrum (Samuels 2009), and GI mice eat birds and a variety of invertebrates (Jones, Chown, and Gaston 2003). Changes in limb proportions are likely to affect locomotion. Mammalian species living in open habitats have relatively long femurs (Brown and Yalden 1973; Herrel et al. 2002), a characteristic that can facilitate running (Samuels and Van Valkenburgh 2008). Mice on Gough Island experience an open habitat compared to mainland mice, which primarily live in and around human structures. Functional and ecological studies will be required to test these hypotheses.

Some of the results highlight differences between the skull and postcranium. The most severe shape changes are found in the skull. Some QTL act only (chromosomes 17 and 19) or primarily (chromosomes 3 and 6) in the skull. Skull width and depth likely completed growth by 5 weeks of age; early growth differences between GI mice and WSB could be reflected in QTL specific to 5 weeks. An example is the chromosome 16 QTL that controls the width of the skull at 5 weeks, but is not detected at 10 and 16 weeks. The skull length measurement includes both the length of the braincase and the length of the face. Combining these early and late growing

regions in one measurement might have reduced power to detect QTL. Measuring the craniofacial region with higher resolution is an important goal for future genetic studies of skeletal evolution in GI mice.

Evolution of the GI mouse skeleton appears to have been highly integrated. The similarity of phenotypic correlations across time points suggests that skeletal modules are largely determined by 5 weeks of age and that timing during prenatal development is a key component of inferred modules. For the whole skeleton, our results are consistent with processes observed in a variety of mammals, with skeletal development proceeding first along the proximal-distal axis, followed by development along the appendicular axis (Bronner, Farach-Carson, and Roach 2010). For limb traits, lengths appear to form distinct clusters from diameters. This pattern may also reflect developmental timing, since long bone lengths develop first at the epiphyseal plate with the addition of bone tissue, followed by thickening of bone via appositional growth (Pourquié 2009). Our results indicate that the joint consideration of suites of skeletal traits based on their phenotypic correlations and developmental origins leads to better connections between QTL and potential biological mechanisms.

Similar genetic studies in laboratory populations of house mice and in wild populations of other vertebrates provide illuminating comparisons to skeletal evolution in GI mice. The LG (Large) and SM (Small) strains of mice were artificially selected for body size, resulting in a >20 gram disparity in adult body mass (Goodale 1938; Goodale 1941; Macarthur 1944). Skeletal differences that arose as correlated responses to selection were mapped (Cheverud et al. 1996; Vaughn et al. 1999; Leamy, Routman, and Cheverud 1999; Klingenberg et al. 2001a; Klingenberg and Leamy 2001; Kenney-Hunt et al. 2006; Kenney-Hunt et al. 2008; E. Norgard et al. 2008; Sanger et al. 2011; Norgard et al. 2011). A subset of nine common measurements

collected at the same age (10 weeks) enables comparison to our results, including skull (SW, ZW, HCV), pelvic (SVL), forelimb (UL), and hindlimb (FL, TL) traits (Kenney-Hunt et al. 2008). Fourteen percent of QTL for seven of the nine traits from the LGxSM cross overlap with the GIxWSB cross. For example, QTL on chromosomes 3, 4, 7, 10, and 15 are identified in both crosses and exhibit similar additive and dominance effects. This sharing is disproportionately driven by loci that are pleiotropic. Although wide confidence intervals on QTL location raise caution in interpreting this pattern, it suggests that a small subset of the detected genetic changes could involve the same biological pathways, genes, and/or mutations. Distributions of standardized additive effects across all QTL (shared and unshared) are similar in the two studies, implying that artificial and natural selection acted on mutations with common properties. Nevertheless, the observation that most QTL locations appear to be distinct suggests that the evolution of large size in GI and LG mice mostly involved different genes.

The threespine stickleback, *Gasterosteus aculeatus,* a target of extensive genetic studies of skeletal evolution, also provides useful context for our findings. Sticklebacks that recently adapted to new freshwater environments diverged in skeletal morphology, including bony plate armor loss and pelvic reduction (Peichel et al. 2001; Shapiro et al. 2004). In contrast to skeletal evolution in GI mice, changes in both skeletal variants (*e.g.* bony lateral plate number, gill raker number, and presence/absence of bony plates) and some continuous traits (*e.g.* spine length, pelvic size, and bony plate size) involve loci with substantial phenotypic effects (Peichel et al. 2001; Colosimo et al. 2004; Cresko et al. 2004; Shapiro et al. 2004; Berner et al. 2014). However, genetic studies of smaller components of stickleback morphology have found hundreds of QTL with small to moderate effects (Miller et al. 2014; Conte et al. 2015). Therefore, some skeletal traits in stickleback display genetic properties distinct from those

observed in GI mice, but the breakdown of stickleback skeletal morphology into smaller components reveals a similar evolutionary trajectory involving many mutations of modest effect.

Finally, our results speak indirectly to the evolutionary causes of skeletal divergence in GI mice. Evolution of the skeleton was presumably rapid and occurred in a new environment, observations consistent with natural selection as a primary evolutionary mechanism. The finding that QTL alleles from GI mice increase skeletal size in almost all cases suggests that natural selection targeted the skeleton or a correlated trait (Orr 1998). Body weight and body condition of GI mice correlate with overwinter survival, and mice that prey upon nestling seabird chicks maintain higher body weights during the winter season (Cuthbert et al. 2016). These patterns raise the prospect that natural selection targeted overall body size in GI mice, driving substantial and rapid evolution of the skeleton.

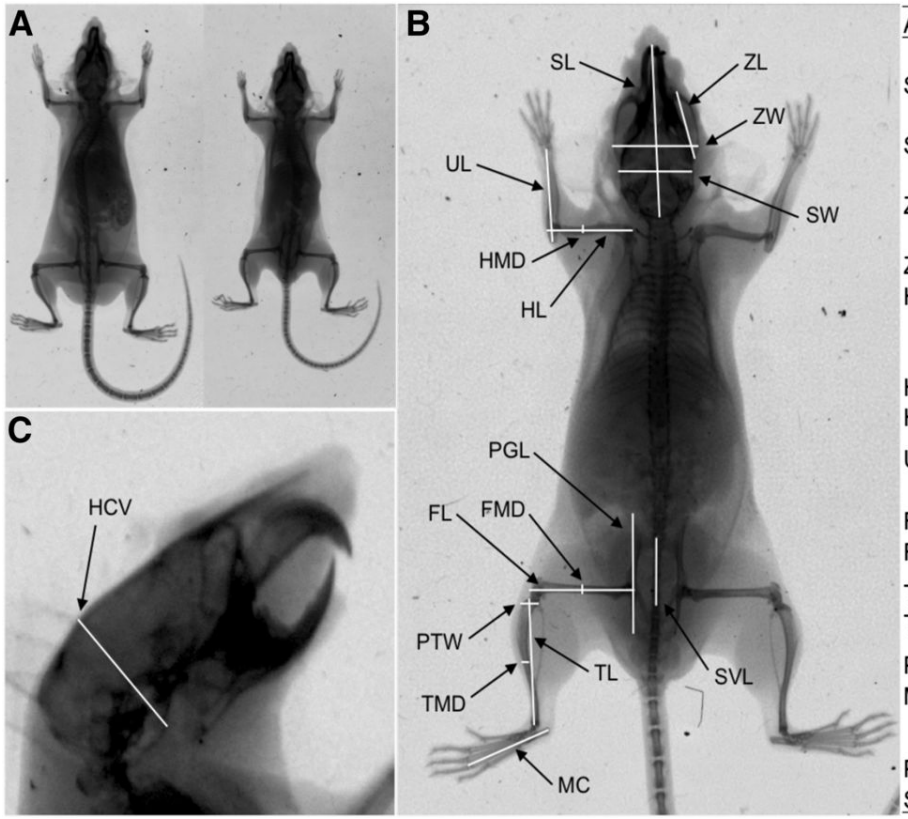

Abbrev.	Trait	Description
	Skull traits	
SL	Skull length	Length from occipital crest (inion) to nasal bone
SW	Skull width	Maximum skull width across parietal bones
ZW	Bi-Zygomatic width	Maximum width of skull across zyogmatic arches
ZL	Zygomatic length	Maximum length of zygomatic arch
HCV	Height of cranial vault	Superior point of parietal bone to inferior of tympanic bulla
	Forelimb traits	
HL	Humerus length	Capitulum to head of humerus
HMD	Humerus midshaft diameter	Shaft diameter taken at midpoint of HL
UL	Ulna length	Styloid process to olecranon process
	Hindlimb traits	
FL	Femur length	Head of femur to femoral condyle
FMD	Femur midshaft diameter	Shaft diameter taken at midpoint of FL
TL	Tibia length	Head of tibia to lateral malleolus
TMD	Tibia midshaft diameter	Shaft diameter taken at midpoint of UL
PTW	Proximal tibia width	Maximum width of proximal epiphysis
MC	Metatarsal-calcaneal length	Distal calcaneus to distal III metatarsal
	Pelvic traits	
PGL	Pelvic girdle length	Illiac crest to ischial tuberosity
SVL	Sacral vertebrae length	Maximum length of sacral vertebrae

Figure 2.1 X-ray image of mouse skeleton and locations of phenotypes.

An X-ray image illustrating the size comparison of a GI mouse (left) and a WSB mouse (right) at 16 weeks of age. (B) Locations of skeletal traits on an X-ray image taken from a dorsal view. (C) Location of the height of the cranial vault (HCV) on an X-ray image taken from a lateral view. The right panel lists the 16 skeletal traits measured, and includes names, acronyms, and descriptions of each trait.

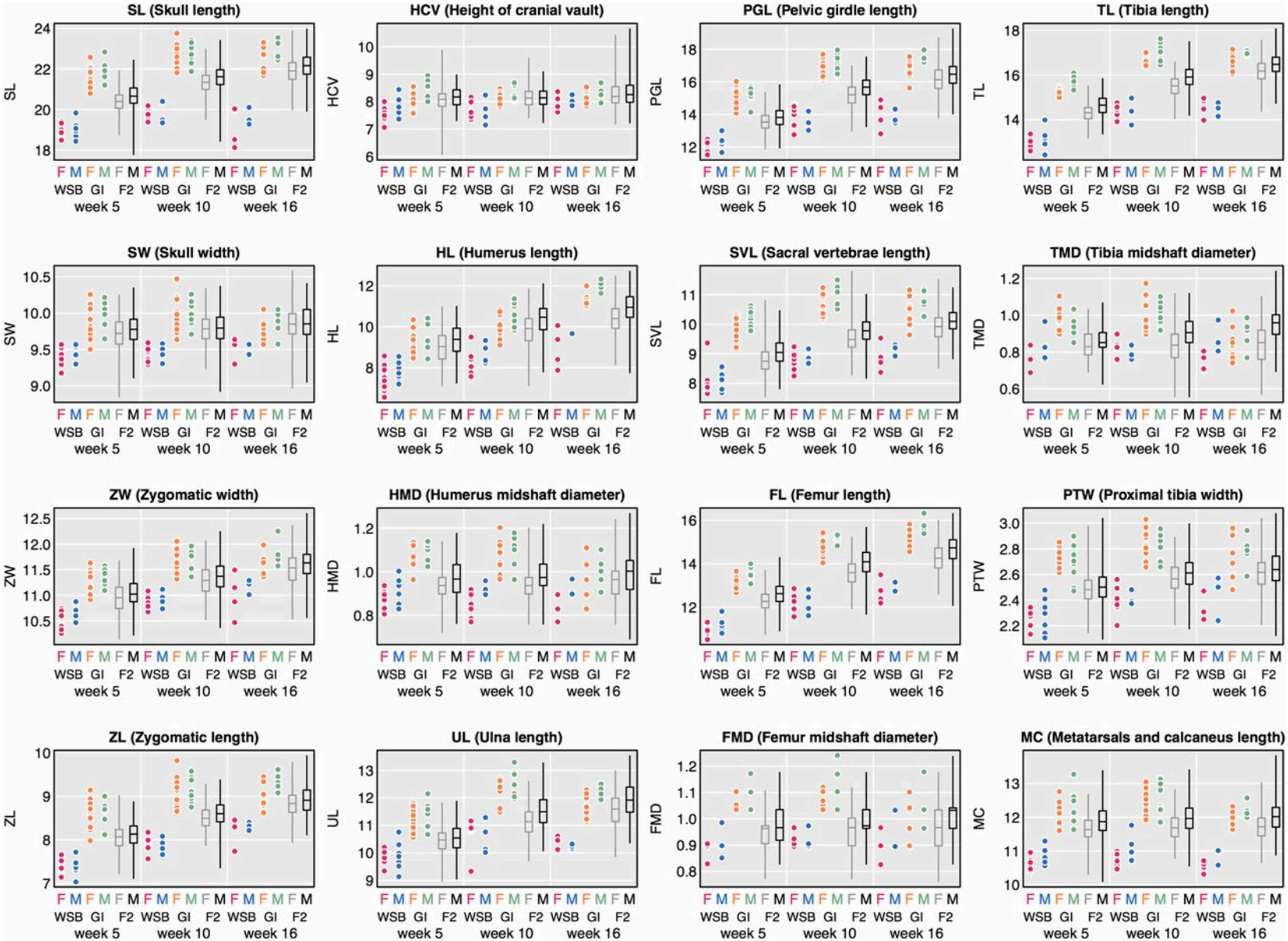
SL (Skull length)
HCV (Height of cranial vault)
PGL (Pelvic girdle length)
TL (Tibia length)
SW (Skull width)
HL (Humerus length)
SVL (Sacral vertebrae length)
TMD (Tibia midshaft diameter)
ZW (Zygomatic width)
HMD (Humerus midshaft diameter)
FL (Femur length)
PTW (Proximal tibia width)
ZL (Zygomatic length)
UL (Ulna length)
FMD (Femur midshaft diameter)
MC (Metatarsals and calcaneus length)
F M F M F M F M F M F M F M F M F M F M F M F M
WSB GI F2 WSB GI F2 WSB GI F2
week 5
week 10
week 16

Figure 2.2 Phenotypic distributions of skeletal traits

Phenotypic distributions of 16 skeletal traits (in millimeters) for female (pink) and male (blue) WSB, female (orange) and male (green) GI, and female (gray) and male (black) F_2 animals at 5, 10, and 16 weeks of age. GI and WSB data are represented as scatter plots and F_2 data are represented with box plots.

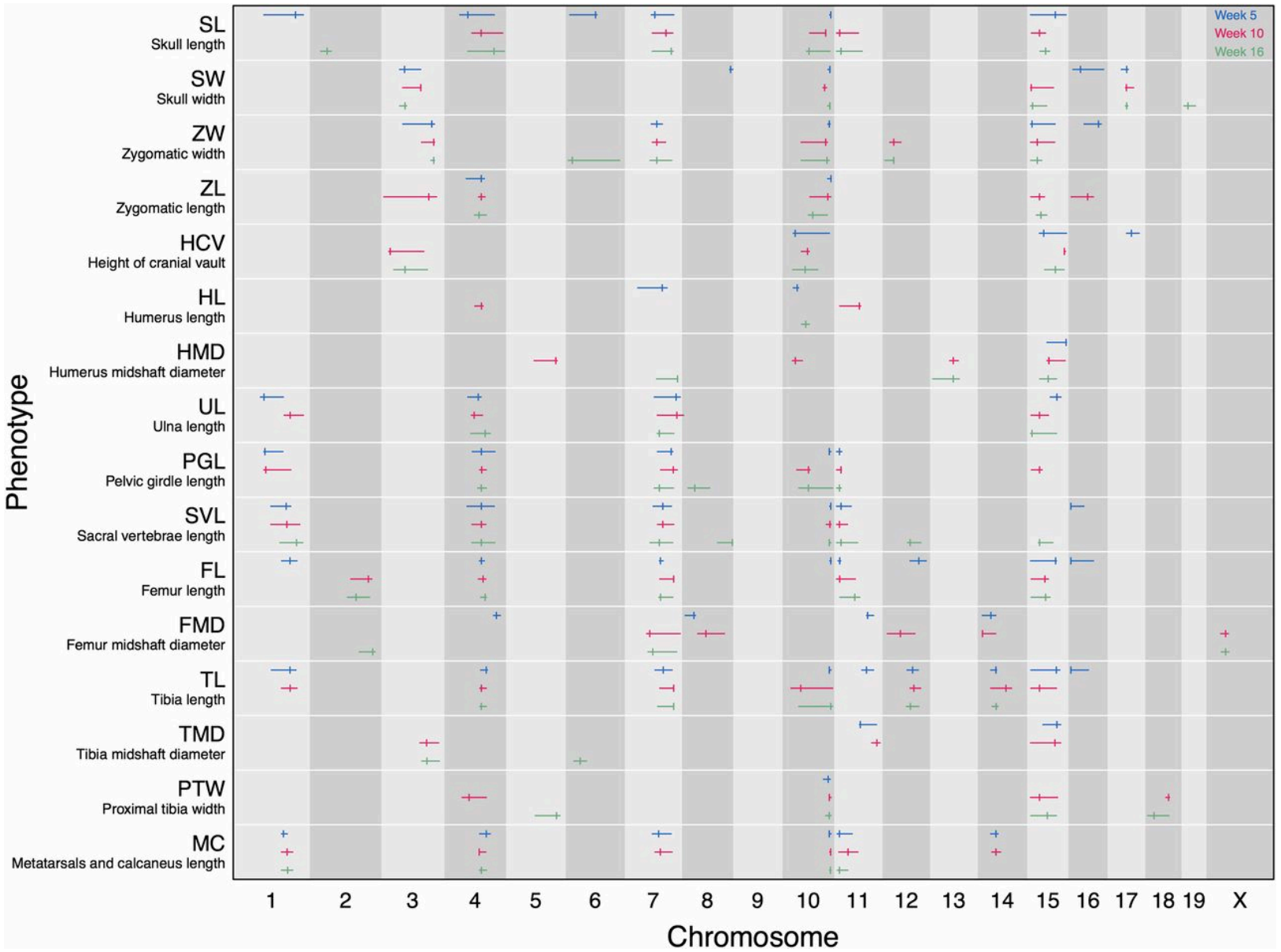
Phenotype
SL
Skull length
SW
Skull width
ZW
Zygomatic width
ZL
Zygomatic length
HCV
Height of cranial vault
HL
Humerus length
HMD
Humerus midshaft diameter
UL
Ulna length
PGL
Pelvic girdle length
SVL
Sacral vertebrae length
FL
Femur length
FMD
Femur midshaft diameter
TL
Tibia length
TMD
Tibia midshaft diameter
PTW
Proximal tibia width
MC
Metatarsals and calcaneus length
Week 5
Week 10
Week 16
1
2
3
4
5
6
7
8
9
10
11
12
13
14
15
16
17
18
19
X
Chromosome

Figure 2.3 Genomic intervals of QTL for skeletal measurements

Genomic intervals (in megabases) of all significant QTL for 16 skeletal measurements at 5 (in blue), 10 (in pink), and 16 (in green) weeks of age. Tick marks indicate the maximum LOD of the QTL. Confidence intervals are the 1.5 LOD intervals.

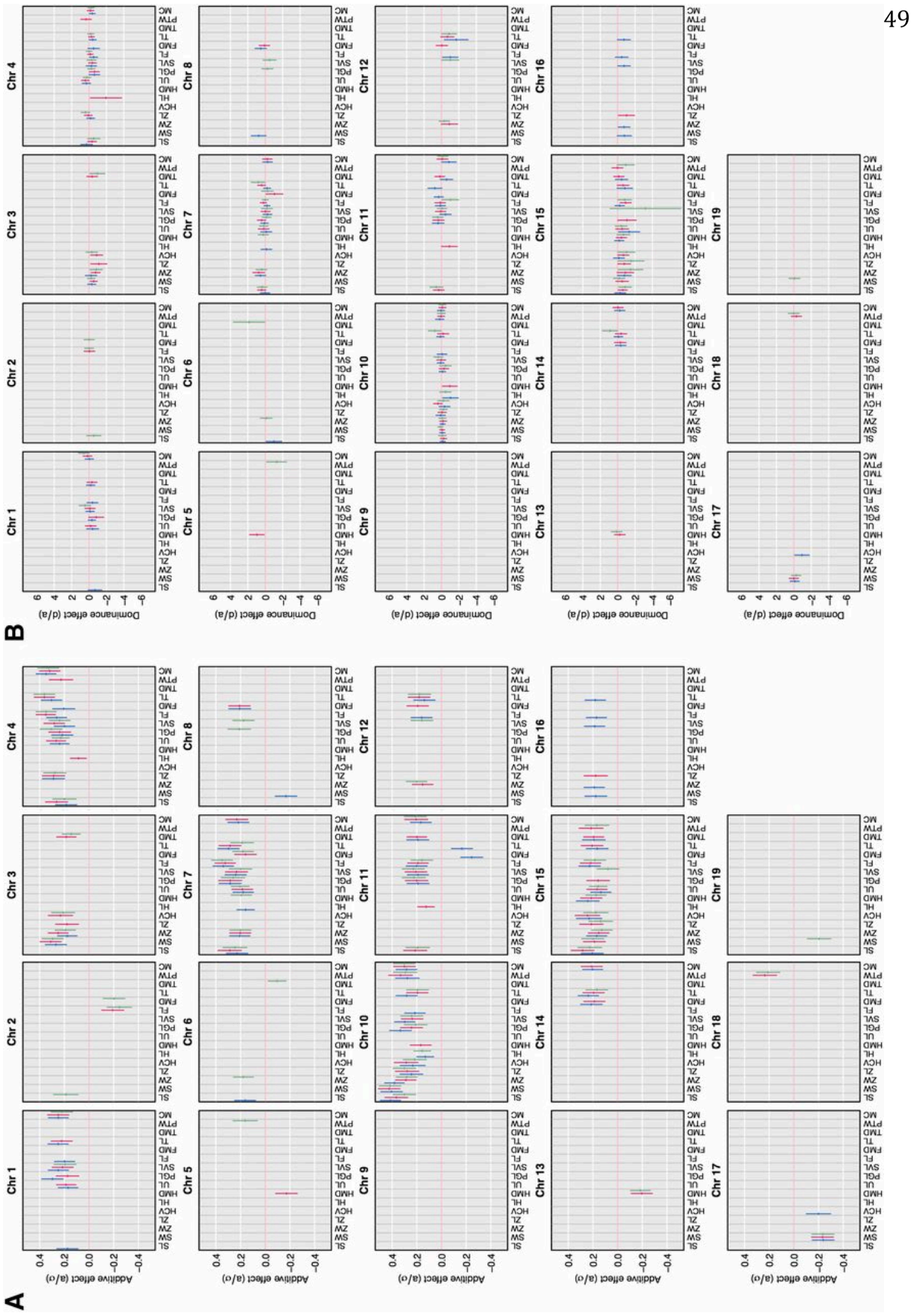
A
B
Chr 1
Chr 2
Chr 3
Chr 4
Chr 5
Chr 6
Chr 7
Chr 8
Chr 9
Chr 10
Chr 11
Chr 12
Chr 13
Chr 14
Chr 15
Chr 16
Chr 17
Chr 18
Chr 19
Additive effect (a/σ)
Dominance effect (d/a)
SL SW ZW ZL HCV HL HMD UL PGL SVL FL FMD TL TMD PTW MC

Figure 2.4 Standardized additive and dominance effects

Standardized (A) additive (a/σ) and (B) dominance (d/a) effects of skeletal trait QTL for 16 skeletal traits at 5 (in blue), 10 (in pink), and 16 (in green) weeks of age.

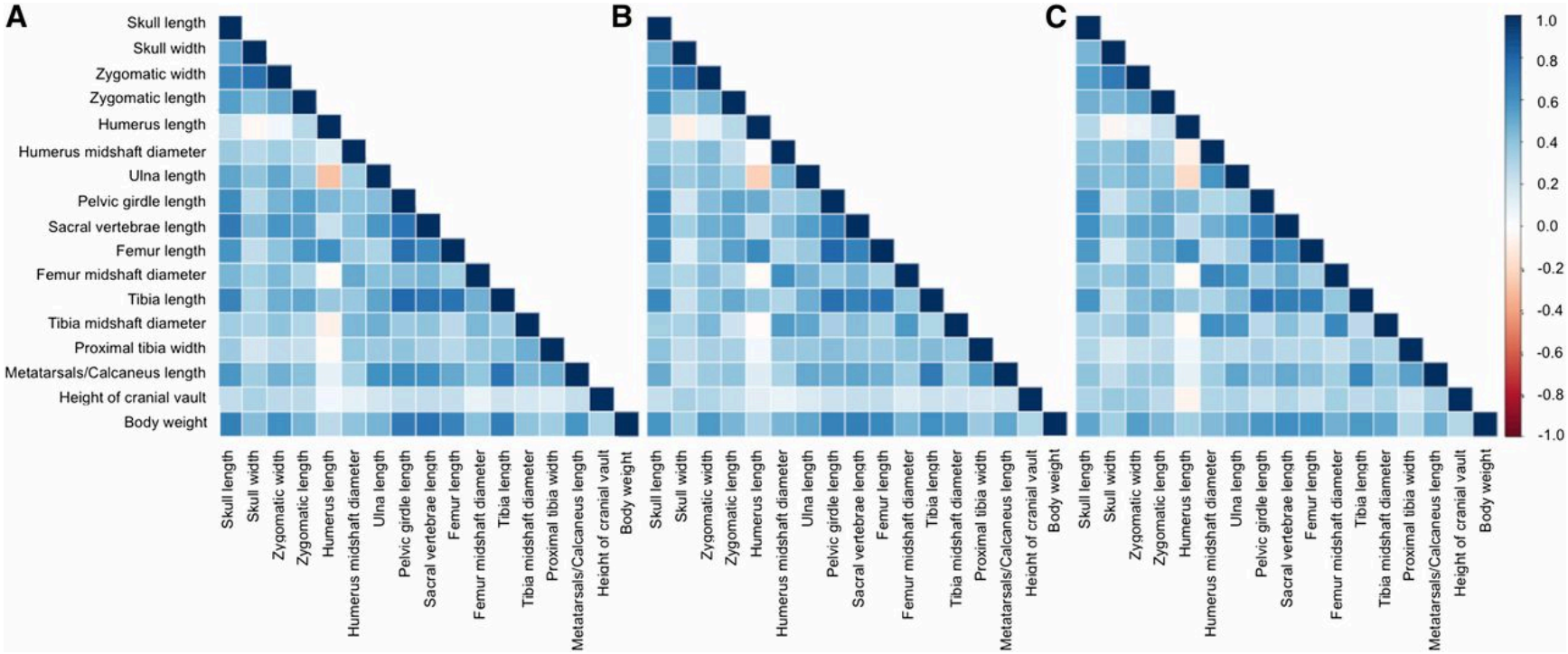

Figure 2.5 Phenotypic correlations among skeletal traits
All pairwise phenotypic correlations among the 16 skeletal traits at 5 (A), 10 (B), and 16 (C) weeks of age. Values represent the Pearson product moment. A positive correlation is represented in blue, and a negative correlation is represented in red. The depth of color indicates the strength of the correlation.

Table 2.1 Shape evolution in GI mice

	F 5 week		F 10 week		F 16 week		M 5 week		M 10 week		M 16 week	
Shape Index	WSB	GI	WSB	GI	WSB	GI	WSB	GI	WSB	GI	WSB	GI
Intermembral index	72.3	72.0	70.9	70.6	70.6	70.6	73.0	71.3	72.5	71.7	72.4	73.9
Humerofemoral index	68.0	70.7	66.6	67.2	70.3	73.9	70.3	70.3	71.4	69.7	74.3	75.5
Crural index	118.8	117.4	117.3	112.6	114.6	108.2	118.0	116.5	117.6	112.5	111.2	107.0
Brachial index	132.5	121.5	131.6	123.3	115.6	104.1	126.4	119.4	121.0	118.8	106.0	102.4

Shape index values for GI and WSB mice for females (F) and males (M) at 5, 10, and 16 weeks of age. The intermembral index is the ratio of the forelimb to hindlimb [(HL + UL)/(FL + TL) × 100], the humerofemoral index is the ratio of proximal elements of the limb [(HL/FL) × 100], the crural index is the ratio of distal to proximal elements of the hindlimb [(TL/FL) × 100], and the brachial index is the ratio of distal to proximal elements of the forelimb [(UL/HL) × 100].

Table 2.2 Tests of pleiotropy *vs.* close linkage

Wk	Chr	Traits with overlapping QTL	p	LOD	QTL 1 Pos	QTL 1 Pos	QTL 1 traits	QTL 2 traits
5	1	SL,UL,PGL,SVL,FL,TL,MC, BW	0.13	12.0	73.7			
	3	SW,ZW,BW	0.52	6.3	58.3			
	4	SL,ZL,UL,PGL,SVL,FL,FMD,TL,MC,BW	<0.01*	24.7	93.6	133.0	SL,ZL,UL,PGL, SVL,FL,TL,MC, BW	FMD
	7	SL,ZW,HL,UL,PGL,SVL,FL,TL,MC,BW	0.96	17.0	146.0			
	10P	HCV,HL,BW	0.22	6.4	119.4			
	10D	SL,SW,ZW,ZL,HCV,PGL,SVL,FL,TL,PTW,MC,BW	0.95	27.5	124.8			
	11P	PGL,SVL,FL,MC,BW	0.23	8.1	19.3			
	11D	FMD,TL,TMD,BW	0.19	16.8	96.5			
	12	FL,TL,BW	0.16	5.5	75.6			
	14	FMD,TL,MC,BW	0.87	7.9	71.9			
	15	SL,ZW,HCV,HMD,UL,FL,TL,TMD,BW	0.81	11.6	48.7			
	16	SL,ZW,SVL,FL,TL,BW	0.23	9.5	21.9			
	17	SW,HCV,BW	0.86	5.6	49.8			
10	1	UL,PGL,SVL,TL,MC,BW	0.07	6.9	159.6			
	3	SW,ZW,ZL,HCV,TMD,BW	0.36	12.7	49.7			
	4	SL,ZL,HL,UL,PGL,SVL,FL,TL,PTW,MC,BW	0.38	24.0	104.1			
	7	SL,ZW,UL,PGL,SVL,FL,FMD,TL,MC,BW	0.25	14.9	95.4			
	10	SL,SW,ZW,ZL,HCV,HMD,PGL,SVL,TL,PTW,MC,BW	0.97	26.5	120.8			
	11	SL,HL,PGL,SVL,FL,MC,BW	0.06	6.8	19.3			
	12	ZW,FMD,TL,BW	0.02*	8.7	27.7	79.8	ZW,FMD	TL,BW
	14	FMD,TL,MC,BW	0.06	6.0	40.0			
	15	SL,SW,ZW,ZL,HCV,HMD,UL,PGL,FL,TL,TMD,PTW,BW	0.10	16.2	51.5			
16	1	SVL,MC,BW	0.04*	6.1	136.2	170.1	MC	SVL,BW

2	FL,FMD,BW	0.01*	10.4	120.7	161.3	FL,BW	FMD
3	SW,HCV,BW	0.19	7.1	47.7			
4	SL,ZL,UL,PGL,SVL,FL,TL,MC,BW	<0.01*	32.2	86.5	105.0	UL,TL,BW	SL,ZL,PGL, SVL,FL,MC
6	ZW,TMD,BW	0.03*	9.1	46.2	82.0	ZW,BW	TMD
7	SL,ZW,HMD,UL,PGL,SVL,FL,FMD,TL,BW	0.34	16.9	95.4			
10	SL,SW,ZW,ZL,HCV,HL,PGL,SVL,TL,PTW,MC,BW	0.58	26.5	121.2			
11	SL,PGL,SVL,FL,MC,BW	0.66	7.6	16.8			
12	SVL,TL,BW	0.16	4.1	98.9			
15	SL,SW,ZW,ZL,HCV,HMD,UL,SVL,FL,PTW,BW	0.38	14.6	51.5			

Tests for the rejection of pleiotropy (H_0) for sets of QTL for skeletal traits from single-trait analyses and QTL for body weight (from Gray *et al.* 2015) that have overlapping 1.5 LOD intervals. QTL positions (in megabases), LOD scores, and *P*-values (*P*) are provided for each set of QTL on a given chromosome (Chr). A large *P*-value indicates that the data are consistent with the pleiotropic model (H_0). An asterisk indicates statistical significance to reject pleiotropy (H_0), providing support for a model of close linkage. If linkage is supported, QTL 1 and QTL 2 positions, along with the partitioning of traits affected by each of the two linked QTL, are listed. Please see right panel in Figure 2.1 for the 16 skeletal traits measured, including names, acronyms, and descriptions of each trait

Chapter 3

Genetics and Functional Morphology of Mandibular Evolution in Giant Mice from Gough Island

Michelle D. Parmenter, Jacob P. Nelson, Sara Weigel, Christopher J. Vinyard,

and Bret A. Payseur

Contributions were as follows: MDP, CJV, and BAP designed the study. MDP, JPN, SW, and CJV collected data. MDP and CJV conducted analyses. MDP and BAP wrote the manuscript.

Supplementary information from this chapter can be found in Appendix B.

Abstract

Islands often facilitate rapid evolution of organismal morphology, providing a rich resource for studying phenotypic evolution. In vertebrates, examples of island evolution often involve changes in the skeleton, including the mandible. Due to its important role in organismal function, such as feeding and predation, changes to mandibular morphology could have important implications to the performance and fitness of the organism. There have been extensive comparative studies on mandibular morphology on islands, particularly in the house mouse *Mus musculus domesticus*. However, little is known about the genetic basis and functional morphology of mandibular evolution on islands. We utilized house mice from Gough Island, an emerging model for rapid evolution of extreme size, to genetically and functionally characterize mandible evolution in a natural context. Gough Island mice are the largest wild house mice in the world and display pronounced changes in skeletal size and shape. Compared to a mainland reference strain from the same subspecies (WSB/EiJ), we found that Gough Island mice exhibit an expansion of the mandible. We also found significant shape change in the mandible, including the narrowing of the mandible and widening of the condyle. Through biomechanical tests of jaw performance, Gough Island mice deliver relatively larger bite forces than WSB/EiJ. The relative increase in load resistance traits is predicted to be functionally associated with the increase in bite force. Quantitative trait locus (QTL) mapping in a F_2 intercross between Gough Island mice and WSB/EiJ identified QTL underlying mandible traits within particular mandible regions. Two QTL affecting a suite of mandible traits were identified, consistent with an important contribution of pleiotropy to the global regulation of mandible growth. We provide evidence for QTL underlying variation in mandible shape distinct from those identified for mandible size. By

combining functional morphology and quantitative genetic techniques, this study provides a rare insight into rapid morphological evolution on islands.

Introduction

Islands have environments and conditions distinct from mainland habitats, including changes in resource availability, diet, and predation (Losos and Ricklefs 2009). These shifts can facilitate rapid and extreme evolution of morphological traits in insular populations (Losos et al. 1997; Scott et al. 2003; Millien 2006; Kirchman 2009). Morphological traits determine how an organism interacts with its environment, and are therefore potentially important targets of natural selection. How morphological traits evolve in nature is of major interest to biologists, however its genetic basis remains poorly understood.

Rapid changes in morphology on islands have been documented extensively across mammalian taxa, including body size (Foster 1964; Case 1978; Adler and Levins 1994; Lomolino 2005; Meiri, Dayan, and Simberloff 2005; Raia and Meiri 2006; Thomas, Meiri, and Phillimore 2009; Lyras, van der Geer, and Rook 2010; Millien 2011) and skeletal traits (Berry 1964; Sondaar 1977; Pergams and Ashley 2001; Brown et al. 2004; Shapiro et al. 2004; Colosimo et al. 2005; Parmenter et al. 2016, see Chapter 2). Many of these studies have focused on the mandible due to its importance to organismal function (Herring 1993). The mandible plays a vital role in food processing (Albertson et al. 2005; Michaux, Chevret, and Renaud 2007; Leandro R Monteiro and Nogueira 2010; Parsons, Márquez, and Albertson 2012) and predatory behaviors (Therrien 2005; Meloro et al. 2011). Island environments present suites of differences that could facilitate the evolution of the mandible, including shifts in food resources (Losos and Ricklefs 2009). Mandible morphology could potentially be shaped by selective pressures unique to the island environment. Changes to mandibular morphology could have important implications to the function, performance, and fitness of the organism (Babiker and Tautz 2015).

Divergence of mandible form has been well documented in island populations of house mice and other Murine rodents (Berry 1964; Berry and Jakobson 1975a; Berry, Peters, and Aarde 1978; Davis 1983; Berry 1986; Scriven and Bauchau 1992; Michaux, Chevret, and Renaud 2007; Renaud and Auffray 2010; Babiker and Tautz 2015). This is in part due to their widespread distribution and successful colonization of a diverse array of island environments (Bonhomme and Searle 2012), allowing for patterns of microevolution to be studied extensively (Pergams and Ashley 2001). Island house mice often display increases in mandible size (Berry, Jakobson, and Peters 1978; Davis 1983) and exhibit distinct shapes (Berry, Jakobson, and Peters 1978; Davis 1983; Scriven and Bauchau 1992; Renaud and Auffray 2010; Boell and Tautz 2011; Renaud et al. 2013; Babiker and Tautz 2015) compared to mainland populations. In a study investigating patterns of evolution across wild house mouse populations, the populations with the highest levels of mandible divergence were those on islands (Boell and Tautz 2011). Common shape differences associated with the island mandible form across populations from multiple island groups include a narrowing of the proximal end of the mandible (ascending ramus) and a more robust distal region (alveolar region; Davis 1983; Renaud et al. 2013).

Relationships between mandible morphology and ecological niche have been characterized at both the between-species and intraspecific level in rodents (Caumul and Polly 2005; Monteiro and dos Reis 2005; Perez et al. 2009). This includes linking morphological changes of the island mandible form with changes in diet (Renaud and Auffray 2010; Babiker and Tautz 2015). Mice on the Piana islet of Corsica in the Mediterranean exhibit an elongation of the condyle, which may be due to a shift in the type of food available, which consists of softer foods, such as tender plant material and invertebrates (Renaud and Auffray 2010). Similar plastic changes of the mandible were identified when laboratory strains were raised on soft vs. hard food

diets (Renaud and Auffray 2010). Mice on Heligoland Island near Germany also display mandible characteristics that suggest a shift towards a carnivorous and/or insectivorous diet, including the elongation of the mandible and condyle, and a robust angular process (Babiker and Tautz 2015). Although these studies provide a rich comparative framework for differences between island and mainland mandible forms, the genetic basis of mouse mandible evolution on islands is poorly understood. Additionally, very few studies of island populations have investigated how changes in morphology may affect function of the mandible (Renaud and Auffray 2010; Babiker and Tautz 2015).

Much is known about the mandible in laboratory strains of house mice (Atchley, Newman, and Cowley 1988), as it is an established model for the study of genetic and developmental mechanisms of morphological variation (Atchley and Hall 1991b; Chen et al. 1989; Corner and Shea 1995; McAlarney et al. 2001; Leamy, Routman, and Cheverud 2002; Klingenberg, Mebus, and Auffray 2003; Klingenberg 2004; Zelditch et al. 2008; Keller, Huet-Hudson, and Leamy 2008; Klingenberg, Navarro, and Pialek 2012; Leamy et al. 2015). The mandible is a complex skeletal structure, partitioned into two developmental modules, the ascending ramus and the alveolar regions (Atchley and Hall 1991b). These regions are influenced by growth patterns and morphogenesis within their individual functional units. Suites of genetic, biomechanical, hormonal, and dietary factors have been shown to influence mandible form (Atchley, Plummer, and Riska 1985a). Genetic loci responsible for size and shape variation of the mandible have been identified (Cheverud, Routman, and Irschick 1997; Leamy, Routman, and Cheverud 1997; Mezey, Cheverud, and Wagner 2000; Klingenberg and Leamy 2001; Klingenberg et al. 2001b; Ehrich et al. 2003b; Christians et al. 2003; Klingenberg 2004; Christians and Senger 2007; Kenney-Hunt et al. 2008; Leamy et al. 2008; Suto 2009; Boell

2013; Pallares et al. 2015). Through examining the spatial patterning and distribution of effects of genetic loci based on traits measured from different regions of the mandible, loci identified were found to be restricted to either the ascending ramus or the alveolar region of the mandible (Cheverud 1997; Mezey et al. 2000; Klingenberg and Leamy 2001; Klingenberg et al. 2001), along with loci found to influence morphology of the whole mandible (Cheverud 1997, Klingenberg et al. 2001).

Studies have identified morphological characteristics of the mandible that are predicted to affect aspects of jaw performance, particularly maximum bite force (Hylander 1979; Demes and Creel 1988) and maximum gape (Herring 1974, Vinyard et al. 2003) The ability of the jaw to open or to deliver a bite are vital to an organism's ability to capture prey and process food (Herring et al. 1972; Herring 1974; Hylander 1979; Emerson and Radinsky 1980; Smith 1984; Dumont and Herrel 2003; Vinyard et al. 2003; Vinyard and Payseur 2008). The masseter muscle is a primary jaw muscle that is highly positively correlated with bite force, as it is the major muscle involved in biting (Bakke et al 1992; Raadsheer et al. 1999). Changes in masseter size, morphology, and location on the jaw has been shown to affect the maximum bite force an organism can deliver (Herring 1974; Raadsheer et al. 1999; Herrel et al. 2008; Williams, Peiffer, and Ford 2009). In nature, variation in bite force and jaw gape may be due to selection acting on these performances and their correlated morphologies (Vinyard and Payseur 2008).

Although an extensive amount of knowledge has been gained from studies utilizing laboratory strains of house mice, studies on the genetics of mandible morphology in natural populations are limited (Pallares et al. 2014). Additionally, much of the research on jaw performance and biomechanics has been in the context of human and primate models (Hylander 1979; Richard J. Smith 1984; Hirsch et al. 2006; Vinyard et al. 2011; Terhune et al. 2015), and

the house mouse has not been fully utilized as a model for studying the genetics and evolution of functional morphology and jaw performance (Vinyard and Payseur 2008).

In this study, we use a population of wild house mice from Gough Island mice to investigate the functional morphology and genetic basis of rapid mandibular evolution in nature while taking advantage of the expansive knowledge and resources of the house mouse model.

Gough Island, a remote island located near the center of the South Atlantic Ocean, is home to the world's heaviest known wild house mouse (Rowe-Rowe and Crafford 1992). Gough Island mice have approximately doubled their body weight since colonizing the island less than 200 generations ago (Jones et al. 2003; Gray et al. 2014; Gray et al. 2015). They also underwent a correlated expansion of the skeleton (Parmenter et al. 2016). Additionally, there is evidence of shape change in the Gough Island skeleton, most notably in the elongation of the skull (Parmenter et al. 2016). The elongation of the skull suggests that the mandible has undergone changes in shape. It is possible that these changes may have been shaped by selective pressures unique to their island environment.

The ecology of Gough Island is distinct from continental Western Europe, the likely origin of Gough Island mice (Gray et al. 2014). The island flora and fauna are distinct, which affects the diet of Gough Island mice (Wace 1961; Rowe-Rowe and Crafford 1992; Ryan, Cooper, and Glass 2001). Their diet consists primarily of plant material and earth worms throughout a large portion of the year (Jones, Chown, and Gaston 2002), however during the austral summer the majority of their diet is composed of avian material, as they are known to prey on nestling chicks belonging to a variety of seabird species (Ryan et al. 2001; Jones, Chown, and Gaston 2002). Both earth worms and live birds are not preferred food sources for

most wild populations of mice (Roux et al. 2002). These novel dietary conditions may have facilitated mandible size and shape evolution in mice on Gough Island.

Our approach utilizes comparisons between Gough Island mice and a representative mainland strain, WSB/EiJ, to identify patterns of divergence in mandible size and shape. We also use a biomechanical approach to assess divergence in jaw performance. By investigating aspects of mandible and masseter morphology predicted to affect jaw performance, we identified traits that may be functionally related to the evolution of jaw performance divergence in Gough Island mice. Through quantitative approaches we identified genetic loci that underlie changes in mandible morphology. By combining quantitative genetic analysis and functional approaches we provide novel insights into our understanding of mandible evolution in a natural population.

Materials and Methods

Gough Island and its mice

Gough Island is part of the United Kingdom Overseas Territory of Tristan da Cunha and is located in the South Atlantic Ocean approximately halfway between South America and South Africa (40° 19'S and 9° 55'W). Fifty mice live trapped on Gough Island in September 2009 were transferred to the Charmany Instructional Facility in the School of Veterinary Medicine at the University of Wisconsin-Madison. Upon their arrival, 46 mice (25 female and 21 male) were used to establish a breeding colony.

All Gough Island mice (subsequently abbreviated GI) used in this study were housed at the University of Wisconsin-Madison Charmany Instructional Facility (Madison, WI). Female and male mice were housed separately in micro-isolator cages with a maximum of four mice per cage. Ground corn cobs (1/8th inch; Waldschmidt and Sons, Madison, WI) were used as bedding; nesting material and irradiated sunflower seeds (Harlan Laboratories, Madison, WI) were provided for enrichment. The room was temperature controlled (68-72 °F) and set on a 12-hour light/dark cycle. Water and rodent chow (Teklad Global 6% fat mouse/rat diet; Harlan Laboratories, Madison, WI) was provided ad libitum. Breeding individuals were fed breeder chow (Teklad Global 19% protein/9% fat; Harlan Laboratories, Madison, WI) ad libitum. All mice were weaned between 3 and 4 weeks of age.

Intercross experiments

Two partially inbred lines of GI mice were generated through full-sib mating for 4 filial generations, a procedure expected to reduce within-line heterozygosity (Silver 1995). One pair of male and female siblings from each partially inbred line was crossed with WSB/EiJ

(subsequently abbreviated as WSB; Jackson Laboratories, Bar Harbor, ME) to generate four independent F2 intercrosses (see Gray et al. 2015; Parmenter et al. 2016; Figure S2.1). F2 analyses of the mandible focused on 768 mice: 354 from Cross A (WSBxGI=199 and GIxWSB=155) and 366 from Cross B (WSBxGI=214 and GIxWSB=152).

Landmark analysis

All F2 mice were weighed at 16 weeks of age, and then euthanized by either CO_2 asphyxiation or by decapitation. GI and WSB mice were also phenotyped (GI N = 30; WSB N = 22). Only 7 and 6 GI and WSB were weighed at 16 weeks of age, respectively. Body weight at 16 weeks was estimated for the remaining GI and WSB mice based on their age using known GI and WSB growth curves (Gray et al. 2015). All euthanized mice were stored at -80°C. Euthanized mice were sent to Northeast Ohio Medical University (NEOMED, Rootstown, OH) for further processing.

Mice were skeletonized using dermestid beetles in a colony at NEOMED by Christopher Vinyard and Sara Weigel. Mandibles were isolated and 2D digital images were taken of lateral and medial views of each hemimandible. Sixteen landmarks (x, y coordinates) were chosen in order to capture the outline of the mandible (see Figure 3.1). Fourteen of these landmarks are previously characterized landmarks used to derive shape information from the house mouse mandible (Klingenberg, Mebus, and Auffray 2003). Two additional landmarks were used to generate Euclidean distances that estimate aspects of jaw performance. Landmarks were digitized from the lateral view of the left hemimandible for each animal using ImageJ (Scheider et al. 2012). Landmark and Euclidean distance data was collected by Jacob Nelson. All pairwise

Euclidean distances (n=120) were measured to the nearest 0.01 millimeter from landmark coordinate data using the Euclidean distance equation:

$$(dist(x, y) = \sqrt{\sum_{i=1}^{n}(x_i - y_i)^2}).$$

Geometric Morphometric Analyses

All geometric morphometric analyses were implemented in MorphoJ (Klingenberg 2011). Landmark coordinates for all mandible specimens were aligned using Procrustes superimposition, which removes variation due to size, location, and rotation, leaving only shape variation for further analyses. Procrustes-fit landmarks are referred to as Procrustes coordinates. Centroid size, defined as the square root of the sum of squared distances of a set of landmarks from their centroid, was generated for each specimen prior to Procrustes analysis.

To identify aspects of mandible shape variation that best distinguish among strain and sex, Canonical Variates Analysis (CVA) was applied to Procrustes coordinates. Statistical significance was determined using permutation tests of pairwise distances between groups. CVA was performed using strain and sex as a priori groups and 10,000 permutations were performed to determine statistical significance. Shape variation underlying each CV was then visualized as a deformation of landmark points in shape space, revealing group differences in shape.

Using the full set of Procrustes coordinates, the covariance matrices for F2s were generated in order to perform Principal Component Analysis (PCA). PCA was used to identify major features of mandible shape variation in the F2 population.

Potential outliers were examined using the Find Outliers function in MorphoJ. When it was concluded that outliers reflected reduced measurement accuracy caused by degraded or

damaged mandibles, they were removed. This included a small number of landmark data points of GI, WSB, and F2 specimens (1, 1, and 34 data points, respectively).

Jaw performance

To evaluate jaw performance, I measured maximum bite force and maximum passive jaw gape in 25 WSB (10 female and 15 male) mice and 23 partially inbred (12 filial generations inbred) GI mice (14 female and 9 male) from cross B. All bite force tests were performed using live animals at 16 weeks of age. Christopher Vinyard provided training and equipment for bite force and gape procedures. Bite force was measured at the incisor using a custom-made bite force transducer designed after Dechow and Carlson (1983). The transducer consists of two aluminum beams, each instrumented with two single-element strain gauges (TML UFLA-1-350-11-3LT). The four strain gauges are connected in a Wheatstone bridge. The beams are mounted parallel to each other using adjustable screws. Deformation of the beams results in a proportional change in resistance in the gauges and subsequently, in the voltage output in the Wheatstone bridge. One end of each beam served as the bite plate and was covered with a rubber coating to protect the animals' teeth from injury.

Prior to bite force tests, an anesthetic (50-100 mg/kg ketamine/0.5-1.0 mg/kg dexmedetomidine) was administered via intraperitoneal injection. Needle electrodes (30 gauge) were inserted into both masseters and anterior temporalis muscles. Electrodes were attached to a Grass stimulator to provide an electrical pulse that stimulated the jaw muscles. The transducer was placed onto the tip of the incisors of the animal and forces elicited by the jaw muscles were recorded when stimulated. Jaw muscles were stimulated for 400 milliseconds (ms) at a repeated rate of 40 Hz with each repetition lasting between 15-25 ms.

To determine the maximum jaw muscle stimulation, stimulations began at a low voltage while recording the bite force data output. The voltage was continually increased over small increments (1-2 volts) until no increase in bite force was detected after an increase in voltage. After determining the appropriate voltage, 2 sets of 3 stimulations were given and maximum bite force was recorded. Stimulations between each set were separated by one-minute intervals to limit muscle fatigue. We were unable to collect bite force data for three WSB animals due to the failure of the mice to go completely under anesthesia during the procedure.

After bite force collection, maximum passive gape was measured either while the animal was still under anesthesia or immediately after euthanasia prior to postmortem rigor. Maximum passive gape was measured to the nearest 0.01 millimeter by manually opening the jaws to their maximum passive motion and recording the linear distance between the upper and lower incisors using digital calipers (Wall 1999). Animals were euthanized by CO_2 asphyxiation and stored at -80°C until further processing.

Jaw performance estimates

A subset of the Euclidean distances in this study can be used to characterize leverage, movement, and load resistance (Herring et al. 1972; Herring 1974; Jablonski 1993; Vinyard et al. 2003). Distances were adjusted for body weight (trait/body weight$^{1/3}$) in order to make direct comparisons of mandible differences between strains. The cross-sectional area (CA) at the M1 where the corpus begins to thin into the diastema is an estimate of load resistance. Thirty GI (17 female, 13 male) and 24 WSB (13 female, 11 male) mandibles were μCT scanned at 70kVp/114mA in a vivaCT 70 scanner (Scanco) at 20.5μm voxel resolution. Scans were output as 2048x2048 tiff images and cropped to relevant anatomical regions in Adobe Photoshop

(CS3). Stacked tiff images were imported into Avizo software (FEI) where digital reconstructions were re-sliced at the M1 to provide images for cross-sectional analysis. Cross-sectional measurements were calculated from the resulting images using the MomentMacro plugin in ImageJ. All μCT scans, reconstructions, and cross-sectional data collection were performed by Christopher Vinyard and Sara Weigel. See Table 3.3 for detailed descriptions of the jaw performance estimates.

Characteristics of the masseter muscle are also predicted to affect jaw performance. To estimate aspects of relative masseter stretch, the ratio of masseter attachment points was measured. The masseter attachment ratio is the ratio of the condyle-superior masseter attachment distance to the condyle-inferior masseter attachment distance. Prior to masseter dissection, superficial tissue was cut away from the head and 2D digital images were taken of each side of the head. Jaw lengths (defined as the distance from landmark 1 to landmark 7) were measured from the exposed mandibles to the nearest 0.01 millimeter using digital calipers. The attachment points (superior, inferior, and condyle) were digitized using ImageJ. The distance from the condyle to the superior attachment point and the distance from the condyle to the inferior attachment point were measured to the nearest 0.01 millimeter from the landmark data using the Euclidean distance equation. Masseter weights were collected from euthanized GI and WSB animals used for bite force and gape tests. The left and right masseter muscles of each animal were dissected cleanly away from the mandible using surgical spring scissors. The masseter muscles were weighed to the nearest 0.001 gram and stored in formalin jars at room temperature. The left and right masseter weights from each animal were averaged prior to analysis. All masseter phenotypes were adjusted for both body weight and jaw length prior to analysis.

Genotyping

All F2 mice were genotyped using the Mega Mouse Universal Genotyping Array (MegaMUGA; Geneseek, Lincoln, NE), an Illumina array platform containing 77,800 single nucleotide polymorphisms (SNPs), along with some structural variants and transgenic markers. The markers are densely and relatively evenly spread throughout the mouse genome, with an average spacing of 33 kb (Threadgill and Churchill 2012). Liver tissue from the F2 population and the GI and WSB parents of the cross were sent to Geneseek (NeoGene Corporation) for DNA extraction and genotyping. The use of controls and the examination of errors are described in Chapter 2 and Parmenter et al. (2016).

QTL mapping

Single-trait QTL analyses were performed using Haley–Knott regression (Haley and Knott 1992) on a 0.5-cM grid across the genome, as implemented in R/qtl (Broman and Sen 2009). Analyses were conducted for (1) the thirty Euclidean distances exhibiting greater than 20 percent divergence between GI and WSB (includes the 9 estimates of jaw performance) (2) centroid size and (3) each principal component from the PCA performed for F2 mandible shape. Sex and parental grandmother (pgm) were used as additive covariates for all QTL models. Genome-wide significance thresholds were determined by permutation (Churchill and Doerge 1994), with adjustments for the X chromosome (Broman et al. 2006). Numbers of permutations were 10,000 and 180,000 for the autosomes and the X chromosome, respectively. A QTL was considered significant if its maximum LOD score met a 5% genome-wide significance threshold. Additional single-trait scans were performed for Euclidean distances using two different methods to control for effects of body size: (1) by using relative distances as traits and (2) by treating

body weight as an additive covariate in the model. Relative distances were calculated by dividing each Euclidean distance by the cube root of body weight for each individual (distance/body weight$^{1/3}$) and is referred to as the shape ratio (Mosimann 1970; Jungers *et al.*1995). The use of shape ratios accounts for the isometric component of body size, while maintaining allometric (size correlated) shape and non-allometric (size independent) shape. Alternatively, the treatment of body weight as a covariate accounts for both isometric shape and allometric shape, leaving only non-allometric shape.

Genetic effects

QTL effects include both additive and dominance effects. Additive effects were calculated as half the difference in genotype means between the GI and WSB homozygotes. Dominance effects were calculated as the difference between the genotypic mean of the GI/WSB heterozygote and the average genotypic mean of the GI and WSB homozygotes. To compare effects across traits of varying sizes, additive effects were standardized by dividing the additive value by the phenotypic SD (a/SD), and dominance effects were standardized by dividing the dominance effects by the additive effects (d/a).

Results

Phenotypic divergence in mandible size

Gough Island mice have larger mandibles than WSB, with the GI mouse mandible exhibiting a significantly larger centroid size than WSB (ANOVA; P-value < 0.001; Table 3.1). Additionally, nearly all Euclidean distances between landmarks show significant expansions in the GI mandible (t-test; females: maximum P-value < 0.03; males: maximum P-value < 0.04; Table S3.1). Thirty Euclidean distances show a greater than 20% expansion in GI mandibles relative to WSB (t-test; maximum P-value < 0.001; Figure 3.2 and Table S3.1). These distances were used for the remaining analyses due to their high level of divergence between the island and mainland strains. A higher proportion of distances within the ascending ramus and those found across the two regions ("trans-regional") have diverged significantly compared to those in the alveolar region (Table S3.1).

There are notable differences between the sexes. A higher number of Euclidean distances exhibit significant differences between GI and WSB for males than for females (94% in males and 87% in females; Figure 3.1B). Most of these distances involve landmark 5 and are height dimensions of the ascending ramus. Centroid size also displays significant sex effects: males are larger than females in GI and WSB (P-value = 0.002; Table 3.1).

Phenotypic divergence in mandible shape

The GI and WSB mandible exhibit significant shape differences. CVA of Procrustes coordinates resulted in the extraction of 100 percent of mandible shape variation. The first canonical variate (CV1) accounted for 90% of shape variance and was principally associated with the separation of strains as illustrated by the resulting Mahalanobis distances (Table 3.2 and

Figure 3.3A). The shape changes associated with CV1 are visualized as deformations of landmarks in shape space (Figure 3.3C). Compared to WSB, GI display deformations primarily in the widening and shortening of the condyle (landmarks 7 and 8), a narrowing and elongation of the angular process (landmarks 10 and 11), and a deepening of the depression between the angular process and the incisor ramus (landmarks 12 and 13; Figure 3.3C). The majority of these shape differences are within the ascending ramus.

CV2 accounted for 8% of shape variance and is principally associated with the separation of the sexes (Figure 3.3B). Compared to males, females display a narrowing of the space between the condyle and coronoid, along with an elongation of the coronoid (landmarks 4 and 5), a shortening of angular process (landmarks 10 and 11), and a narrowing of the incisor alveolus (landmarks 1 and 12; Figure 3.3D). CV3 accounted for the remaining 2% of variation (Figure S3.1), contributing little to the total shape variation. These shape changes that have occurred in localized regions of the GI mandible may have led to changes in the function or performance of the jaw of Gough Island mice.

Direct measures of divergence in jaw performance

GI mice exhibit a larger bite force than WSB (ANOVA; P-value < 0.001; Figure 3.4 and Table S3.2). After corrections for either body weight or jaw length, GI mice retain a relatively larger bite force (ANOVA; P-value = 0.001; P-value = 0.004, respectively). GI mice exhibit a larger maximum gape than WSB (ANOVA; P-value = 0.001). However, GI mice show no significant divergence in maximum gape after correcting for either body weight or jaw length (ANOVA; P-value = 0.25; P-value = 0.09, respectively). There are no significant effects of sex on maximum bite force and gape (ANOVA; minimum P-value = 0.06; Table S3.2), except for bite force relative to jaw length (ANOVA; P-value = 0.01; Table S3.2).

Morphological measures of jaw performance

Some aspects of mandibular morphology are predicted to affect maximum bite force and maximum passive gape, which are described in Table 3.3. All 9 Euclidean distances predicted to affect performance show significant expansions in the GI mandible (t-test; maximum P-value = 0.0007; Table 3.3). After adjusting for body weight, four functional estimates remain significant, including corpus depth (L3-12), symphysis length (L1-13), temporalis load arm length (L8-4), and condyle length (L6-7; t-test; maximum P-value = 0.001; Table 3.3). All four of these distances are larger in GI than WSB. Two of these distances are predicted to increase load resistance, and therefore may be associated with the divergence of jaw performance in GI mice. GI mice have a larger cross-sectional area (CA) at the M1. This suggests that load resistance is increased, and therefore may be associated with the relatively larger bite force of GI mice.

GI mice have heavier masseters than WSB (ANOVA; P-value < 0.001; Table 3.3). However, WSB exhibit relatively heaver masseters after adjusting for either body weight or jaw length (ANOVA; P-value = 0.01, P-value = 0.02, respectively; Table 3.3). The masseter attachment ratio quantifies the level of jaw-muscle stretch, which is predicted to limit maximum gape (Herring 1974). There are no significant strain or sex differences in the masseter attachment ratio between GI and WSB (ANOVA; strain: P-value = 0.48; sex: P-value = 0.46; Table 3.3). These results suggest that masseter morphology does not explain observed divergence in maximum bite force or maximum gape between GI and WSB mice.

Shape variation in the F2 population

The majority of Euclidean distances exhibit significant sex and parental grandmother (pgm) effects (ANOVA; sex: maximum P-value = 0.04; pgm: maximum P-value = 0.04; data not

shown), and were therefore used as additive covariates in all subsequent QTL models. Principal components analysis (PCA) of Procrustes coordinates revealed that PC1 accounts for 17 percent of the total variance in mandible shape within the F2 population (Figure S3.2). PC 1-5 account for over half of the variance in mandible shape. Although PCA captures a modest amount of F2 shape variation, a common set of landmarks contribute to the variation underlying PC 1-5. These are mostly x-axis components of landmarks found primarily in the ascending ramus, including landmarks within the condyle, angular, and coronoid processes (Figure S3.2). Thus, a significant portion of mandible shape variation among the F2 population is localized to the ascending ramus and represents horizontal shifts in shape.

QTL mapping of mandible size

A total of 77 genotype-phenotype associations were identified for nearly all 30 Euclidean distances exhibiting high levels of divergence measured across the GI mandible (except for L2-3, L11-16, L2-11, and L3-11; Figure 3.5A and Table S3.3). Multiple QTL are detected for all traits, with the exception of L11-12. An average of 2.6 QTL were identified per trait. QTL were found across most chromosomes (except for chromosomes 5, 8, 18, 19, and X). A large portion of QTL co-localize based on overlapping confidence intervals. Nearly half of all QTL are found on chromosomes 10 and 11 and span the entire mandible (Figure 3.5A). Additionally, two QTL were identified for centroid size and also are located on chromosomes 10 and 11 (Figure 3.6). These highly co-localizing QTL are potentially pleiotropic and may act as global regulators of mandibular growth.

Mandibular regions also show differences in their genetic architectures. A higher proportion of unique QTL are found for traits within the alveolar region than traits within the

ascending ramus. In fact, there are very few QTL that co-localize across traits within the alveolar region, suggesting that the alveolar region evolved as a distinct module. Trans-regional traits have relatively simple genetic architectures, with most QTL co-localized to chromosomes 10 and 11, suggesting that the evolution of overall length of the mandible is due to loci with global effects on size. The majority of the remaining QTL co-localize to a region on chromosome 12 and were identified for traits describing variation in expansion between the central region of the mandible to the end of the condyle. This suggests that a pleiotropic locus on chromosome 12 contributes to variation in the extension of the proximal end of the mandible.

Some QTL are restricted to traits found within particular mandibular regions. QTL on chromosomes 4, 9, and 15 are identified for distances located almost exclusively in the ascending ramus, all of which co-localize on their respective chromosomes (Figure 3.5A). These QTL contribute to variation in distances between the condyle and coronoid. QTL on chromosomes 4 and 9 also contribute to variation in the expansion from the central region of the mandible to the condyle and QTL on chromosome 15 also contribute to variation in the area between the condyle and the angular process. This supports the idea that three pleiotropic loci contribute to variation primarily located within the ascending ramus of the GI mandible. Other QTL contribute to variation in particular dimensions of the mandible. QTL on chromosomes 7, 15, and 16 predominately contribute to variation in height dimensions rather than length dimensions. Lastly, trait-specific QTL were identified, including those identified for symphysis height (L1-15; chromosome 1), a trans-regional length (L7-13; chromosome 3), a length within the ascending ramus (L8-16; chromosome 13), and the height between the minimum depression between the condyle and the angular process (L9-10; chromosome 14).

The standardized additive effects for the Euclidean distance QTL are small to moderate, ranging from 1 to 19% of the mean phenotypic differences between GI and WSB mice (Figure 3.5A and Table S3.3). The largest additive effect is 0.14 mm for jaw length (L1-7; chromosome 10 QTL and Table S3.3). There are large differences in additive effects depending on chromosomal location. The majority of QTL have positive effects, where a GI allele confers a larger size. However, nearly all QTL that have negative effects (where the GI allele confers a smaller size) are located on chromosomes 4 and 9, and all QTL on chromosomes 4 and 9 have negative effects (except for the QTL on chromosome 4 for L3-12; Figure 3.5A and Table S3.3). QTL for traits representing the elongation of the condyle primarily have negative effects, indicating the presence of GI alleles at these loci are associated with the shortening of the condyle. The effects of the chromosome 10 and 11 QTL for centroid size are both modest and additive (Table S3.3).

For distances adjusted for body weight, the resulting QTL patterns show notable differences. The majority of the QTL on 10 and 11 are no longer significant, evidence that these QTL contribute significantly to variation in mandible size (Figure 3.5B; Table S3.3). QTL on chromosome 4 and 9 are maintained and increase in number, spanning the entire mandible. A QTL on chromosome 9 was identified for nearly all 30 traits. A higher proportion (60%) of QTL exhibit negative effects for body weight-adjusted traits (Figure 3.5B; Table S3.3). The vast majority (67%) of negative effect QTL are located on chromosomes 4 and 9. Nearly all negative effect QTL affect body weight-adjusted traits localized to the ascending ramus or overall length dimensions (trans-regional traits), and are relatively smaller in GI mice or not significantly different from WSB (Table S3.3). This suggests that QTL with negative effects underlie traits that exhibit negative allometry between GI and WSB mice. In other words, these traits are not as

large in GI mice as expected based on their body size, indicating a change in shape, suggesting that QTL on chromosomes 4 and 9 likely contribute to aspects of shape variation in the ascending ramus and overall length of the GI mandible. When body weight is used as a covariate in the QTL model, the resulting QTL are similar in location and effects (Table S3.3), with the exception of a higher number of QTL identified on chromosome 12.

Standardized dominance effects are minimal for all Euclidean distance QTL (including unadjusted and weight-adjusted distances) except for a subset of the QTL that co-localize to chromosome 12, which confer moderate to strong dominance (Figure S3.3). When dominance was present, the GI allele was typically dominant to the WSB allele. Dominance appears to play a greater role for QTL on chromosome 12 than other QTL.

QTL mapping of mandibular shape

QTL were identified for almost all principal components (PCs) underlying variation in mandible shape, with an average of 3 QTL per trait (Table S3.3). QTL on chromosomes 4 and 9 were the most commonly identified for PCs 1-5, which harbors greater than half of mandibular shape variation. The traits contributing most to variation underlying PCs 1-5 were landmarks within the condyle, coronoid, angular process, and the incisor alveolus, suggesting that these QTL contribute to shape variation within these regions. Additionally, these QTL co-localize with QTL for distances on chromosomes 4 and 9, which are located in the same regions. Additionally, they also co-localize with the size-corrected distance QTL on chromosomes 4 and 9, providing evidence that these loci act in pleiotropy to contribute to shape variation in the GI mandible, particularly in the ascending ramus.

QTL mapping of jaw performance estimates

For relative Euclidean distances that represent estimates of jaw performance, there are both shared and distinct QTL identified based on the different categories of jaw performance: leverage, load resistance, and movement (Figure S3.4). For the four relative Euclidean distances that are significantly different between GI and WSB mice, QTL on chromosome 2 are found for all four traits across all performance categories. QTL on chromosome 9 are found exclusively for estimates located within the ascending ramus, representing a movement and leverage trait. A single QTL on chromosome 12 is identified for corpus depth (L3-12), a load resistance estimate. This is the only QTL found on chromosome 12 for relative Euclidean distances, suggesting that this QTL exclusively effects variation in corpus depth, which is predicted to affect load resistance of the mandible.

Discussion

The Gough Island mouse mandible is distinct from its mainland counterpart. The entire Gough Island mouse mandible has expanded. There is heterogeneity in the magnitude of expansion, indicating local regions of increased expansion. Overall length dimensions of the mandible are disproportionately represented among individual mandible traits showing highest divergence in Gough Island mice, illustrating that a major morphological change was the elongation of the mandible. Size traits showing high degrees of expansion were also concentrated in the ascending ramus region of the mandible. Additionally, this region was identified as a major region of shape divergence between Gough Island mice and mainland WSB, most notably the widening and shortening of the condyle and the narrowing of the angular process. These shape changes may have functional implications for Gough Island mouse jaw performance.

Previous studies identifying mandibular shape differences among island and mainland populations allow for illuminating comparisons. Notable differences in mandible shape of mice of North Atlantic Islands (including Shetland, Orkney, and Faroe Islands) and those from the British mainland were identified, including the narrowing of the ascending ramus and a more robust alveolar region (Davis 1983). Similar shape differences associated with the island mandible were identified in mice from the Sub-Antarctic Kerguelen Archipelago (Renaud et al. 2013). We find a similar pattern in the ascending ramus, however shapes within the alveolar region associated with Gough Island mouse mandibles are distinct from the island forms from these studies. Mice from Heligoland Island near Germany display an elongation of the condyle, a less robust angular process and an overall elongation of the mandible. It has been argued that these characteristics point towards an adaptation to a carnivorous or insectivorous diet (Babiker and Tautz 2015). Gough Island mice display similar patterns, including a narrower angular

process and elongation of the mandible, although Gough Island mice do not share similar condyle morphology with the Heligoland mice. Similarities in mandibular evolution among these island populations could reflect common adaptations to an island environment. On the other hand, differences among island populations could reflect patterns of local adaptation.

Mandible morphology is susceptible to environmental conditions, such as diet and age, and show plastic responses to changes in these conditions (Renaud and Auffray 2010; Renaud, Auffray, and de la Porte 2010; Boell and Tautz 2011). Environmental noise was minimized by utilizing age-staged mice and raising both strains on a common diet and uniform laboratory conditions. Additionally, uncovering loci contributing significantly to variation in mandibular morphology demonstrates that there is a large genetic component. It has been demonstrated that genetic effects are typically larger than any environmental effects in mandible variation among natural populations of rodents (Boell and Tautz 2011).

We identified QTL for mandible morphology that have region-specific effects and QTL that affect all regions of the mandible. We found that 53% of QTL were localized to the ascending ramus, 17% within the alveolar region, and 30% of QTL were found across both regions. Similar results were found in a study identifying QTL for mandible morphology between an F_2 intercross between LG/J and SM/J, laboratory strains that have been artificially selected for extreme size divergence (50% in the ascending ramus, 27% in the alveolar region, and 23% across the whole mandible; Cheverud 1997). Some Chromosomal locations of QTL are similar across the two studies, including QTL associated with traits spanning the whole mandible located on chromosomes 11 and 12, QTL associated with traits within the ascending ramus (on chromosomes 2 and 4), within molar, condyle, and coronoid processes (on chromosome 15), restricted to the molar and angular processes (on chromosome 17), and traits concentrated in the

condyle (on chromosome 9). There are also notable differences. One of the largest discrepancies is that QTL on 10 in our study are found across the whole mandible, but are restricted to molar and condyle in Cheverud 1997 study. Similarities in the distribution and location of QTL could reflect similar genetic and developmental pathways underlying correlated changes in mandibular morphology during selection on large body size. However, confidence intervals of the QTL are large, and therefore it is not possible to determine if QTL identified between the two studies are the same loci and these preliminary comparisons should be taken with caution.

Most of the variation in shape among the first five PCs is localized to the ascending ramus, along with the incisor region. Similar shape changes were identified in a study investigating mandible shape variation between the LG/J and SM/J strains (Klingenberg et al. 2004). Although QTL for principal components of mandible shape from the two studies exhibit similar distributions across the genome, the number of QTL and their locations differ. This suggests that the evolution of the mandible involved different genetic loci between Gough Island mice and the LG/J and SM/J strains.

Loci were identified for almost every PC for Procrustes coordinates of mandibular shape. This is a surprising result, as many of the PCs contribute very little to the total F_2 variation in shape and are therefore expected to not be very informative. This suggests that even a small amount of mandible shape variation can be explained by genetic loci with statistical confidence. This phenomenon has been seen in other studies investigating the genetic basis of mandibular shape in house mice (Boell 2013; Pallares et al. 2014).

The Gough Island house mouse has a larger bite force than expected for a mammal of its size. The relative increase in Gough Island mouse bite force could be associated with the relative increase in corpus depth and the increase in cross-sectional area of the corpus at the M1,

increasing mandible load resistance. The relative increase in bite force is likely not influenced by the majority of leverage and movement traits, due to their isometric scaling with body weight. Bite force and jaw gape are known to be negatively correlated (Dumont and Herrel 2003). The lack of divergence of relative maximum gape in Gough Island mice is therefore not a surprising result given their increased bite force. This lack of divergence could be associated with the isometric scaling of performance estimates predicted to affect gape. The divergence of relative condyle length and temporalis load arm length seen in Gough Island mice were not strong enough to confer significant changes in relative maximum gape. A more detailed analysis of jaw morphology and mechanics will be necessary in order to draw further conclusions.

The physiological maximum bite force measured in this study may not reflect the typical bite forces that mice on Gough Island exhibit in their natural environment. The physiological analyses may fail to link function with particular biological roles specific to the mouse's natural environment, which would limit our ability to understand their evolution (Lande and Arnold 1983; Wainwright, Reilly, and Reilly 1994). However, the quantification of physiological bite force still reflects possible consequences of changes to mandibular morphology of Gough Island mice.

Masseter weight is known to be positively correlated with maximum bite force (Bakke et al. 1992; Raadsheer et al. 1999). It is therefore surprising that Gough Island mice have relatively smaller masseters than WSB while also exhibiting a relatively larger maximum bite force. This suggests that the relative increase in bite force was not associated with aspects of masseter architecture measured in this study. A more detailed characterization of all major jaw muscle groups, along with their muscle fiber architecture, would allow us to better understand contributions of jaw musculature to jaw performance divergence.

The evolution of a larger bite force could have occurred in multiple ways. Bite force could have been directly targeted by selection, or may have increased as a correlated response to changes in mandibular morphology being targeted by selection. Changes in jaw performance could be related to the unique diet of the mice on the island. Aspects of jaw anatomy and performance have been compared between rodent populations that have adopted distinct diets (Satoh and Iwaku 2006; Michaux, Chevret, and Renaud 2007; Cox et al. 2012). Compared to the herbivorous deer mouse *Peromyscus maniculatus*, the carnivorous grasshopper mouse *Onychomys leucogaster* has an elongated jaw and a relatively larger bite force, without a correlated change in gape (Satoh and Iwaku 2006). These carnivorous adaptations are similar to those found in the Gough Island mice, and could be associated with the adoption of carnivory and predation on seabird chicks.

Our results provide indirect insights into the evolutionary causes of mandibular evolution in Gough Island mice. It is plausible that selection targeted body size, which resulted in a correlated response in skeletal and mandible size. QTL on chromosomes 10 and 11 were identified for traits across the entire mandible, and co-localize to regions containing QTL identified for body weight, growth rate, and a suite of skeletal size dimensions in previous studies using the same cross (Gray et al. 2015; Parmenter et al. 2016, see Chapter 2). The genetic control of overall organismal size by a small number of pleiotropic loci is potentially more likely for a population whose recent colonization suggests few genetic changes of large effect. However, we also detected additional loci associated with morphological variation within specific mandibular regions, which are distinct from those involved in global size regulation. This reflects a more complex genetic architecture. The recent colonization of mice on Gough

Island suggests standing variation as a source of genetic variation, which could explain the suite of unique QTL identified for mandible morphology.

Although we cannot directly address the link between jaw traits and diet in this study, there is evidence that differences in diet may be functionally related to mandible morphology. Mice from two Sub-Antarctic islands have been shown to share similar mandible morphologies that are distinct from mainland wild house mice, including the length of the coronoid process and the height of the ascending ramus (Boell and Tautz 2011). These mice have similar colonization times as Gough Island mice, arriving on the islands less than 200 years ago (Hardouin et al. 2010). These island mice have a unique diet, exhibiting a preference for earthworms, which are not a preferred food choice of most populations of mice (Le Roux et al. 2002), but interestingly make up a large portion of the diet of Gough Island mice (Jones, Chown, and Gaston 2003). There is also evidence that bird eating may increase mouse survival rates. Gough Island mice that exhibit high levels of predation on seabird chicks have a higher body mass and greater overwinter survival (Cuthbert et al. 2016). There is likely selection for these traits in order for mice to avoid high winter mortality rates, which is common among island populations (Cuthbert et al. 2016). Lastly, Gough Island mouse predatory behavior is unusual. Most mice on islands prey upon small-sized chicks (less than 50 grams) and target weak or sick animals (Wanless et al. 2007). However, Gough Island mice often attack healthy chicks, and in the case of the Tristan Albatross, is up to 300 times the size of the mice. Optimization of jaw morphology and performance to allow for the predation of large prey would be advantageous in this case.

Acknowledgements

We would like to thank Peter Ryan and Richard Cuthbert for arranging the trapping and shipment of mice from Gough Island to Wisconsin. We thank the staff at Charmany Instructional Facility for mouse colony maintenance and animal care. We thank Melissa Gray for her substantial contributions toward the generation of the F2 intercross, colony management, and phenotyping. We also thank Kaitlyn Sonnentag, Claire Walker, Erin Lalor, Megan Latsch, Hannah Van Rossom, Michelle Heal, and William Matzke for their dedication to mouse husbandry, phenotyping, and assistance in generating animals for our experiments. We also thank Dan O'Neal, Lauren Taylor, Shawn Mercer, Nathan Yu, and Graham Hughes for additional skeletonizing and phenotyping of mandibles. We also thank laboratory members Amy Dapper, Megan Frayer, April Peterson, and Jered Stratton for useful comments on the manuscript. We appreciate the support and stimulating scientific conversations provided by Payseur Lab members and alumni, including Amy Dapper, Megan Frayer, Peicheng Jing, Mark Nolte, April Peterson, Jered Stratton, and Richard Wang. This research was supported by National Institutes of Health (NIH) grant R01-GM100426A to B.A.P., a National Science Foundation (NSF) graduate research fellowship to M.D.P., and a dissertation completion fellowship provided by the University of Wisconsin-Madison Graduate School to M.D.P.

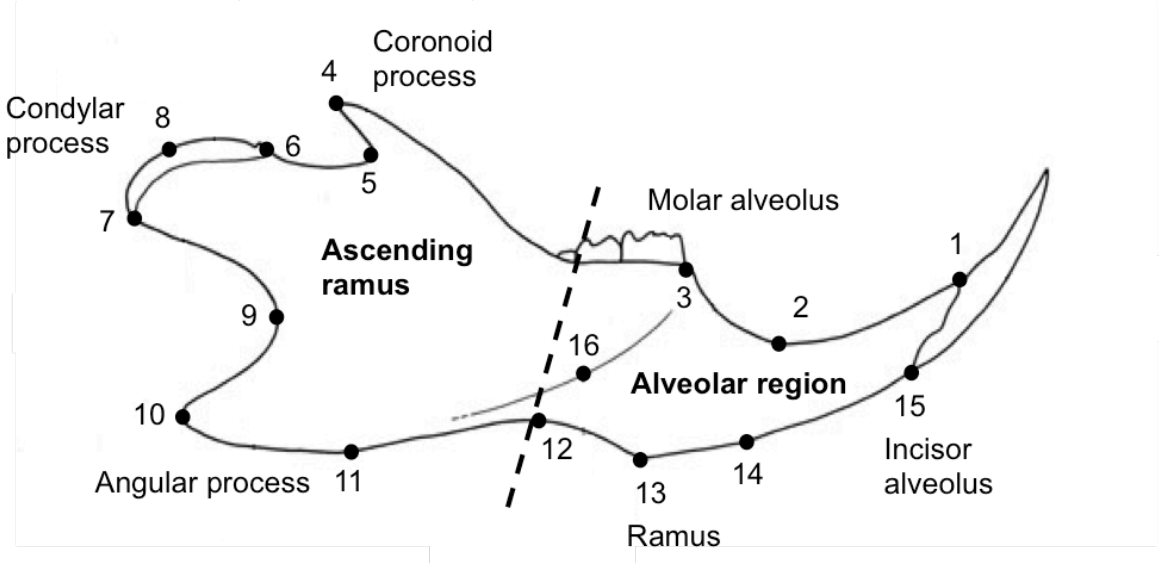

Figure 3.1 Diagram of mouse mandible and location of landmarks

Diagram of a house mouse mandible indicating the two major anatomical regions and positions of the 16 landmarks used in this study. Mandible diagram adapted from The Anatomy of the Laboratory Mouse (Cook 1965).

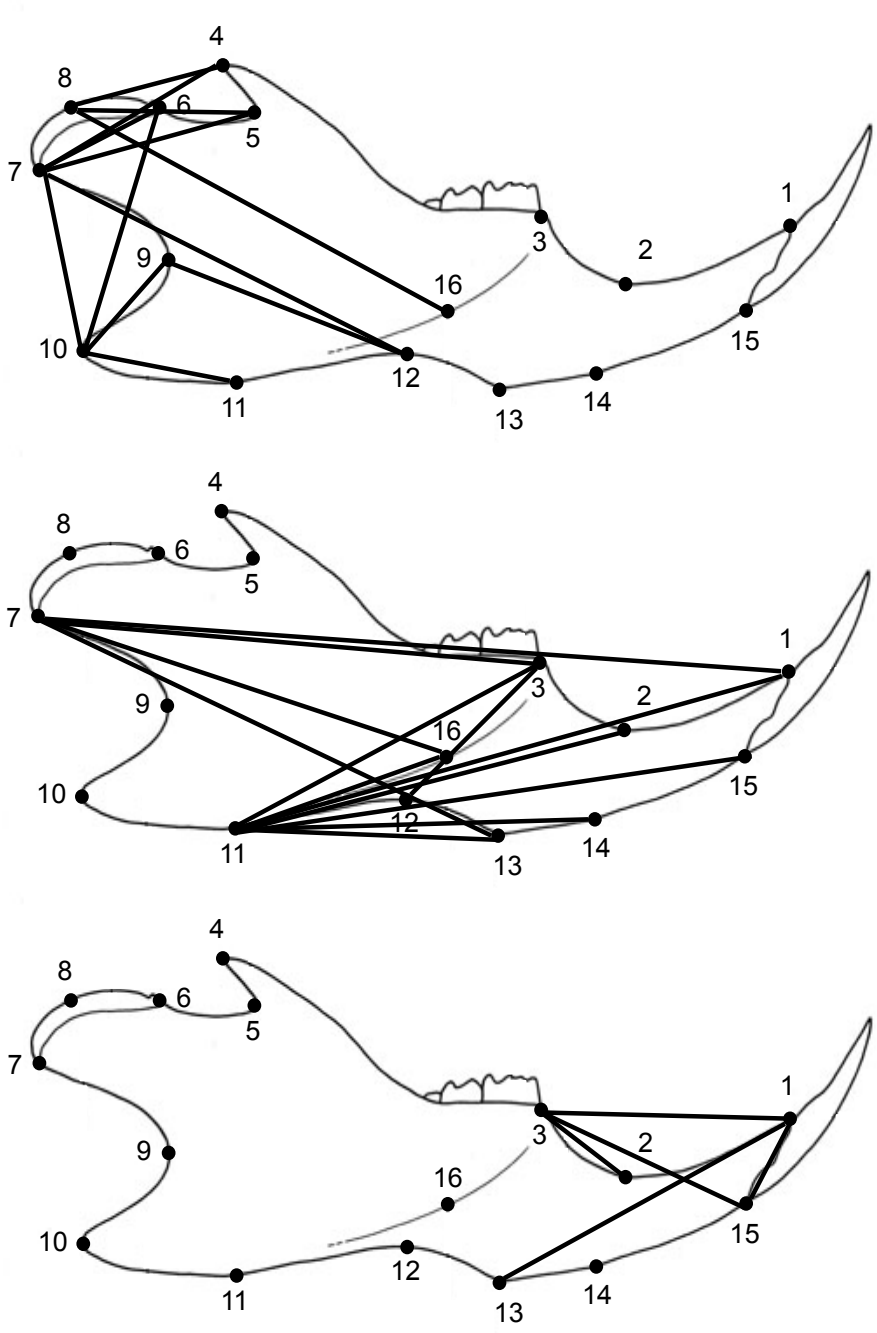

Figure 3.2 Locations of highly diverged Euclidean distances
Locations of all Euclidean distances that exhibit a greater than 20% difference between GI and WSB within the ascending ramus (top), the alveolar region (bottom), and across both regions, referred to here as “trans-regional” (middle). Mandible diagram adapted from The Anatomy of the Laboratory Mouse (Cook 1965).

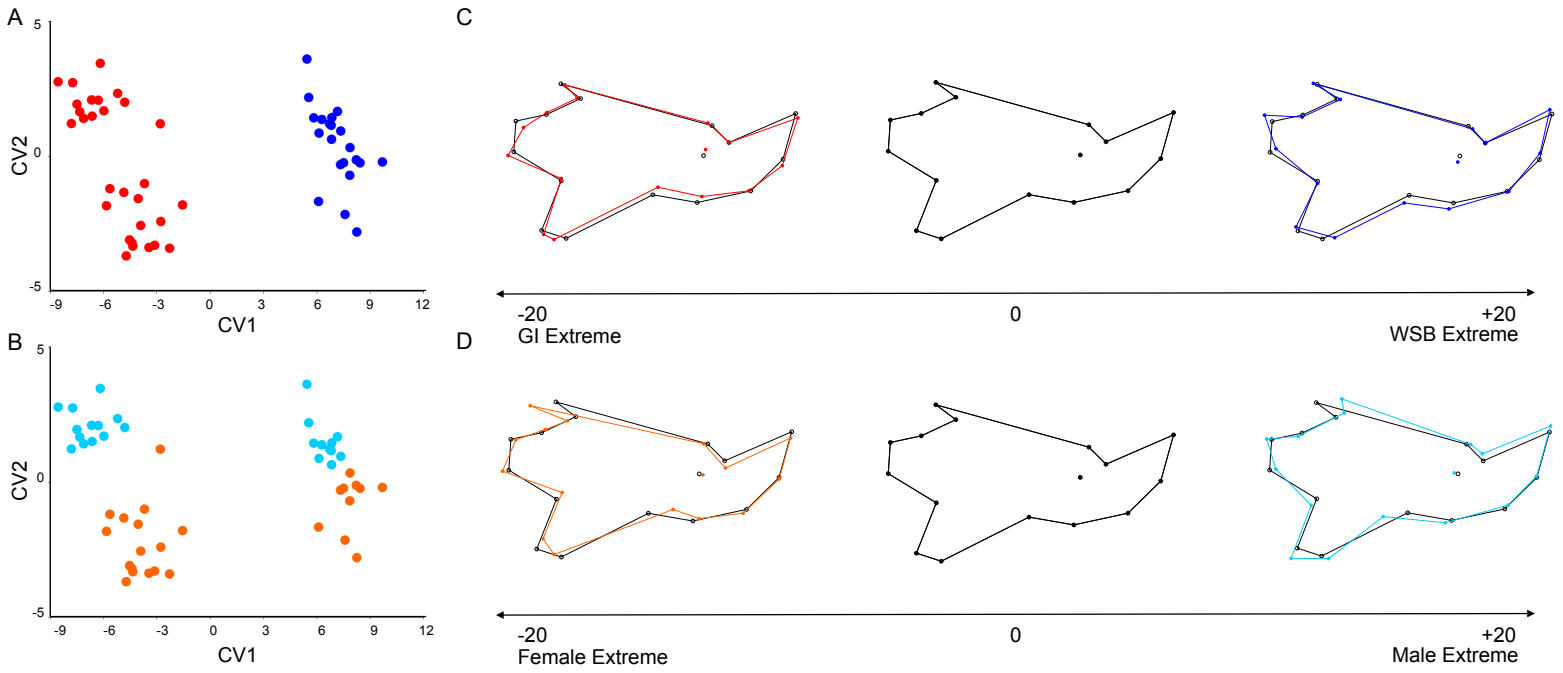

Figure 3.3 CVA of mandible shape

Plot of CV1 and CV2 scores for GI and WSB mandible specimens based on Procrustes coordinate data. CV scores are color-coded based on (A) strain: GI = red; WSB = blue, and (B) sex: females = orange; males = light blue. (C) Mandible shape variation associated with CV1 using wireframe deformations. Deformations represent the shape change along the CV1 axis, separating GI (wireframe at negative end of axis), WSB (wireframe at positive end of axis) and their mean (wireframe when CV1 score is zero). (D) Mandible shape variation associated with CV2 using wireframe deformations. Deformations represent the shape change along the CV2 axis, separating females (wireframe at negative end of axis), males (wireframe at positive end of axis) and their mean (wireframe when CV2 score is zero). Each deformation is exaggerated by 20 times.

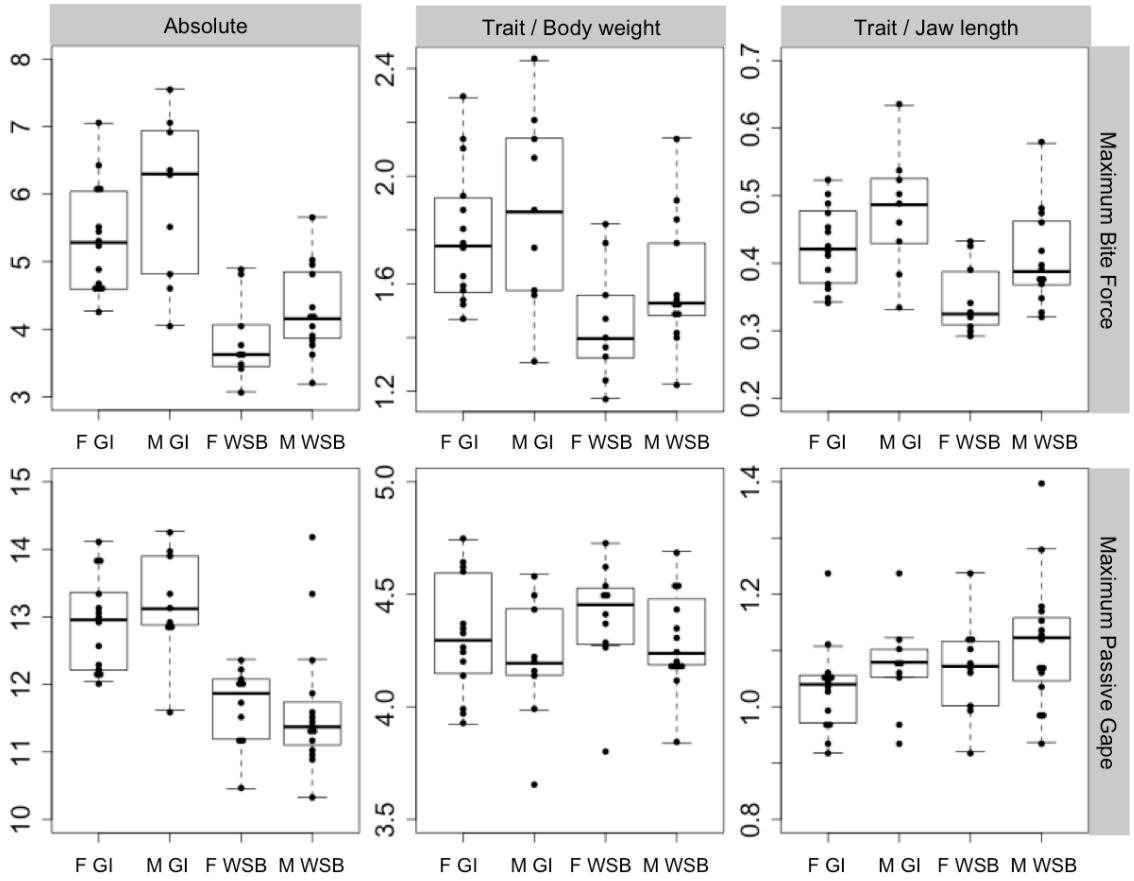

Figure 3.4 Maximum bite force and maximum passive jaw gape

Dotplots of maximum bite force and maximum passive gape for GI and WSB. Absolute trait values are reported for maximum bite force and maximum gape, along with trait values adjusted for body weight (trait/body weight$^{1/3}$) for maximum bite force and maximum gape, along with trait values adjusted for jaw length (trait/jaw length) for maximum bite force and maximum gape. F = females and M = males.

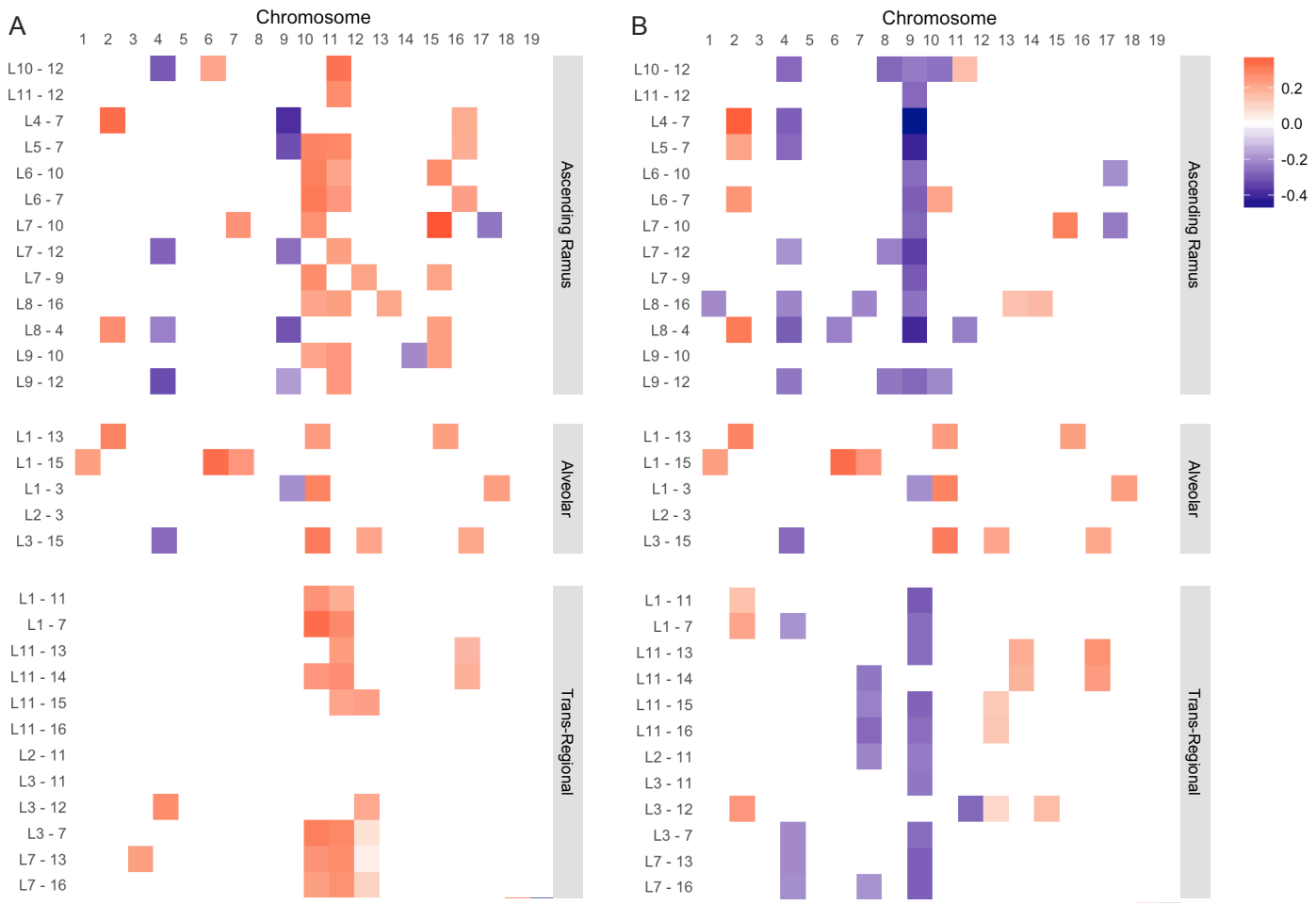

Figure 3.5 Chromosomal locations of QTL for mandible traits

Locations of all significant QTL identified for absolute (A) and relative (B) Euclidean distances. Relative distance is defined as the distance divided by body weight$^{0.33}$. Heat map colors represent the standardized additive effect (a/SD) of each QTL. A positive effect is represented in red and a negative effect is represented in purple. The depth of color indicates the magnitude of the effect.

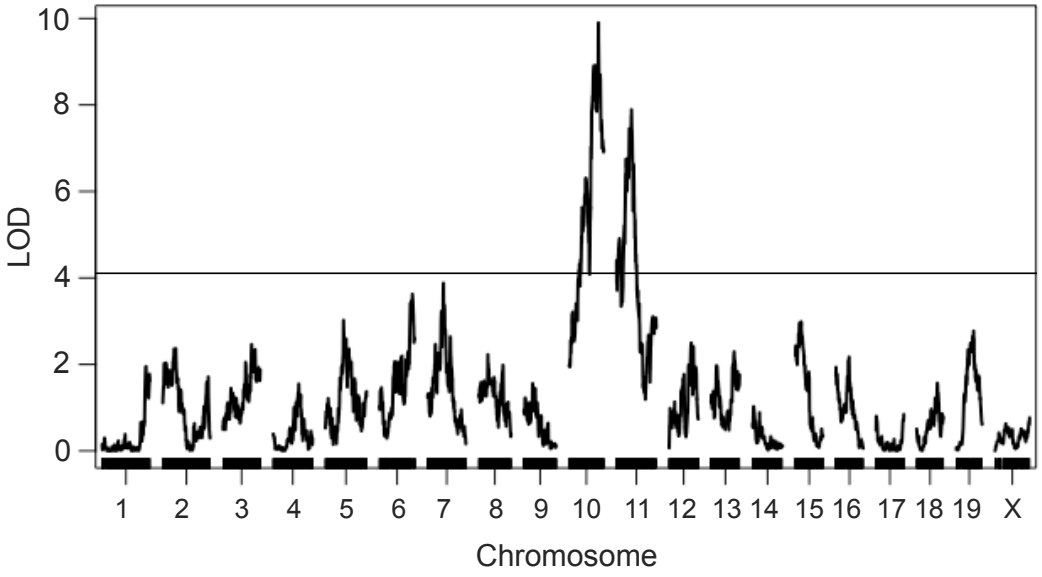

Figure 3.6 Centroid size QTL

QTL scan of centroid size. The 5% genome-wide significance threshold is indicated with a horizontal line.

Table 3.1 ANOVA table for centroid size

Variable	d.f.	MS	F	P
Strain	1	869573	230.13	< 0.0001
Sex	1	40319	10.67	0.002
Strain x Sex	1	637	0.17	0.683
Residuals	48	3779		

ANOVA table demonstrating significant divergence in centroid size between GI and WSB mice.

Table 3.2 Mahalanobis distances and Procrustes distances from CVA

	GI F	GI M	WSB F	WSB M
GI F	-	5.27*	11.95*	10.99*
GI M	0.0198*	-	14.93*	13.31*
WSB F	0.0397*	0.0424*	-	3.63*
WSB M	0.0408*	0.0365*	0.0185	-

Mahalanobis distances (above the diagonal) and Procrustes distances (below the diagonal) from canonical variate analysis (CVA) for GI and WSB Procrustes coordinates with sex and strain as a priori groups. P-values are based on permutation testing (1000 replicates). Statistical significance (P-value < 0.05) is indicated with an asterisk.

Table 3.3 Estimates of jaw performance

Trait Name	Trait	Predicted change to jaw performance	GI Average	GI SD	WSB Average	WSB SD	P
Leverage							
Jaw length	L1-7	Gape increases and bite force decreases with increase in trait due to increased jaw leverage	13.65 (4.52)	0.47 (0.27)	11.47 (4.57)	0.48 (0.29)	<0.0001 (0.5268)
Molar load arm	L3-7		9.57 (3.16)	0.36 (0.19)	8.12 (2.93)	0.30 (0.73)	<0.0001 (0.1967)
Masseter lever arm	L7-16		9.16 (3.03)	0.39 (0.20)	7.63 (3.03)	0.28 (0.22)	<0.0001 (0.9437)
Temporalis load arm	L5-7		4.10 (1.40)	0.30 (0.10)	3.37 (1.04)	0.12 (0.36)	<0.0001 (<0.0001)
Load Resistance							
Corpus depth	L3-12	Bite force increases with increase in load resistance traits. Traits are related to the amount of bone present at distal region of mandible and are predicted to correlate with load resistance.	4.14 (1.42)	0.19 (0.07)	3.84 (1.18)	0.17 (0.29)	0.0007 (0.0014)
Symphysis length	L1-13		6.18 (2.10)	0.27 (0.10)	5.53 (1.87)	0.27 (0.10)	<0.0001 (<0.0001)
Cross-sectional area at M1	CA		2.03	0.25	1.49	0.23	<0.0001
Movement							
Condyle length	L6-7	Gape increases with increased condyle length as rotation is increased	2.50 (0.50)	0.27 (0.06)	1.89 (0.42)	0.22 (0.11)	<0.0001 (0.0030)
Temporalis moment arm length	L8-4	Gape decreases with increased moment arm lengths due to an increase in muscle stretch	2.65 (0.91)	0.30 (0.09)	2.24 (0.85)	0.17 (0.29)	0.0006 (0.2750)
Masseter moment arm length	L8-16		8.98 (2.98)	0.32 (0.18)	7.95 (3.00)	0.42 (0.73)	<0.0001 (0.8343)
Masseter							
Masseter weight	MW	Bite force increases as masseter weight increases	0.09 (0.003) [0.036]	0.01 (0.001) [0.003]	0.06 (0.003) [0.04]	0.01 (0.001) [0.002]	< 0.0001 (0.01) [0.02]
Masseter attachment ratio	MA	Gape increases as ratio deviates from 1.0 due to reduction in muscle stretch	1.40	0.07	1.41	0.06	0.48

Trait names, definitions, predicted influences on jaw performance, and means, standard deviations (SD), and P-values (P) of two-tailed T-tests between GI and WSB for Euclidean distances, cross-sectional area (CA), and masseter traits. Values in parentheses are body weight-adjusted traits (trait/body weight$^{1/3}$). Values in brackets are for masseter traits adjusted for jaw length (trait/jaw

length). Predictions are based off of studies investigating changes in morphology and their effect on maximum gape and maximum bite force (Herring and Herring 1974; Vinyard et al. 2003; Vinyard and Payseur 2008).

Chapter 4

Conclusions and Future Directions

The work presented in this thesis provides a rare portrait of the genetics of morphological evolution on islands in efforts to obtain a better understanding of complex trait evolution in a natural context. In Chapter 2, we found that the overall growth of the skeleton is largely controlled by loci that are found on only a handful of chromosomal regions, suggesting that the Gough Island mouse skeleton evolved through a few genetic loci acting in pleiotropy with global effects on growth. We also investigated the genetics and morphology of mandibular evolution of Gough Island mice in Chapter 3. We found that overall growth of the mandible is largely controlled by loci located on two chromosomes that co-localize with skeletal growth and body weight QTL. However, mandibular regions show distinct differences in their genetic architectures, suggesting that aspects of mandible evolution in Gough Island mice are modular. We provided evidence that the evolution of mandible size and shape are likely controlled by distinct genetic loci. We also demonstrated that Gough Island mice have a stronger bite than expected for a mammal of its size, which may be adaptive to the island environment. Biomechanical predictions of morphological variation on jaw performance allowed us to begin to characterize mandibular morphologies that may be functionally related to jaw performance in Gough Island mice.

The work presented in this thesis demonstrates the power of studying a model system with extensive resources in its natural context and is the first study to detail the genetics and functional morphology of skeletal evolution of an island population.

One of the major questions we sought to address was how did the Gough Island mouse skeleton evolve. The evolution of the Gough Island mouse skeleton was in part due to a small number of loci that act pleiotropically to expand the size of the skeleton and overall body size. Pleiotropy has implications for evolution, as it is one mechanism in which traits can co-evolve.

Selection acting on a pleiotropic locus can cause changes to functionally or developmentally related traits that are correlated, which could facilitate rapid morphological evolution (Lande 1980). This suggests that pleiotropy could have facilitated the rapid evolution of skeletal size in Gough Island mice through selection on loci controlling overall organismal size.

The pleiotropic loci identified in these studies likely have systemic effects, such as hormone signaling, or roles in pathways with large downstream effects. For example, Gli1 is located within the confidence interval of the chromosome 11 QTL identified across body size, skeletal, and mandibular traits. Gli1 codes for a zinc finger protein that controls transcription in the Hedgehog pathway, and is important in neuronal development, skeletal formation, and overall body size (Park et al. 2000; Kimura et al. 2005). Although it is possible that pleiotropic loci control variation in overall growth through systematic effects, it is also possible that pleiotropic loci identified across multiple skeletal traits control growth specific to the skeleton. The gene Pth (parathyroid hormone) regulates serum calcium levels, is important for skeletal growth (Ascenzi et al. 1978; Iwaniec et al. 2007; Yuan et al. 2012) and is located within the confidence interval of the pleiotropic locus on chromosome 7.

It is worth pointing out that although pleiotropy likely plays a role in rapid skeletal evolution, the Gough Island mouse skeleton is morphologically and genetically complex. Numerous unique loci were identified for skeletal and mandibular traits. The recent colonization time of Gough Island mice (less than 200 years), suggests that some of the genetic changes that occurred may have been due to standing genetic variation. It has been argued that evolution of complex traits involving multiple loci is more likely to utilize standing genetic variation in recently colonized island populations (Barrett and Schluter 2008). Evolution is thought to occur faster from standing variation than from new mutations, as it is not dependent on the time for

new mutations to arise and alleles that are present are at higher frequencies (Innan and Kim 2004).

We uncovered numerous unique loci that contribute to variation within particular mandibular regions. This speaks to the complexity of the structure, and suggests modular evolution of the mandible. Modularity has been shown to facilitate evolution because traits from different modular structures can evolve relatively independently with little interference between traits (Wagner, Pavlicev, and Cheverud 2007). This has been shown to facilitate beak evolution in Darwin's finches, where two regulatory pathways, the BMP-4 and the calmodulin-dependent pathway, independently regulate beak length and depth with little interference between traits (Abzhanov et al. 2004, 2006).

Another question to explore is whether the evolution of the Gough Island mouse is unique to Gough Island, or if it reflects common evolutionary patterns across island systems. In other words, can we use Gough Island mice as a representative of island evolution to explain general evolutionary mechanisms across island systems? Pleiotropy can drive rapid evolution in cases of recent colonization events. Insular mice experienced relatively recent colonization so any changes to the population were likely rapid, which raises the prospect that pleiotropy could be a common mechanism for evolution on islands. For example, the chromosome 10 QTL overlaps with genomic regions underlying variation in body size (Chan et al. 2012) and skeletal size (Kenney-Hunt et al. 2008) in laboratory mouse strains. This is evidence that this QTL may cause size changes across multiple populations. However, evolution from standing genetic variation suggests that differentiation of recently colonized island populations from the mainland is likely due to founder effects. This suggests that different genetic patterns would be observed across island populations with different founders and source populations.

Similar morphological changes that were identified in the Gough Island mouse mandible were also seen in other island mouse populations, such as the elongation of the mandible. However, Gough Island mice also exhibit changes in mandible morphology that do not reflect a common trend across islands. This may be due to the adaptation of particular mandible forms to the specific island environment, such as shifts in diet mouse populations experience after island colonization. There is evidence for selection acting on mandibular morphology in wild house mouse populations, where similar shapes were identified for populations from similar habitats (Boell and Tautz 2011). In order to evaluate broad patterns of mandibular evolution across island populations, it would require more extensive morphological characterization of mandibles from multiple island populations.

Some aspects of Gough Island mouse biology fit the expected trends of the island syndrome. Given the size and degree of isolation of Gough Island, the direction of change in traits observed fits expectations (Adler and Levins 1994). This includes an increase in population density, increased survival, and increased body size.

At the same time, Gough Island mice depart from the island syndrome, mostly in regards to the magnitude of change in traits compared to mouse populations on islands with similar sizes and degrees of isolation. Gough Island mice are much larger than expected, and also exhibit much lower seasonal variation in survival (Cuthbert et al. 2016a). Gough Island mouse predation behavior and diet are unique. Mice on Gough Island take advantage of seabird chicks as an energetically rich food source, making up a large portion of their diet, which is not common among wild house mice (Jones, Chown, and Gaston 2003; Roux et al. 2002). Mice in high predation areas exhibit higher overwinter survival rates, which has been argued to drive selection for extreme body size and predatory behaviors (Jones et al. 2003a; Cuthbert and Hilton 2004;

Cuthbert et al. 2016a). Although not unique to Gough Island, the complete absence of mouse predators and competitors on islands is not common (Heaney and Holdgate 1957; Jones et al. 2003a; Wanless et al. 2009) and likely reduces selective pressures related to the presence of predators and competitors. These unusual characteristics of the Gough Island mouse have been argued to drive their exceptional body size (Cuthbert et al. 2016a).

Do these patterns tell us whether we can we use Gough Island mice as a representative of island evolution to explain general evolutionary mechanisms across island systems? It may not be sufficient to use a single island population to explain general patterns of island evolution. Rather, it requires the investigation of populations from multiple islands (see Future Directions). Each island has its own set of conditions and history that likely affect the relative importance of genetic and environmental factors underlying evolution on islands.

The studies presented in this thesis are the first steps taken toward a better understanding of skeletal and mandibular evolution on islands from a morphological and genetic perspective. Although we have helped lay the foundation for the study of skeletal evolution in an island context, this work also leads to many more questions. Described below are potential future directions of the work presented here in this thesis.

Future directions

Comparison of morphology and genetic properties of skeletal evolution in multiple island populations

As discussed above, comparisons between the results presented in this thesis to other large-bodied island mouse populations could reveal if they exhibit similar morphological and genetic changes. This would provide insights into whether phenotypic convergence and parallel evolution play a role in island evolution. Although body size has been catalogued across insular

mouse populations, detailed systematic characterizations of the house mouse skeleton across island populations are lacking. To better understand patterns of skeletal evolution on islands, a thorough phenotypic and genetic characterization of skeletal morphology of large-bodied mice from additional islands would be extremely valuable and would provide insights into whether there are shared patterns of morphological evolution across islands and whether they reflect a common genetic basis. Using the 16 skeletal traits measured in the research presented in this thesis (Parmenter et al. 2016, see Chapter 2) would allow for direct comparisons. Mice from Islands such as Papa Westray and Salvagem Grande make promising candidates since they evolved similar large body sizes as Gough Island mice. QTL mapping of skeletal traits between other island populations and WSB would allow us to directly compare the genetic mapping results between Gough Island mice and WSB presented in this thesis. This would provide insights into whether the evolution of skeletal expansion across island populations reflect a common genetic basis. QTL mapping of multiple populations may be prohibitive. In this case crossing the island populations with WSB to evaluate the distribution of phenotypic effects among the offspring could be informative.

Characterize differences between high and low elevation populations of mice on Gough Island

Islands have heterogeneous environments, and Gough Island is no exception. There are major differences between the high and low elevation areas of the island. The majority of the island is mountainous, rising steeply from sea level to the highlands at over 900 meters above sea level and experiences strong westerly winds. The island's Southeast side is closer to sea level and much more forgiving, with more grass and shrub land and is more protected from the harsh

winds (Heaney and Holdgate 1957). There is also 50% more rainfall at high elevations, and vegetation types show strong altitudinal trends (Wace 1961).

Mice used in the research presented in this thesis originated from mice caught from the low elevation areas. The biology of high elevation mice is distinct from those at low elevations (Rowe-Rowe and Crafford 1992; Jones, Chown, and Gaston 2003). High elevation mice are smaller (an average body weight of 24 grams; Jones, Chown, and Gaston 2003), and have distinct diets. Low elevation mice primarily eat bird and earthworm material, whereas the high elevation mice primarily eat plant material and do not predate on birds (Jones, Chown, and Gaston 2003). The biological differences between high and low elevation mice on Gough Island could be the result of adaptations to their unique microenvironment. This suggests that interpretations of results presented in this thesis may not accurately extend to the evolution of high elevation mice on Gough Island.

Detailed comparisons of skeletal variation in high and low elevation mice would allow us to determine if the two groups of mice differ in phenotype. Measurements could include skeletal traits used in the studies presented in this thesis (Parmenter et al. 2016, see Chapter 2) to allow for direct comparisons. Phenotypes could initially be measured from high elevation mouse specimens collected from the island in order to capture phenotypic variation present on the island. Collection of skeletal data from low-elevation specimens would also be useful since skeletal data collected in this thesis are from lab-reared animals. This is feasible since skeletons can be preserved and measured conveniently in the lab. Raising high elevation Gough Island mice in the laboratory on a common diet under the same conditions as the lab-raised low elevation Gough Island mice would determine if the high elevation skeletal phenotypes are maintained in the lab, and therefore likely genetic in origin, suggesting that the high and low

elevation mice evolved different skeletal morphologies. It is possible that high elevation mice could experience a shift in phenotype after lab rearing, which would suggest that it is likely due to environmental effects specific to their high elevation environment.

Additionally, identifying any population structure between mice from areas of high and low elevation could provide illuminating insights into the evolution of mice on the island. Using genotype data from mice from high and low elevation areas (along with genotypes from potential mainland source populations; see Gray et al. 2014) we could infer the likelihood of whether low and high elevation mice make up one single population or two separate populations (with a program such as STRUCTURE (Pritchard, Stephens, and Donnelly 2000). If there is evidence for population structure on the island, this could indicate that mice underwent specific adaptations to their respective environments. Selective pressures within their particular niches may be important in shaping the phenotypic and genotypic divergence between the high and low elevation mice on Gough Island.

Fine mapping of QTL underlying morphological evolution in Gough Island mice

Fine mapping of QTL underlying the extreme morphological evolution in Gough Island mice could lead to the identification of causative mutations. It would also yield direct insights into the function of the QTL. The distal chromosome 10 QTL is likely a global regulator of growth, as it controls body weight and underlies the expansion of the skeleton. Using a congenic approach, we would isolate the Gough Island mouse distal chromosome 10 QTL onto the background of WSB. Characterizing morphological phenotypes of the congenic line will determine the direct effects of the QTL. Characterizing the direct effect of the chromosome 10 QTL will provide insights into its role in pleiotropy on skeletal evolution. Phenotypes would include skeletal traits and growth rate, which would allow for direct comparisons to the results

presented in this thesis. Additional phenotypes (such as body fat percentage, organ weights, and muscle architecture) could also be collected to further characterize the function of the distal chromosome 10 QTL.

References

Abzhanov, A., W. P. Kuo, C. Hartmann, B. R. Grant, P. R. Grant, and C. J. Tabin. 2006. "The Calmodulin Pathway and Evolution of Elongated Beak Morphology in Darwin's Finches." *Nature* 442 (7102): 563–67.

Adler, G. H., and R. Levins. 1994. "The Island Syndrome in Rodent Populations." *The Quarterly Review of Biology* 69 (4): 473–90.

Albertson, R. C., J. T. Streelman, T. D. Kocher, and P. C. Yelick. 2005. "Integration and Evolution of the Cichlid Mandible: The Molecular Basis of Alternate Feeding Strategies." *PNAS* 102 (45): 16287–92.

Allendorf, F. W. 1986. "Genetic Drift and the Loss of Alleles versus Heterozygosity." *Zoo Biology* 5 (2): 181–90.

Ascenzi, A., E. Bonucci, A. Ripamonti, and N. Roveri. 1978. "X-Ray Diffraction and Electron Microscope Study of Osteons during Calcification." *Calcified Tissue Research* 25 (1): 133–43.

Atchley, W. R., and B. K. Hall. 1991a. "A Model for Development and Evolution of Complex Morphological Structures." *Biological Reviews of the Cambridge Philosophical Society* 66 (2): 101–57.

Atchley, W. R., S. Newman, and D. E. Cowley. 1988. "Genetic Divergence in Mandible Form in Relation to Molecular Divergence in Inbred Mouse Strains." *Genetics* 120 (1). Genetics Society of America: 239–53.

Atchley, W. R., and B. K. Hall. 1991b. "A Model for Development and Evolution of Complex Morphological Structures." *Biological Reviews of the Cambridge Philosophical Society* 66 (2): 101–57.

Atchley, W. R., A. A. Plummer, and B. Riska. 1985a. "Genetics of Mandible Form in the Mouse." *Genetics* 111 (3): 555–77.

Atchley, W. R., A. A. Plummer, and B. Riska. 1985b. "Genetic Analysis of Size-Scaling Patterns in the Mouse Mandible." *Genetics* 111 (3): 579–95.

Atchley, W. R., J. J. Rutledge, and D. E. Cowley. 1981. "Genetic Components of Size and Shape. II. Multivariate Covariance Patterns in the Rat and Mouse Skull." *Evolution* 35 (6): 1037–55.

Aylor, D. L., W. Valdar, W. Foulds-Mathes, R. J. Buus, R. A. Verdugo, R. S. Baric, M. T. Ferris, et al. 2011. “Genetic Analysis of Complex Traits in the Emerging Collaborative Cross.” *Genome Research* 21 (8): 1213–22.

Babiker, H., and D. Tautz. 2015. “Molecular and Phenotypic Distinction of the Very Recently Evolved Insular Subspecies *Mus Musculus Helgolandicus Zimmerman*, 1953.” *BMC Evolutionary Biology* 15 (January): 160.

Bakke, M., A. Tuxetv, P. Vilmann, B. R. Jensen, A. Vilmann, and M. Toft. 1992. “Ultrasound Image of Human Masseter Muscle Related to Bite Force, Electromyography, Facial Morphology, and Occlusal Factors.” *European Journal of Oral Sciences* 100 (3): 164–71.

Barrett, R. D. H., and D. Schluter. 2008. “Adaptation from Standing Genetic Variation.” *Trends in Ecology & Evolution* 23 (1): 38–44.

Beck, J. A., S. Lloyd, M. Hafezparast, M. Lennon-Pierce, J. T. Eppig, M. F. Festing, and E. M. Fisher. 2000. “Genealogies of Mouse Inbred Strains.” *Nature Genetics* 24 (1): 23–25.

Beheregaray, L. B., J. P. Gibbs, N. Havill, T. H. Fritts, J. R. Powell, and A. Caccone. 2004. “Giant Tortoises Are Not so Slow: Rapid Diversification and Biogeographic Consensus in the Galápagos.” *PNAS* 101 (17): 6514–19.

Berner, D., D. Moser, M. Roesti, H. Buescher, and W. Salzburger. 2014. “Genetic Architecture of Skeletal Evolution in European Lake and Stream Stickleback.” *Evolution* 68 (6): 1792–1805.

Berry, R. J. 1964. “The Evolution of an Island Population of the House Mouse.” *Evolution* 18 (3): 468–83.

Berry, R. J. 1968. “The Ecology of an Island Population of the House Mouse.” *Journal of Animal Ecology* 37 (2): 445–70.

Berry, R. J. 1970. *Natural History of the House Mouse*. Field Studies Council.

Berry, R. J. 1985. “The Processes of Pattern: Genetical Possibilities and Constraints in Coevolution.” *Oikos* 44 (1): 222.

Berry, R. J. 1986. “Genetics of Insular Populations of Mammals, with Particular Reference to Differentiation and Founder Effects in British Small Mammals.” *Biological Journal of the Linnean Society* 28 (1-2): 205–30.

Berry, R. J., W. N Bonner, and J. Peters. 1979. “Natural Selection in House Mice (Mus Musculus) from South Georgia (South Atlantic Ocean).” *Journal of Zoology* 189 (3): 385–98.

Berry, R. J., and F. H Bronson. 1992. “Life History and Bioeconomy of the House Mouse.” *Biological Reviews* 67 (4): 519–50.

Berry, R. J., and W. B. Jackson. 1979. “House Mice on Enewetak Atoll.” *Journal of Mammalogy* 60 (1). Oxford University Press: 222–25.

Berry, R. J., and M. E Jakobson. 1974. “Vagility in an Island Population of the House Mouse.” *Journal of Zoology* 173 (3): 341–54.

Berry, R. J., and M. E Jakobson. 1975a. “Ecological Genetics of an Island Population of the House Mouse (Mus Musculus).” *Journal of Zoology* 175 (4): 523–40.

Berry, R. J., and M. E Jakobson. 1975b. “Adaptation and Adaptability in Wild-living House Mice (Mus Musculus).” *Journal of Zoology* 176 (3): 391–402.

Berry, R. J., M. E Jakobson, and J. Peters. 1978. “The House Mice of the Faroe Islands: A Study in Microdifferentiation.” *Journal of Zoology* 185 (1): 73–92.

Berry, R. J., M. E Jakobson, and J. Peters. 1987. “Inherited Differences within an Island Population of the House Mouse (Mus Domesticus).” *Journal of Zoology* 211 (4): 605–18.

Berry, R. J., and J. Peters. 1975. “Macquarie Island House Mice: A Genetical Isolate on a sub-Antarctic Island.” *Journal of Zoology* 176 (3): 375–89.

Berry, R. J., J. Peters, and R. J. Van Aarde. 1978. “Sub-antarctic House Mice: Colonization, Survival and Selection.” *Journal of Zoology* 184 (1): 127–41.

Berry, R. J., R. D. Sage, W. Z. Lidicker, and W. B. Jackson. 1981. “Genetical Variation in Three Pacific House Mouse (Mus Musculus) Populations.” *Journal of Zoology* 193 (3): 391–404.

Berry, R. J., G. S. Triggs, P. P. King, H. R. Nash, and L. R. Noble. 1991. “Hybridization and Gene Flow in House Mice Introduced into an Existing Population on an Island.” *Journal of Zoology London* 225 (Pt4): 615–32.

Biewener, A. A. 2005. “Biomechanical Consequences of Scaling.” *The Journal of Experimental Biology* 208 (Pt 9): 1665–76.

Bock, W. J., and G. von Wahlert. 1965. "Adaptation and the Form-Function Complex." *Evolution* 19 (3): 269.

Boell, L. 2013. "Lines of Least Resistance and Genetic Architecture of House Mouse (Mus Musculus) Mandible Shape." *Evolution & Development* 15 (3): 197–204.

Boell, L., and D.Tautz. 2011. "Micro-Evolutionary Divergence Patterns of Mandible Shapes in Wild House Mouse (Mus Musculus) Populations." *BMC Evolutionary Biology* 11 (1): 306.

Bonhomme, F., and J. B. Searle. 2012. *Evolution of the House Mouse*. Edited by M Macholan, Stuart Baird, Pavel Munclinger, and Jaroslav Pialek. 1st ed. Cambridge University Press.

Bonner, W. N. 1984. "Introduced Mammals." In: Antarctic Ecology (ed. by R. M. Laws), Vol. I, pp. 237-278. Academic Press, London.

Bookstein, F. L. 1991. *Morphometric Tools for Landmark Data : Geometry and Biology*. Cambridge University Press.

Brockmann, G. A., C. S. Haley, U. Renne, S. A. Knott, and M. Schwerin. 1998. "Quantitative Trait Loci Affecting Body Weight and Fatness from a Mouse Line Selected for Extreme High Growth." *Genetics* 150 (1): 369–81.

Broman, K. W., and S. Sen. 2009. *A Guide to QTL Mapping with R/qtl*. Springer Science & Business Media.

Broman, K. W., S. Sen, S. E. Owens, A. Manichaikul, E. M. Southard-Smith, and G. A. Churchill. 2006. "The X Chromosome in Quantitative Trait Locus Mapping." *Genetics* 174 (4): 2151–58.

Bronner, F., M. C. Farach-Carson, and H. I. Roach. 2010. *Bone and Development*. Springer Science & Business Media.

Brown, J. C., and D. W. Yalden. 1973. "The Description of mammals–2 Limbs and Locomotion of Terrestial Mammals." *Mammal Review* 3 (4): 107–34.

Brown, P., T. Sutikna, M. J. Morwood, R. P. Soejono, N. Jatmiko, E. W. Saptomo, and R. A. Due. 2004. "A New Small-Bodied Hominin from the Late Pleistocene of Flores, Indonesia." *Nature* 431 (7012): 1055–61.

Calder, W. A. 1996. *Size, Function, and Life History*. Dover Publications.

Carapuço, M., A. Nóvoa, N. Bobola, and M. Mallo. 2005. “Hox Genes Specify Vertebral Types in the Presomitic Mesoderm.” *Genes & Development* 19 (18): 2116–21.

Carson, E. A., J. P. Kenney-Hunt, M. Pavlicev, K. A. Bouckaert, A. J. Chinn, M. J. Silva, and J. M. Cheverud. 2012. “Weak Genetic Relationship between Trabecular Bone Morphology and Obesity in Mice.” *Bone* 51 (1): 46–53.

Carter, T. C., and D. S. Falconer. 1951. “Stocks for Detecting Linkage in the Mouse, and the Theory of Their Design.” *Journal of Genetics* 50 (2): 307–23.

Case, Ted J. 1978. “A General Explanation for Insular Body Size Trends in Terrestrial Vertebrates.” *Ecology* 59 (1): 1-18.

Caumul, R., and P. D. Polly. 2005. "Phylogenetic and environmental components of morphological variation: skull, mandible, and molar shape in marmots (marmota rodentia)" *Evolution* 59 (11): 2460–72.

Chan, Y. F., F. C. Jones, E. McConnell, J. Bryk, L. Bünger, and D. Tautz. 2012. “Parallel Selection Mapping Using Artificially Selected Mice Reveals Body Weight Control Loci.” *Current Biology* 22 (9): 794–800.

Chapuis, J.L., P. Boussès, and G. Barnaud. 1994. “Alien Mammals, Impact and Management in the French Subantarctic Islands.” *Biological Conservation* 67 (2): 97–104.

Chase, K., D. R. Carrier, F. R. Adler, T. Jarvik, E. A. Ostrander, T. D. Lorentzen, and K. G. Lark. 2002. “Genetic Basis for Systems of Skeletal Quantitative Traits: Principal Component Analysis of the Canid Skeleton.” *PNAS* 99 (15): 9930–35.

Chen, W. H., M. Hosokawa, T. Tsuboyama, T. Ono, T. Iizuka, and T. Takeda. 1989. “Age-Related Changes in the Temporomandibular Joint of the Senescence Accelerated Mouse. SAM-P/3 as a New Murine Model of Degenerative Joint Disease.” *The American Journal of Pathology* 135 (2): 379–85.

Cheverud, J. M., E. J. Routman, F. A. Duarte, B. van Swinderen, K. Cothran, and C. Perel. 1996. “Quantitative Trait Loci for Murine Growth.” *Genetics* 142 (4): 1305–19.

Cheverud, J. M., E. J. Routman, and D. J. Irschick. 1997. “Pleiotropic Effects of Individual Gene Loci on Mandibular Morphology.” *Evolution* 51 (6): 2006.

Chown, S. L., and V. R. Smith. 1993. “Climate Change and the Short-Term Impact of Feral House Mice at the Sub-Antarctic Prince Edward Islands.” *Oecologia* 96 (4): 508–16.

Christians, J. K., V. K. Bingham, F. K. Oliver, T. T. Heath, and P. D. Keightley. 2003. "Characterization of a QTL Affecting Skeletal Size in Mice." *Mammalian Genome* 14 (3): 175–83.

Christians, J. K., and L. K. Senger. 2007. "Fine Mapping Dissects Pleiotropic Growth Quantitative Trait Locus into Linked Loci." *Mammalian Genome* 18 (4): 240–45.

Churchill, G. A., D. C. Airey, H. Allayee, J. M. Angel, A. D. Attie, J. Beatty, W. D. Beavis, et al. 2004. "The Collaborative Cross, a Community Resource for the Genetic Analysis of Complex Traits." *Nature Genetics* 36 (11): 1133–37.

Churchill, G. A., and R. W. Doerge. 1994. "Empirical Threshold Values for Quantitative Trait Mapping." *Genetics* 138 (3): 963–71.

Collaborative Cross Consortium. 2012. "The Genome Architecture of the Collaborative Cross Mouse Genetic Reference Population." *Genetics* 190 (2): 389–401.

Colosimo, P. F., K. E. Hosemann, S. Balabhadra, G. Villarreal, M. Dickson, J. Grimwood, J. Schmutz, R. M. Myers, D. Schluter, and D. M. Kingsley. 2005. "Widespread Parallel Evolution in Sticklebacks by Repeated Fixation of Ectodysplasin Alleles." *Science* 307 (5717): 192 8–33.

Colosimo, P. F., C. L. Peichel, K. Nereng, B. K. Blackman, M. D. Shapiro, D. Schluter, and D. M. Kingsley. 2004. "The Genetic Architecture of Parallel Armor Plate Reduction in Threespine Sticklebacks." *PLoS Biology* 2 (5): E109.

Conte, G. L., M. E. Arnegard, J. Best, Y. F. Chan, F. C. Jones, D. M. Kingsley, D. Schluter, and C. L. Peichel. 2015. "Extent of QTL Reuse During Repeated Phenotypic Divergence of Sympatric Threespine Stickleback." *Genetics* 201 (3): 1189–1200.

Corbet, G. B. 1961. "Origin of the British Insular Races of Small Mammals and of the 'Lusitanian' Fauna." *Nature* 191 (4793): 1037–40.

Corner, B. D., and B. T. Shea. 1995. "Growth Allometry of the Mandibles of Giant Transgenic Mice: An Analysis Based on the Finite-Element Scaling Method." *Journal of Craniofacial Genetics and Developmental Biology* 15 (3): 125–39.

Corva, P. M., and J. F. Medrano. 2001. "Quantitative Trait Loci (QTLs) Mapping for Growth Traits in the Mouse: A Review." *Genetics Selection Evolution* 33 (2): 105.

Cox, P. G., E. J. Rayfield, M. J. Fagan, A. Herrel, T. C. Pataky, and N. Jeffery. 2012. "Functional Evolution of the Feeding System in Rodents." *PLoS ONE* 7 (4): e36299.

Cresko, W. A., A. Amores, C. Wilson, J. Murphy, M. Currey, P. Phillips, M. A. Bell, C. B. Kimmel, and J. H. Postlethwait. 2004. "Parallel Genetic Basis for Repeated Evolution of Armor Loss in Alaskan Threespine Stickleback Populations." *PNAS* 101 (16): 6050–55.

Cuthbert, R. J., and G. Hilton. 2004. "Introduced House Mice Mus Musculus: A Significant Predator of Threatened and Endemic Birds on Gough Island, South Atlantic Ocean?" *Biological Conservation* 117 (5): 483–89.

Cuthbert, R. J., H. Louw, G. Parker, K. Rexer-Huber, and P. Visser. 2013. "Observations of Mice Predation on Dark-Mantled Sooty Albatross and Atlantic Yellow-Nosed Albatross Chicks at Gough Island." *Antarctic Science* 25 (06): 763–66.

Cuthbert, R. J., R. M. Wanless, A. Angel, M. Burle, G. M. Hilton, H. Louw, P. Visser, J. W. Wilson, and P. G. Ryan. 2016a. "Drivers of Predatory Behavior and Extreme Size in House Mice Mus Musculus on Gough Island." *Journal of Mammalogy* 97 (2): 533-44.

Darwin, C. 1859. *The Origin of Species: By Means of Natural Selection, Or the Preservation of Favoured Races in the Struggle for Life*. Cambridge University Press.

Davis, M. J. 1983. "Morphometric Variation of Populations of House Mice Mus Demesticus in Britain and Faroe." *Journal of Zoology* 199 (4): 521–34.

Dechow, P. C., and D. S. Carlson. 1983. "A Method of Bite Force Measurement in Primates." *Journal of Biomechanics* 16 (10): 797–802.

Demes, B., and N. Creel. 1988. "Bite Force, Diet, and Cranial Morphology of Fossil Hominids." *Journal of Human Evolution* 17 (7): 657–70.

Diamond, J. M. 1975. "The Island Dilemma: Lessons of Modern Biogeographic Studies for the Design of Natural Reserves." *Biological Conservation* 7 (2): 129–46.

Dilley, B. J., D. Davies, A. L. Bond, P. G. Ryan, P. D. Boersma, N. T. Wheelwright, A. M. Booth, et al. 2015. "Effects of Mouse Predation on Burrowing Petrel Chicks at Gough Island." *Antarctic Science* 27 (06): 543–53.

Dryden, I. L., and K. V. Mardia. 1998. *Statistical Shape Analysis*. Wiley.

Dumont, E. R., and A. Herrel. 2003. "The Effects of Gape Angle and Bite Point on Bite Force in Bats." *The Journal of Experimental Biology* 206 (13): 2117–23.

Durst, P. A. P., and V. L. Roth. 2012. "Classification Tree Methods Provide a Multifactorial Approach to Predicting Insular Body Size Evolution in Rodents." *The American Naturalist* 179 (4): 545–53.

Durst, P. A. P., and V. L. Roth. 2015. "Mainland Size Variation Informs Predictive Models of Exceptional Insular Body Size Change in Rodents." *Proc. R. Soc. B* 282 (1810): 1–7.

Ehrich, T.H., T. T. Vaughn, S. F. Koreishi, R. B. Linsey, L. S. Pletscher, and J. M. Cheverud. 2003. "Pleiotropic Effects on Mandibular Morphology I. Developmental Morphological Integration and Differential Dominance." *J Exp Zool B Mol Dev Evol.* 296 (1): 58–79.

Emerson, S. B., and L. Radinsky. 1980. "Functional Analysis of Sabertooth Cranial Morphology." *Paleobiology* 6 (3): 295–312.

Festing, M.F. W. 1979. *Inbred Strains in Biomedical Research*. London: Macmillan Education UK.

Foster, J. B. 1964. "Evolution of Mammals on Islands." *Nature* 202 (4929): 234-35.

Francis-West, P., R. Ladher, A. Barlow, and A. Graveson. 1998. "Signalling Interactions during Facial Development." *Mechanisms of Development* 75 (1): 3–28.

Gillespie, R. G., and D. A. Clague. 2009. *Encyclopedia of Islands*. 1st ed. University of California Press.

Gliwicz, J. 1980. "Island populations of rodents: their organization and functioning." *Biological Reviews* 55 (1): 109–38.

Goodale, H. D. 1938. "A Study of the Inheritence of Body Weight in the Albino Mouse by Selection." *J. Hered.* 29 (3): 101–12.

Goodale, H. D. 1941. "Progress Report on Possibilities in Projeny-Test Breeding." *Science* 94 (2445): 442–43.

Grant, P. R. 1999. *Ecology and Evolution of Darwin's Finches*. Princeton University Press.

Grant, P. R., and Royal Society (Great Britain). Discussion Meeting. 1998. *Evolution on Islands*. Oxford University Press.

Gray, M. M., M. D. Parmenter, C. Hogan, I. Ford, R. J. Cuthbert, P. G. Ryan, K. W. Broman, and B. A. Payseur. 2015. "Genetics of Rapid and Extreme Size Evolution in Island Mice." *Genetics* 201 (1): 213-28.

Gray, M. M., D. Wegmann, R. J. Haasl, M. A. White, S. I. Gabriel, J. B. Searle, R. J. Cuthbert, P. G. Ryan, and B. A. Payseur. 2014. "Demographic History of a Recent Invasion of House Mice on the Isolated Island of Gough." *Molecular Ecology* 23 (8): 1923–39.

Gross, J. B., and J. Hanken. 2008. "Review of Fate-Mapping Studies of Osteogenic Cranial Neural Crest in Vertebrates." *Developmental Biology* 317 (2): 389–400.

Haley, C. S., and S. A. Knott. 1992. "A Simple Regression Method for Mapping Quantitative Trait Loci in Line Crosses Using Flanking Markers." *Heredity* 69 (4): 315–24.

Hall, B. K. 2005. "Consideration of the Neural Crest and Its Skeletal Derivatives in the Context of Novelty/innovation." *Journal of Experimental Zoology. Part B, Molecular and Developmental Evolution* 304 (6): 548–57.

Hanken, J., and B. K. Hall. 1993. *The Skull: Development*. University of Chicago Press.

Hardouin, E. A., J. Chapuis, M. I. Stevens, J. B. van Vuuren, P. Quillfeldt, R. J. Scavetta, M. Teschke, and D. Tautz. 2010. "House Mouse Colonization Patterns on the Sub-Antarctic Kerguelen Archipelago Suggest Singular Primary Invasions and Resilience against Re-Invasion." *BMC Evolutionary Biology* 10 (October): 325.

Harrison, G. A., R. J. Morton, and J. S. Weiner. 1959. "The Growth in Weight and Tail Length of Inbred and Hybrid Mice Reared at Two Different Temperatures. I. Growth in Weight. II. Tail Length." *PNAS* 242 (695): 479-516.

Heaney, J. B., and M. W. Holdgate. 1957. "The Gough Island Scientific Survey." *The Geographical Journal* 123 (1): 20–31. doi:10.2307/1790718.

Heaney, L. R. 1978. "Island Area and Body Size of Insular Mammals: Evidence from the Tri-Colored Squirrel (Callosciurus Prevosti) of Southeast Asia." *Evolution* 32 (1): 29.

Herrel, A., K. Huyghe, B. Vanhooydonck, T. Backeljau, K. Breugelmans, I. Grbac, R. Van Damme, and D. J. Irschick. 2008. "Rapid Large-Scale Evolutionary Divergence in Morphology and Performance Associated with Exploitation of a Different Dietary Resource." *PNAS* 105 (12): 4792–95.

Herrel, A., J. J. Meyers, and B. VanHooydonck. 2002. "Relations between Microhabitat Use and Limb Shape in Phrynosomatid Lizards." *Biological Journal of the Linnean Society* 77 (1): 149–63.

Herrel, A., T. Speck, and N. P. Rowe. 2006. *Ecology and Biomechanics : A Mechanical Approach to the Ecology of Animals and Plants*. CRC/Taylor & Francis.

Herring, S. W. 1993. "Formation of the Vertebrate Face Epigenetic and Functional Influences." *American Zoologist* 33 (4): 472–83.

Herring, S. W. 1974. "The Superficial Masseter and Gape in Mammals." *The American Naturalist* 108 (962): 561.

Herring, S. W., G. Clough, H. Copley, R. F. Ewer, H. Frädrich, C. Gans, H. Gundlach, et al. 1972. "The Role of Canine Morphology in the Evolutionary Divergence of Pigs and Peccaries." *Journal of Mammalogy* 53 (3): 500–512.

Hessey R., W. C. Allee, and K. P. Schmidt. 1951. "Ecological Animal Geography." *Soil Science* 72 (6): 479.

Hill, J. 1959. *Results of the Norwegian Scientific Expedition to Tristan Da Cunha. 1937-1938.* Oslo: Norske Videnskaps-akademi i Oslo.

Hirsch, C., M. T. John, C. Lautenschläger, and T. List. 2006. "Mandibular Jaw Movement Capacity in 10 and 17-Yr-Old Children and Adolescents: Normative Values and the Influence of Gender, Age, and Temporomandibular Disorders." *European Journal of Oral Sciences* 114 (6): 465–70.

Hoekstra, H. E., R. J. Hirschmann, R. A. Bundey, P. A. Insel, and J. P. Crossland. 2006. "A Single Amino Acid Mutation Contributes to Adaptive Beach Mouse Color Pattern." *Science* 313 (5783):101–4.

Hooker, J. D. 1867. "On Insular Floras: A Lecture." *Journal of Botany* 5: 23–31.

Huang, Q., F. H. Xu, H. Shen, H. Y. Deng, T. Conway, Y. J. Liu, Y. Z. Liu, et al. 2004. "Genome Scan for QTLs Underlying Bone Size Variation at 10 Refined Skeletal Sites: Genetic Heterogeneity and the Significance of Phenotype Refinement." *Physiological Genomics* 17 (3): 326–31.

Hylander, W. L. 1979. "The Functional Significance of Primate Mandibular Form." *Journal of Morphology* 160 (2): 223–39.

Innan, H., and Y. Kim. 2004. "Pattern of Polymorphism after Strong Artificial Selection in a Domestication Event." *PNAS* 101 (29). National Academy of Sciences: 10667–72.

Ishikawa, A., and S. Okuno. 2014. "Fine Mapping and Candidate Gene Search of Quantitative Trait Loci for Growth and Obesity Using Mouse Intersubspecific Subcongenic Intercrosses and Exome Sequencing." *PloS One* 9 (11): e113233.

Iwaniec, U. T., T. J. Wronski, J. Liu, M. F. Rivera, R. R. Arzaga, G. Hansen, and R. Brommage. 2007.

"PTH Stimulates Bone Formation in Mice Deficient in Lrp5." *Journal of Bone and Mineral Research* 22 (3): 394–402.

Jablonski, N. G. 1993. "Evolution of the Masticatory Apparatus in Theropithecus." In *Theropithecus*, edited by Nina G. Jablonski, 299–330. Cambridge University Press.

Jeong, J., J. Mao, T. Tenzen, A. H. Kottmann, and A. P. McMahon. 2004. "Hedgehog Signaling in the Neural Crest Cells Regulates the Patterning and Growth of Facial Primordia." *Genes & Development* 18 (8): 937–51.

Jiang, X., S. Iseki, R. E. Maxson, H. M. Sucov, and G. M. Morriss-Kay. 2002. "Tissue Origins and Interactions in the Mammalian Skull Vault." *Developmental Biology* 241 (1): 106–16.

Johnson, D. R. 1976. "The Interfrontal Bone and Mutant Genes in the Mouse." *J. Anat* 121 (3): 507–13.

Jones, A. G., S. L. Chown, and K. J. Gaston. 2003. "Introduced House Mice as a Conservation Concern on Gough Island." *Atlantic* 12 (1987): 2107–19.

Jones, A. G., S. L. Chown, P. G. Ryan, N. J. M. Gremmen, and K. J. Gaston. 2003a. "A Review of Conservation Threats on Gough Island: A Case Study for Terrestrial Conservation in the Southern Oceans." *Biological Conservation* 113 (1): 75–87.

Jungers, W. L., A. B. Falsetti, and C. E. Wall. 1995. "Shape, Relative Size, and Size-adjustments in Morphometrics." *American Journal of Physical Anthropology* 38 (S21): 137–61.

Keane, T. M., L. Goodstadt, P. Danecek, M. A. White, K. Wong, B. Yalcin, A. Heger, et al. 2011. "Mouse Genomic Variation and Its Effect on Phenotypes and Gene Regulation." *Nature* 477 (7364): 289–94.

Keightley, P. D., T. Hardge, L. May, and G. Bulfield. 1996. "A Genetic Map of Quantitative Trait Loci for Body Weight in the Mouse." *Genetics* 142 (1): 227–35.

Keller, J. M., Y. Huet-Hudson, and L. J. Leamy. 2008. "Effects of 2,3,7,8-Tetrachlorodibenzo-P-Dioxin on Molar Development among Non-Resistant Inbred Strains of Mice: A Geometric Morphometric Analysis." *GDA* 71 (1): 3–16.

Kenney-Hunt, J. P., T. T. Vaughn, L. S. Pletscher, A. Peripato, E. J. Routman, K. Cothran, D. Durand, E. Norgard, C. Perel, and J. M. Cheverud. 2006. "Quantitative Trait Loci for Body Size Components in Mice." *Mammalian Genome* 17 (6): 526–37.

Kenney-Hunt, J. P., B. Wang, E. Norgard, G. Fawcett, D. Falk, L. S. Pletscher, J. P. Jarvis, C. C. Roseman, J. B. Wolf, and J. M. Cheverud. 2008. "Pleiotropic Patterns of Quantitative Trait Loci for 70 Murine Skeletal Traits." *Genetics* 178 (4): 2275–88.

Kimura, H., D. Stephen, A. Joyner, and T. Curran. 2005. "Gli1 Is Important for Medulloblastoma Formation in Ptc1+/− Mice." *Oncogene* 24 (25): 4026–36.

King, P. P., P. Stokes, and R. Fitz-Roy. 1836. "Sketch of the Surveying Voyages of His Majesty's Ships Adventure and Beagle, 1825-1836." *Journal of the Royal Geographical Society of London* 6: 311.

Kirchmann J. J. 2009. "Genetic tests of rapid parallel speciation of flightless birds from an extant volant ancestor." *Biological Journal of the Linnean Society London* 96 (3): 601-16.

Klingenberg, C. P. 2008a. "Morphological Integration and Developmental Modularity." *Annual Review of Ecology, Evolution and Systematics* 39: 115-32.

Klingenberg, C. P. 2010. "Evolution and Development of Shape: Integrating Quantitative Approaches." *Nature Reviews Genetics* 11 (9): 623–35.

Klingenberg, C. P. 2011. "MorphoJ: An Integrated Software Package for Geometric Morphometrics." *Molecular Ecology Resources* 11 (2): 353–57.

Klingenberg, C. P., and L. J. Leamy. 2001. "Quantitative Genetics of Geometric Shape in the Mouse Mandible." *Evolution* 55 (11): 2342–52.

Klingenberg, C. P., L. J. Leamy, E. J. Routman, and J. M. Cheverud. 2001a. "Genetic Architecture of Mandible Shape in Mice: Effects of Quantitative Trait Loci Analyzed by Geometric Morphometrics." *Genetics* 157 (2): 785–802.

Klingenberg, C. P., L. J. Leamy, E. J. Routman, and J. M. Cheverud. 2001b. "Genetic Architecture of Mandible Shape in Mice: Effects of Quantitative Trait Loci Analyzed by Geometric Morphometrics." *Genetics* 157 (2): 785–802.

Klingenberg, C. P., K. Mebus, and J. C. Auffray. 2003. "Developmental Integration in a Complex Morphological Structure: How Distinct Are the Modules in the Mouse Mandible?" *Evolution & Development* 5 (5): 522–31.

Klingenberg, C. P., N. Navarro, and J. Pialek. 2012. "Development of the Mouse Mandible." In *Evolution of the House Mouse*, edited by Milos Macholan, Stuart J. E. Baird, and Pavel Munclinger, 135–49. Cambridge: Cambridge University Press.

Klingenberg, C. P. 2004. “Integration and Modularity of Quantitative Trait Locus Effects on Geometric Shape in the Mouse Mandible.” *Genetics* 166 (4): 1909–21.

Lack, D. 1947. *Darwin’s Finches*. Cambridge: University Press.

Lande, R. 1979. “Quantitative Genetic Analysis of Multivariate Evolution, Applied to Brain:body Size Allometry.” *Evolution* 33 (1): 402-16.

Lande, R. 1980. “The Genetic Covariance between Characters Maintained by Pleiotropic Mutations.” *Genetics* 94 (1): 203–15.

Lande, R., and S. J. Arnold. 1983. “The Measurement of Selection on Correlated Characters.” *Evolution* 37 (6): 1210.

Lang, D. H., N. A. Sharkey, H. A. Mack, G. P. Vogler, D. J. Vandenbergh, D. A. Blizard, J. T. Stout, and G. E. McClearn. 2005. “Quantitative Trait Loci Analysis of Structural and Material Skeletal Phenotypes in C57BL/6J and DBA/2 Second-Generation and Recombinant Inbred Mice.” *Journal of Bone and Mineral Research* 20 (1): 88–99.

Lawlor, T. E. 1982. “The Evolution of Body Size in Mammals: Evidence from Insular Populations in Mexico.” *The American Naturalist* 119 (1): 54–72.

Leamy, L. J., C. P. Klingenberg, E. Sherratt, J. B. Wolf, and J. M. Cheverud. 2008. “A Search for Quantitative Trait Loci Exhibiting Imprinting Effects on Mouse Mandible Size and Shape.” *Heredity* 101 (6): 518–26.

Leamy, L. J., C. P. Klingenberg, E. Sherratt, J. B. Wolf, and J. M. Cheverud. 2015. “The Genetic Architecture of Fluctuating Asymmetry of Mandible Size and Shape in a Population of Mice: Another Look.” *Symmetry* 7 (1): 46–63.

Leamy, L. J., D. Pomp, E. J. Eisen, and J. M. Cheverud. 2002. “Pleiotropy of Quantitative Trait Loci for Organ Weights and Limb Bone Lengths in Mice.” *Physiological Genomics* 10 (1): 21–29.

Leamy, L. J., E. J. Routman, and J. M. Cheverud. 1999. “Quantitative Trait Loci For Early- and Late-Developing Skull Characters in Mice: A Test of the Genetic Independence Model of Morphological Integration.” *The American Naturalist* 153 (2): 201–14.

Leamy, L. J., E. J. Routman, and J. M. Cheverud. 2002. “An Epistatic Genetic Basis for Fluctuating Asymmetry of Mandible Size in Mice.” *Evolution* 56 (3): 642–53.

Leamy, L. J., E. J. Routman, and J. M. Cheverud. 1997. “A Search for Quantitative Trait Loci Affecting Asymmetry of Mandibular Characters in Mice.” *Evolution* 51 (3): 957.

Lister, A. M., and C. Hall. 2014. “Variation in Body and Tooth Size with Island Area in Small Mammals: A Study of Scottish and Faroese House Mice (Mus Musculus).” *Annales Zoologici Fennici* 51 (1-2): 95–110.

Lomolino, M. V. 1985. “Body Size of Mammals on Islands: The Island Rule Reexamined.” *The American Naturalist* 125 (2): 310–16.

Lomolino, M. V. 2005. “Body Size Evolution in Insular Vertebrates: Generality of the Island Rule.” *Journal of Biogeography* 32 (10): 1683-99.

Lomolino, M. V., D. F. Sax, M. R. Palombo, and A. A. van der Geer. 2012. “Of Mice and Mammoths: Evaluations of Causal Explanations for Body Size Evolution in Insular Mammals.” *Journal of Biogeography* 39 (5): 842–54.

Lomolino, M. V., D. F. Sax, B. R. Riddle, and J. H. Brown. 2006. “The Island Rule and a Research Agenda for Studying Ecogeographical Patterns.” *Journal of Biogeography* 33 (9): 1503–10.

Losos, J. B., K. I. Warheit, and T. W. Schoener. 1997. "Adaptive differentiation following experimental island colonization in Anolis lizards." *Nature* 387 (6628): 70.

Losos, J. B., and R. E. Ricklefs. 2009. “Adaptation and Diversification on Islands.” *Nature* 457 (7231): 830–36.

Luca, L., D. Roberto, S. M. Francesca, and P. Francesca. 2003. “Consistency of Diet and Its Effects on Mandibular Morphogenesis in the Young Rat.” *Progress in Orthodontics* 4: 3–7.

Lynch, M., and B. Walsh. 1998. *Genetics and Analysis of Quantitative Traits*. Sinauer.

Lyras, G. A., A. A. E. van der Geer, and L. Rook. 2010. “Body Size of Insular Carnivores: Evidence from the Fossil Record.” *Journal of Biogeography* 37 (6): 1007–21.

Macarthur, J. W. 1944. “Genetics of Body Size and Related Characters. I. Selecting Small and Large Races of the Laboratory Mouse.” *The American Naturalist* 78 (775): 142–57. doi:10.1086/281181.

MacArthur, R. H., and E. O. Wilson. 1967. *The Theory of Island Biogeography*. Princeton University Press.

Major, O. I. 1902. “On the Pigmy Hippopotamus from the Pleistocene of Cyprus.” *Proceedings of the Zoological Society of London* 72 (3): 107–11.

Mardia, K. V., J. T. Kent, and J. M. Bibby. 1979. *Multivariate Analysis (Probability and Mathematical Statistics)*. Edited by KV Mardia. London: Academic Press.

Marquez, E. J. 2008. "A statistical framework for testing modularity in multidimensional data." *Evolution* 62 (10): 2688-2708.

Mayr, E. 1954. *Change of Genetic Environment and evolution. (1954): 157.*

McAlarney, M. E., M. Rizos, E. G. Rocca, O. F. Nicolay, and S. Efstratiadis. 2001. “The Quantitative and Qualitative Analysis of the Craniofacial Skeleton of Mice Lacking the IGF-I Gene.” *Clinical Orthodontics and Research* 4 (4): 206–19.

Meiri, S., N. Cooper, and A. Purvis. 2008. “The Island Rule: Made to Be Broken?” *Proceedings of the Royal Society of London B: Biological Sciences* 275 (1631): 141-48.

Meiri, S., T. Dayan, and D. Simberloff. 2004. “Body Size of Insular Carnivores: Little Support for the Island Rule.” *The American Naturalist* 163 (3): 469–79.

Meiri, S., T. Dayan, and D. Simberloff. 2005. “Area, Isolation and Body Size Evolution in Insular Carnivores.” *Ecology Letters* 8 (11): 1211-17.

Meiri, S., E. Meijaard, S. A. Wich, C. P. Groves, and K. M. Helgen. 2008. “Mammals of Borneo – Small Size on a Large Island.” *Journal of Biogeography* 35 (6): 1087–94.

Meloro, C., P. Raia, F. Carotenuto, and S. N. Cobb. 2011. “Phylogenetic Signal, Function and Integration in the Subunits of the Carnivoran Mandible.” *Evolutionary Biology* 38 (4): 465–75.

Mezey, J. G., J. M. Cheverud, and G. P. Wagner. 2000. “Is the Genotype-Phenotype Map Modular?: A Statistical Approach Using Mouse Quantitative Trait Loci Data.” *Genetics* 156 (1): 305–11.

Michaux, J., P. Chevret, and S. Renaud. 2007. “Morphological Diversity of Old World Rats and Mice (Rodentia, Muridae) Mandible in Relation with Phylogeny and Adaptation.” *Journal of Zoological Systematics and Evolutionary Research* 45 (3): 263–79.

Miller, C. T., A. M. Glazer, B. R. Summers, B. K. Blackman, A. R. Norman, M. D. Shapiro, B. L. Cole, et al. 2014. “Modular Skeletal Evolution in Sticklebacks Is Controlled by Additive and Clustered Quantitative Trait Loci.” *Genetics* 197 (1): 405–20.

Millien, V. 2006. “Morphological Evolution Is Accelerated among Island Mammals.” *PLoS Biol* 4 (10): e321.

Millien, V. 2011. “Mammals Evolve Faster on Smaller Islands.” *Evolution; International Journal of Organic Evolution* 65 (7): 1935-44.

Millien, V., and J. Damuth. 2004. "Climate change and size evolution in an island rodent species: new perspectives on the island rule" *Evolution* 58 (6): 1353–60.

Monteiro, L. R., and S. F. dos Reis. 2005. “Morphological Evolution in the Mandible of Spiny Rats, Genus Trinomys (Rodentia: Echimyidae).” *Journal of Zoological Systematics and Evolutionary Research* 43 (4): 332–38.

Monteiro, L. R., and M. R. Nogueira. 2010. “Adaptive Radiations, Ecological Specialization, and the Evolutionary Integration of Complex Morphological Structures.” *Evolution* 64 (3): 724–44.

Morriss-Kay, G. M. “Derivation of the Mammalian Skull Vault.” *Journal of Anatomy* 199 (Pt 1-2): 143–51.

Mosimann, J. E. 1970. “Size Allometry: Size and Shape Variables with Characterizations of the Lognormal and Generalized Gamma Distributions.” *Journal of the American Statistical Association* 65 (330): 930-45.

Norgard, E., H. A. Lawson, L. S. Pletscher, B. Wang, V. R. Brooks, J. B. Wolf, and J M Cheverud. 2011. “Genetic Factors and Diet Affect Long-Bone Length in the F34 LG, SM Advanced Intercross.” *Mammalian Genome* 22 (3-4): 178–96.

Norgard, E., C. C. Roseman, G. L. Fawcett, M. Pavlicev, C. D. Morgan, L. S. Pletscher, B. Wang, and J M Cheverud. 2008. “Identification of Quantitative Trait Loci Affecting Murine Long Bone Length in a Two-Generation Intercross of LG/J and SM/J Mice.” *Journal of Bone and Mineral Research* 23 (6): 887–95.

Nowak, R. 1999. *Walker’s Mammals of the World, Volume 1*. JHU Press.

Olsen, E. C., and R. L. Miller. 1958. *Morphological Integration*. University of Chicago Press.

Orr, H. A. 1998. “Testing Natural Selection vs. Genetic Drift in Phenotypic Evolution Using Quantitative Trait Locus Data.” *Genetics* 149 (4): 2099–2104.

Ovchinnikov, D. 2009. “Alcian Blue/alizarin Red Staining of Cartilage and Bone in Mouse.” *Cold Spring*

Harbor Protocols 2009 (3): 5157.

Pallares, L. F., P. Carbonetto, S. Gopalakrishnan, C. C. Parker, C. L. Ackert-Bicknell, A. A. Palmer, and D. Tautz. 2015. "Mapping of Craniofacial Traits in Outbred Mice Identifies Major Developmental Genes Involved in Shape Determination." *PLoS Genetics* 11 (11): e1005607.

Pallares, L. F., B. Harr, L. M. Turner, and D. Tautz. 2014. "Use of a Natural Hybrid Zone for Genomewide Association Mapping of Craniofacial Traits in the House Mouse." *Molecular Ecology* 23 (23): 5756–70.

Palombo, M. R. 2009. "Body Size Structure of Pleistocene Mammalian Communities: What Support Is There for The 'island Rule'?" *Integrative Zoology* 4 (4): 341–56.

Park, H. L., C. Bai, K. A. Platt, M. P. Matise, A. Beeghly, C. C. Hui, M. Nakashima, and A. L. Joyner. 2000. "Mouse Gli1 Mutants Are Viable but Have Defects in SHH Signaling in Combination with a Gli2 Mutation." *Development* 127 (8): 1593–1605.

Parmenter, M. D., M. M. Gray, C. A. Hogan, I. N. Ford, K. W. Broman, C. J. Vinyard, and B. A. Payseur. 2016. "Genetics of Skeletal Evolution in Unusually Large Mice from Gough Island." *Genetics* 204 (4): 1559-72.

Parsons, K. J., E. J. Márquez, and R. C. Albertson. 2012. "Constraint and Opportunity: The Genetic Basis and Evolution of Modularity in the Cichlid Mandible." *The American Naturalist* 179 (1): 64–78.

Pavlicev, M., J. P. Kenney-Hunt, E. Norgard, C. C. Roseman, J. B. Wolf, and J. M. Cheverud. 2008. "Genetic Variation in Pleiotropy: Differential Epistasis as a Source of Variation in the Allometric Relationship between Long Bone Lengths and Body Weight." *Evolution* 62 (1): 199–213.

Peichel, C. L., K. S. Nereng, K. A. Ohgi, B. L. Cole, P. F. Colosimo, C. A. Buerkle, D. Schluter, and D. M. Kingsley. 2001. "The Genetic Architecture of Divergence between Threespine Stickleback Species." *Nature* 414 (6866): 901–5.

Perez, S. I., J. A. F. Diniz-Filho, F. J. Rohlf, and S. F. Dos Reis. 2009. "Ecological and Evolutionary Factors in the Morphological Diversification of South American Spiny Rats." *Biological Journal of the Linnean Society* 98 (3): 646–60.

Pergams, O. R., and M. V. Ashley. 2001. "Microevolution in Island Rodents." *Genetica* 112-113: 245–56.

Peters, R. H. 1986. *The Ecological Implications of Body Size*. Cambridge University Press.

Pool, J. E., and C. F. Aquadro. 2007. "The Genetic Basis of Adaptive Pigmentation Variation in Drosophila Melanogaster." *Molecular Ecology* 16 (14): 2844–51.

Pourquié, O. 2009. *The Skeletal System*. Cold Spring Harbor Laboratory Press.

Pritchard, J. K., M. Stephens, and P. Donnelly. 2000. "Inference of Population Structure Using Multilocus Genotype Data." *Genetics* 155 (2): 945–59.

R Core Team. 2016. "R: A Language and Environment for Statistical Computing." https://www.r-project.org/.

Raadsheer, M.C., T. M. G. J. van Eijden, F. C. van Ginkel, and B. Prahl-Andersen. 1999. "Contribution of Jaw Muscle Size and Craniofacial Morphology to Human Bite Force Magnitude." *Journal of Dental Research* 78 (1): 31–42.

Raia, P., and S. Meiri. 2006. "The Island Rule in Large Mammals: Paleontology Meets Ecology." *Evolution; International Journal of Organic Evolution* 60 (8): 1731–42.

Raia, P., and S. Meiri. 2011. "The Tempo and Mode of Evolution: Body Sizes of Island Mammals." *Evolution* 65 (7): 1927–34.

Rauch, F. 2005. "Bone Growth in Length and Width: The Yin and Yang of Bone Stability." *Journal of Musculoskeletal & Neuronal Interactions* 5 (3): 194–201.

Reed, D. R., A. H. McDaniel, M. Avigdor, and A. A. Bachmanov. 2008. "QTL for Body Composition on Chromosome 7 Detected Using a Chromosome Substitution Mouse Strain." *Obesity* 16 (2): 483–87.

Renaud, S., and J. C. Auffray. 2010. "Adaptation and Plasticity in Insular Evolution of the House Mouse Mandible." *Journal of Zoological Systematics and Evolutionary Research* 48 (2): 138–50.

Renaud, S., J. C. Auffray, and S. de la Porte. 2010. "Epigenetic Effects on the Mouse Mandible: Common Features and Discrepancies in Remodeling due to Muscular Dystrophy and Response to Food Consistency." *BMC Evolutionary Biology* 10: 28.

Renaud, S., E. A. Hardouin, B. Pisanu, and J.-L. Chapuis. 2013. "Invasive House Mice Facing a Changing Environment on the Sub-Antarctic Guillou Island (Kerguelen Archipelago)." *Journal of Evolutionary Biology* 26 (3): 612–24.

Rocha, J. L., E. J. Eisen, L. D. Van Vleck, and D. Pomp. 2004. "A Large-Sample QTL Study in Mice: I. Growth." *Mammalian Genome* 15 (2): 83–99.

Roseman, C. C., J. P. Kenney-Hunt, and J. M. Cheverud. 2009. “Phenotypic Integration Without Modularity: Testing Hypotheses About the Distribution of Pleiotropic Quantitative Trait Loci in a Continuous Space.” *Evolutionary Biology* 36 (3): 282–91.

Roux, V. L., J.-L. Chapuis, Y. Frenot, and P. Vernon. 2002. “Diet of the House Mouse (Mus Musculus) on Guillou Island, Kerguelen Archipelago, Subantarctic.” *Polar Biology* 25 (1): 49–57.

Rowe-Rowe, D. T., and J. E. Crafford. 1992. “Density, Body Size, and Reproduction of Feral House Mice on Gough Island.” *South African Journal of Zoology* 27 (1): 1–5.

Russell, J. C. 2012. “Spatio-Temporal Patterns of Introduced Mice and Invertebrates on Antipodes Island.” *Polar Biology* 35 (8): 1187–95.

Ryan, P. G., J. Cooper, and J. P. Glass. 2001. “Population Status, Breeding Biology and Conservation of the Tristan Albatross Diomedea [Exulans] Dabbenena.” *Bird Conservation International* 11 (01): 35–48.

Samuels, J. X., and B. Van Valkenburgh. 2008. “Skeletal Indicators of Locomotor Adaptations in Living and Extinct Rodents.” *Journal of Morphology* 269 (11): 1387–1411.

Samuels, J. X. 2009. “Cranial Morphology and Dietary Habits of Rodents.” *Zoological Journal of the Linnean Society* 156 (4): 864–88.

Sanger, T. J., E. Norgard, L. S. Pletscher, M. Bevilacqua, V. R. Brooks, L. J. Sandell, and J. M. Cheverud. 2011. “Developmental and Genetic Origins of Murine Long Bone Length Variation.” *Journal of Experimental Zoology. Part B, Molecular and Developmental Evolution* 316B (2): 146–61.

Satoh, K., and F. Iwaku. 2006. “Jaw Muscle Functional Anatomy in Northern Grasshopper Mouse, Onychomys Leucogaster, a Carnivorous Murid.” *Journal of Morphology* 267 (8): 987–99.

Schlosser, G., and G. P. Wagner. 2004. *Modularity in Development and Evolution*. University of Chicago Press.

Schluter, D. 1996. “Adaptive Radiation Along Genetic Lines of Least Resistance.” *Evolution* 50 (5): 1766–74.

Schmidt-Nielsen, K. 1984. *Scaling, Why Is Animal Size so Important?* Cambridge University Press.

Scott, S. N., S. M. Clegg, S. P. Blomberg, J. Kikkawa, I. P. Owens. 2003. "Morphological shifts in island-

dwelling birds: the roles of generalist foraging and niche expansion." *Evolution* 57 (9): 2147-56.

Scriven, P. N., and V. Bauchau. 1992. “The Effect of Hybridization on Mandible Morphology in an Island Population of the House Mouse.” *Journal of Zoology* 226 (4): 573–83.

Sealander, J. A. 1962. “Seasonal Changes in Blood Values of Deer Mice and Other Small Mammals.” *Ecology* 43 (1): 107–19.

Shao, H., D. R. Reed, and M. G. Tordoff. 2007. “Genetic Loci Affecting Body Weight and Fatness in a C57BL/6J X PWK/PhJ Mouse Intercross.” *Mammalian Genome* 18 (12): 839–51.

Shapiro, M. D., M. E. Marks, C. L. Peichel, B. K. Blackman, K. S. Nereng, B. Jónsson, D. Schluter, and D. M. Kingsley. 2004. “Genetic and Developmental Basis of Evolutionary Pelvic Reduction in Threespine Sticklebacks.” *Nature* 428 (6984): 717–23.

Shubin, N., C. Tabin, and S. Carroll. 1997. “Fossils, Genes and the Evolution of Animal Limbs” *Nature* 388 (6643): 639–48.

Siegel, M. I. 1970. “The Tail, Locomotion and Balance in Mice.” *American Journal of Physical Anthropology* 33 (1):101–2.

Silver, L. M. 1995. *Mouse Genetics: Concepts and Applications*. Oxford University Press.

Slábová, M, and D. Frynta. 2007. “Morphometric Variation in Nearly Unstudied Populations of the Most Studied Mammal: The Non-Commensal House Mouse (Mus Musculus Domesticus) in the Near East and Northern Africa.” *Zoologischer Anzeiger* 246 (2): 91–101.

Smith, R. J. 1984. “Allometric Scaling in Comparative Biology: Problems of Concept and Method.” *American Journal of Physiology - Regulatory, Integrative and Comparative Physiology* 246 (2): R152–60.

Smith, R. J. 1984. “Comparative Functional Morphology of Maximum Mandibular Opening (Gape) in Primates.” In *Food Acquisition and Processing in Primates*, 231–55. Boston, MA: Springer US.

Snell, G. D. 1941. *Biology of the Laboratory Mouse*. Dover Publications.

Sondaar, P. Y. 1977. “Insularity and Its Effect on Mammal Evolution.” In *Major Patterns in Vertebrate Evolution*, 671–707. Boston, MA: Springer US.

Stamps, J. A., and M. Buechner. 1985. “The Territorial Defense Hypothesis and the Ecology of Insular Vertebrates.” *The Quarterly Review of Biology* 60 (2): 155–81.

Suto, J.-I. 2009. “Identification of Multiple Quantitative Trait Loci Affecting the Size and Shape of the Mandible in Mice.” *Mammalian Genome* 20 (1): 1–13.

Svenson, K. L., D. M. Gatti, W. Valdar, C. E. Welsh, R. Cheng, E. J. Chesler, A. A. Palmer, et al. 2012. “High-Resolution Genetic Mapping Using the Mouse Diversity Outbred Population.” *Genetics* 190 (2): 437–47.

Tamarin, R. H. 1978. “Dispersal, Population Regulation, and K-Selection in Field Mice.” *The American Naturalist* 112 (985): 545–55.

Terhune, C. E., W. L. Hylander, C. J. Vinyard, and A. B. Taylor. 2015. “Jaw-Muscle Architecture and Mandibular Morphology Influence Relative Maximum Jaw Gapes in the Sexually Dimorphic Macaca Fascicularis.” *Journal of Human Evolution* 82: 145–58.

Therrien, F. 2005. “Mandibular Force Profiles of Extant Carnivorans and Implications for the Feeding Behaviour of Extinct Predators.” *Journal of Zoology* 267 (03): 249.

Thomas, G. H., S. Meiri, and A. B. Phillimore. 2009. “Body Size Diversification in Anolis: Novel Environment and Island Effects.” *Evolution* 63 (8): 2017–30.

Threadgill, D. W., and G. A. Churchill. 2012. “Ten Years of the Collaborative Cross.” *G3* 2 (2): 153–56.

Tian, J., M. P. Keller, A. T. Broman, C. Kendziorski, B. S. Yandell, A. D. Attie, K. W. Broman. 2016. “The Dissection of Expression Quantitative Trait Locus Hotspots.” *Genetics* 202 (4): 1563-74.

Tian, J., and K. W. Broman. 2015. “Testing of Pleotropy versus Close Linkage.” *GitHub Repository*. https://github.com/jianan/qtlpvl.

Van Valen, L. 1973. “Body Size and Numbers of Plants and Animals.” *Evolution* 27 (1): 27.

van der Geer, A., G. Lyras, J. de Vos, and M. Dermitzakis. 2011. *Evolution of Island Mammals Adaptation and Extinction of Placental Mammals on Islands*. John Wiley & Sons.

Vaughn, T. T., L. S. Pletscher, A. Peripato, K. King-Ellison, E. Adams, C. Erickson, and J. M. Cheverud. 1999. “Mapping Quantitative Trait Loci for Murine Growth: A Closer Look at Genetic Architecture.” *Genetical Research* 74 (03): 313–22.

Verill, G. E. 1895. *On Some Birds and Eggs Collected by Mr. Geo. Comer at Gough Island, Kerguelen Island, and the Island of South Georgia: With Extracts from His Notes, Including a Meteorological Record for about Six Months at Gough Island*. Connecticut Academy of Arts and Sciences.

Vinyard, C. J., and B. A. Payseur. 2008. "Of 'mice' and Mammals: Utilizing Classical Inbred Mice to Study the Genetic Architecture of Function and Performance in Mammals." *Integrative and Comparative Biology* 48 (3): 324–37.

Vinyard, C. J., C. E. Wall, S. H. Williams, and W. L. Hylander. 2003. "Comparative Functional Analysis of Skull Morphology of Tree-Gouging Primates." *American Journal of Physical Anthropology* 120 (2): 153–70.

Vinyard, C. J., S. H. Williams, C. E. Wall, A. H. Doherty, A. W. Crompton, and W. L. Hylander. 2011. "A Preliminary Analysis of Correlations between Chewing Motor Patterns and Mandibular Morphology across Mammals." *Integrative and Comparative Biology* 51 (2): 260–70.

Wace, N. M. 1961. "The Vegetation of Gough Island." *Ecological Monographs* 31 (4): 337–67.

Wagner, G. P., M. Pavlicev, and J. M. Cheverud. 2007. "The Road to Modularity." *Nature Reviews. Genetics* 8 (12): 921–31.

Wainwright, P. C., and S. M. Reilly. 1994. *Ecological Morphology : Integrative Organismal Biology*. University of Chicago Press.

Wall, C. E. 1999. "A Model of Temporomandibular Joint Function in Anthropoid Primates Based on Condylar Movements during Mastication." *American Journal of Physical Anthropology* 109 (1): 67–88.

Wallace, A. R. 1880. *Island Life; Or the Phenomena and Causes of Insular Faunas and Floras: Including a Revision and an Attempted Solution of the Problem of Geological Climates*. Macmillan.

Wanless, R. M. 2007. "Impacts of the Introduced House Mouse on the Seabirds of Gough Island." Diss. University of Cape Town.

Wanless, R. M., A. Angel, R. J. Cuthbert, G. M. Hilton, and P. G. Ryan. 2007. "Can Predation by Invasive Mice Drive Seabird Extinctions?" *Biology Letters* 3 (3): 241–44.

Wanless, R. M., P. G. Ryan, R. Altwegg, A. Angel, J. Cooper, R. J. Cuthbert, and G. M. Hilton. 2009. "From Both Sides: Dire Demographic Consequences of Carnivorous Mice and Longlining for the Critically Endangered Tristan Albatrosses on Gough Island." *Biological Conservation* 142 (8): 1710–18.

Wellik, D. M., and M. R. Capecchi. 2003. “Hox10 and Hox11 Genes Are Required to Globally Pattern the Mammalian Skeleton.” *Science* 301 (5631): 363–67.

Whittaker, R. J., and J. M. Fernández-Palacios. 2007. *Island Biogeography : Ecology, Evolution, and Conservation*. Oxford University Press.

Williams, S. H., E. Peiffer, and S. Ford. 2009. “Gape and Bite Force in the Rodents Onychomys Leucogaster and Peromyscus Maniculatus: Does Jaw-Muscle Anatomy Predict Performance?” *Journal of Morphology* 270 (11): 1338–47.

Williamson, M. 1984. *Island Populations*. *Oxford University Press*.

Wilmore, L. G., C. C. Roseman, J. Rogers, J. M. Cheverud, and J. T. Richtsmeier. 2009. “Comparison of Mandibular Phenotypic and Genetic Integration between Baboon and Mouse.” *Evolutionary Biology* 36 (1): 19–36.

Wolf, J. B., L. J. Leamy, E. J. Routman, and J. M. Cheverud. 2005. “Epistatic Pleiotropy and the Genetic Architecture of Covariation within Early and Late-Developing Skull Trait Complexes in Mice.” *Genetics* 171 (2): 683–94.

Wolf, J. B., D. Pomp, E. J. Eisen, J. M. Cheverud, and L. J. Leamy. 2006. “The Contribution of Epistatic Pleiotropy to the Genetic Architecture of Covariation among Polygenic Traits in Mice.” *Evolution & Development* 8 (5): 468–76.

Yamada, K, and D. B. Kimmel. 1991. “The Effect of Dietary Consistency on Bone Mass and Turnover in the Growing Rat Mandible.” *Archives of Oral Biology* 36 (2): 129–38.

Yang H., T. A. Bell, G. A. Churchill, F. P.-M. de Villena. 2007. "On the subspecific origin of the laboratory mouse." *Nature genetics* 39 (9): 1100-07.

Yoshida, T., P. Vivatbutsiri, G. M. Morriss-Kay, Y. Saga, and S. Iseki. 2008. “Cell Lineage in Mammalian Craniofacial Mesenchyme.” *Mechanisms of Development* 125 (9-10): 797–808.

Yuan, Q., T. Sato, M. Densmore, H. Saito, C. Schüler, R. G. Erben, and B. Lanske. 2012. “Deletion of PTH Rescues Skeletal Abnormalities and High Osteopontin Levels in Klotho−/− Mice.” *PLoS Genetics* 8 (5): e1002726.

Zelditch, M. L., A. R. Wood, R. M. Bonett, and D. L. Swiderski. 2008. “Modularity of the Rodent Mandible: Integrating Bones, Muscles, and Teeth.” *Evolution & Development* 10 (6): 756–68.

Appendix A

Supplementary Material for Chapter 2

Figure S2.1 Design of F2 intercrosses for genetic mapping. WSB = parental WSB individual; Gough = parental Gough (GI) individual (full sib inbred for 3 generations); F1 = first filial generation hybrid of WSBxGI; F2 = second filial generation hybrid of F1xF1.

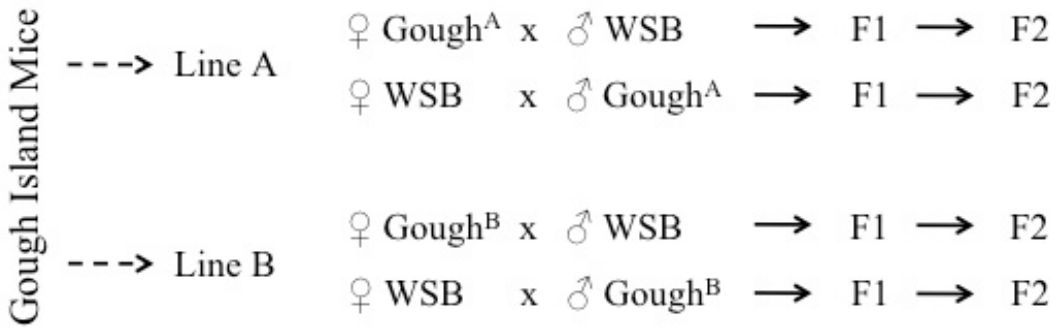

Figure S2.2 WSB, GI and F2 histograms representing the phenotypes of the 16 skeletal traits at (A) 5, (B) 10, and (C) 16 weeks of age. Vertical lines represent the means of the parents (blue = WSB, red = GI) and F2s (green).

A.

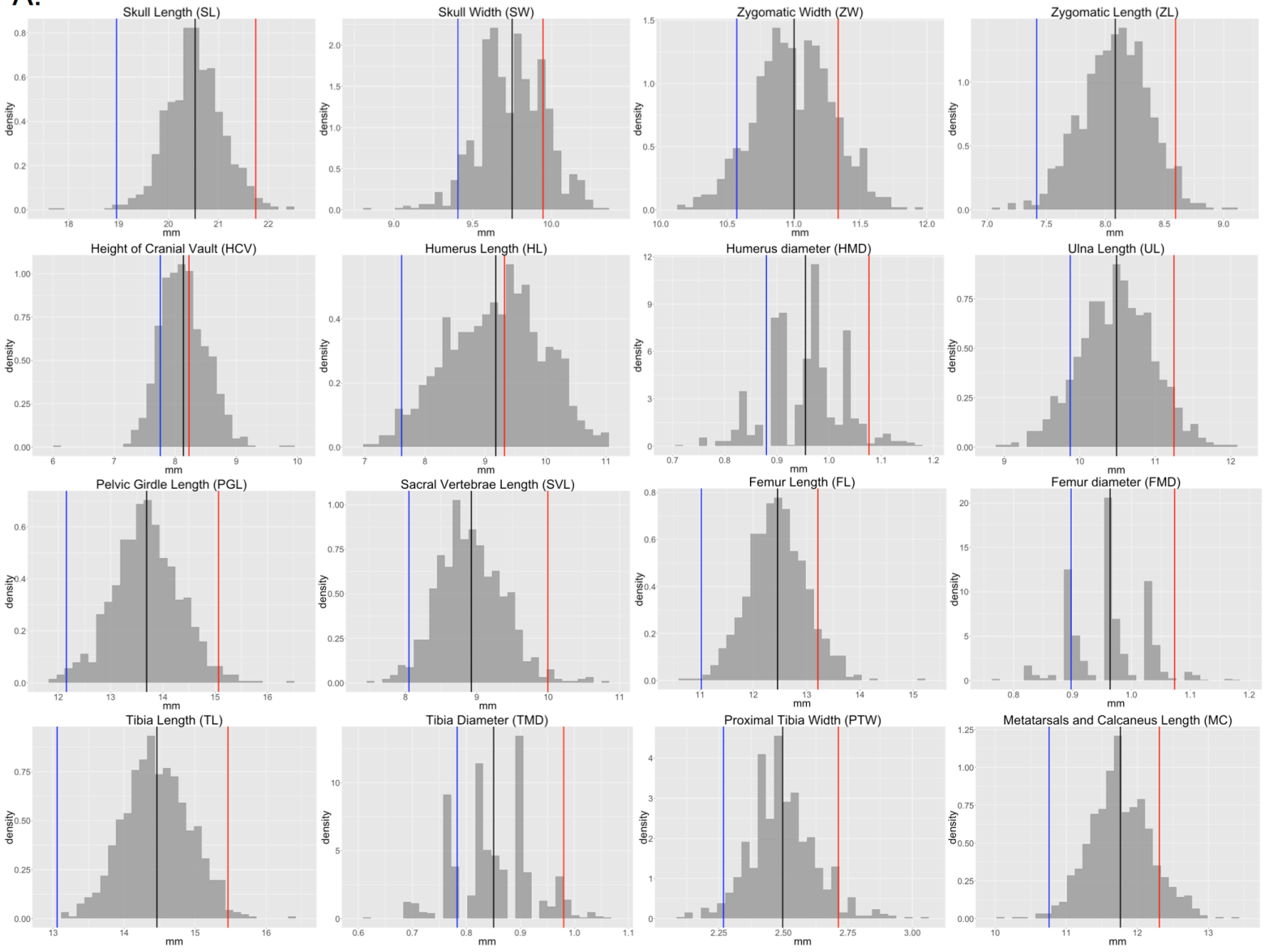
Skull Length (SL)
Skull Width (SW)
Zygomatic Width (ZW)
Zygomatic Length (ZL)
Height of Cranial Vault (HCV)
Humerus Length (HL)
Humerus diameter (HMD)
Ulna Length (UL)
Pelvic Girdle Length (PGL)
Sacral Vertebrae Length (SVL)
Femur Length (FL)
Femur diameter (FMD)
Tibia Length (TL)
Tibia Diameter (TMD)
Proximal Tibia Width (PTW)
Metatarsals and Calcaneus Length (MC)
density
mm

B.

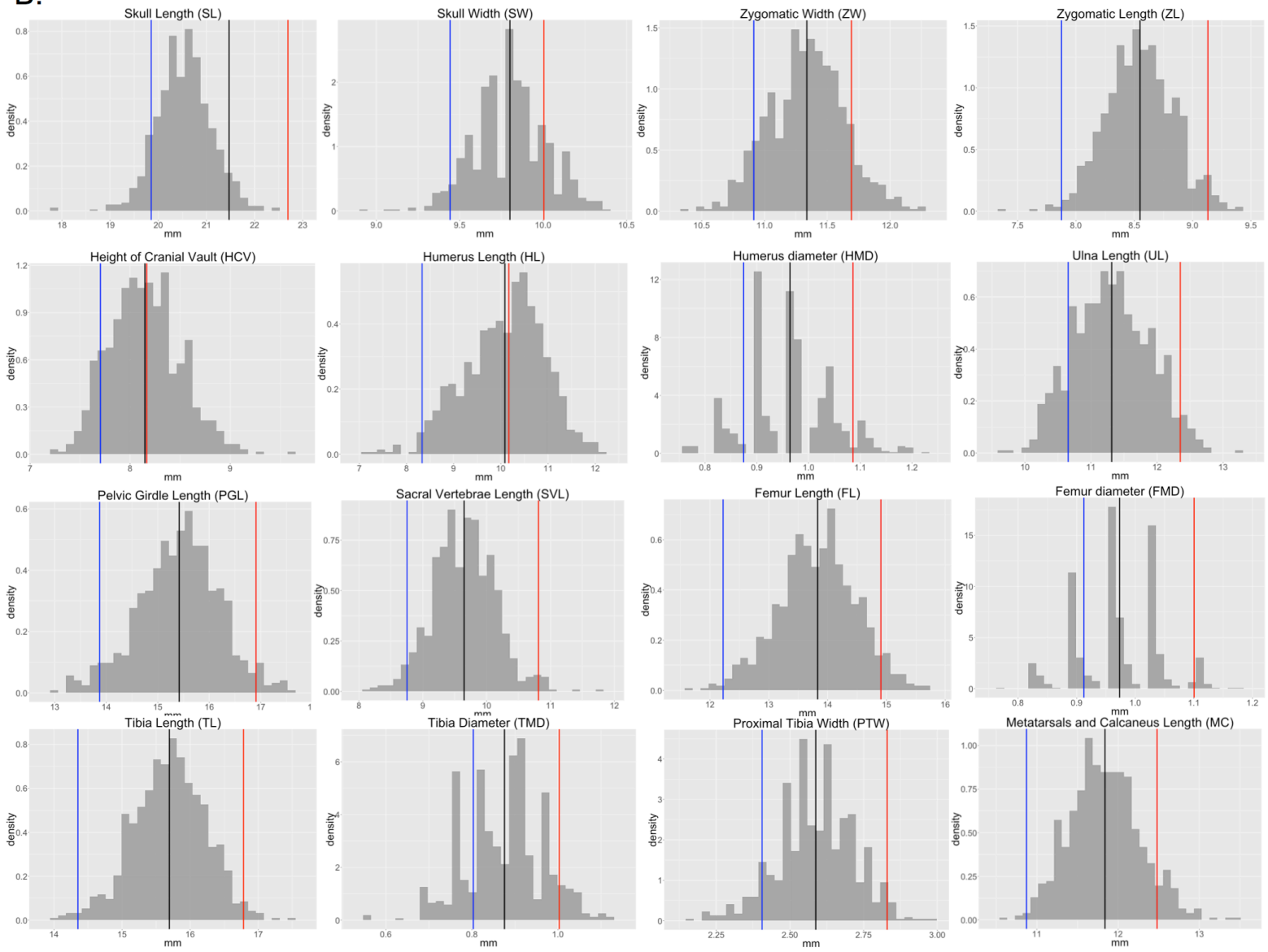
Skull Length (SL)
Skull Width (SW)
Zygomatic Width (ZW)
Zygomatic Length (ZL)
Height of Cranial Vault (HCV)
Humerus Length (HL)
Humerus diameter (HMD)
Ulna Length (UL)
Pelvic Girdle Length (PGL)
Sacral Vertebrae Length (SVL)
Femur Length (FL)
Femur diameter (FMD)
Tibia Length (TL)
Tibia Diameter (TMD)
Proximal Tibia Width (PTW)
Metatarsals and Calcaneus Length (MC)
density
mm

C.

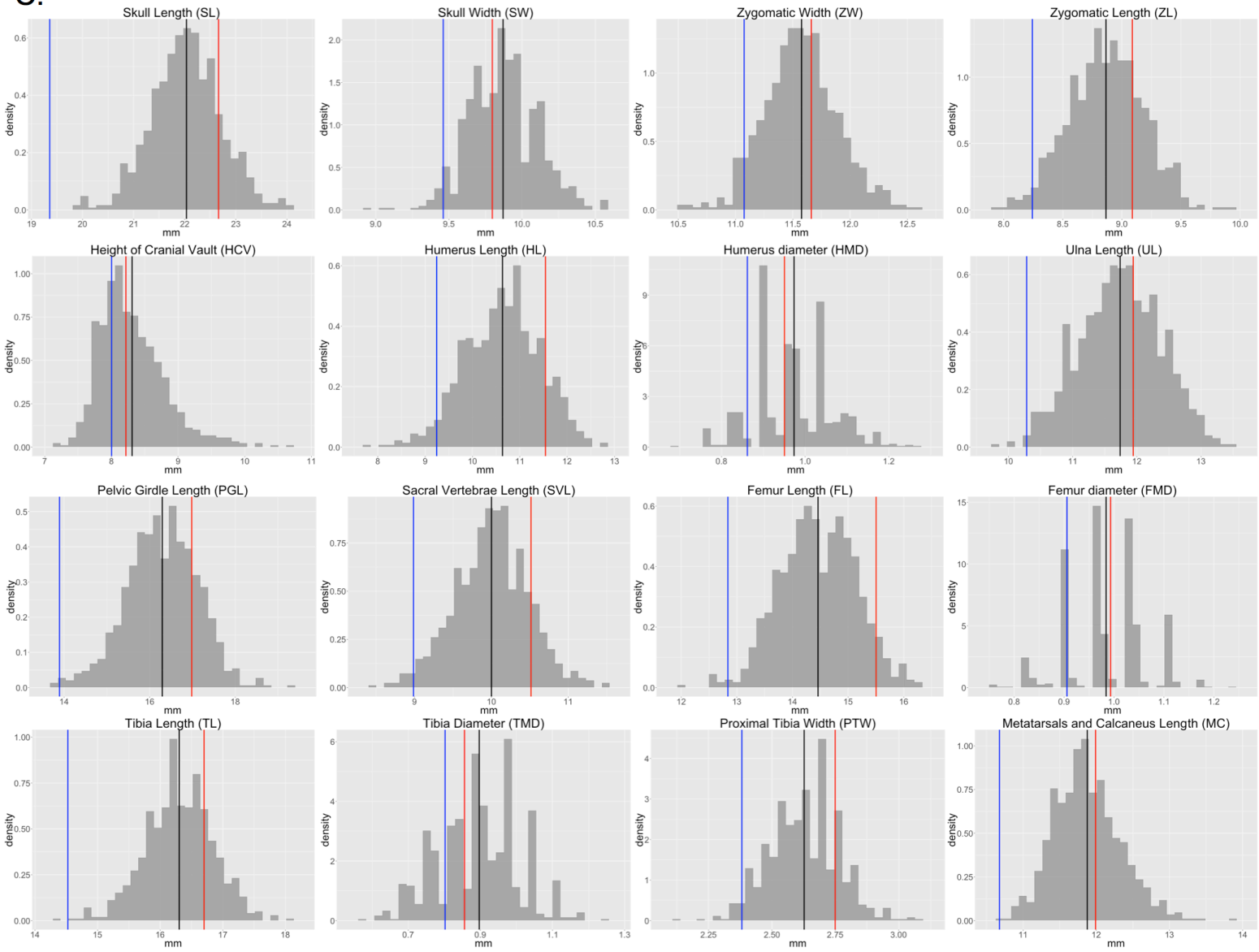
Skull Length (SL)
Skull Width (SW)
Zygomatic Width (ZW)
Zygomatic Length (ZL)
Height of Cranial Vault (HCV)
Humerus Length (HL)
Humerus diameter (HMD)
Ulna Length (UL)
Pelvic Girdle Length (PGL)
Sacral Vertebrae Length (SVL)
Femur Length (FL)
Femur diameter (FMD)
Tibia Length (TL)
Tibia Diameter (TMD)
Proximal Tibia Width (PTW)
Metatarsals and Calcaneus Length (MC)
density
mm

Figure S2.3 Principal Component Analyses on skeletal traits. A. Percent variance explained by each principal component (PC) at 5, 10, and 16 weeks (left, center, and right columns, respectively. B. QTL for PC1 and PC2 at 5, 10, and 16 weeks. Significance is indicated with a dotted line.

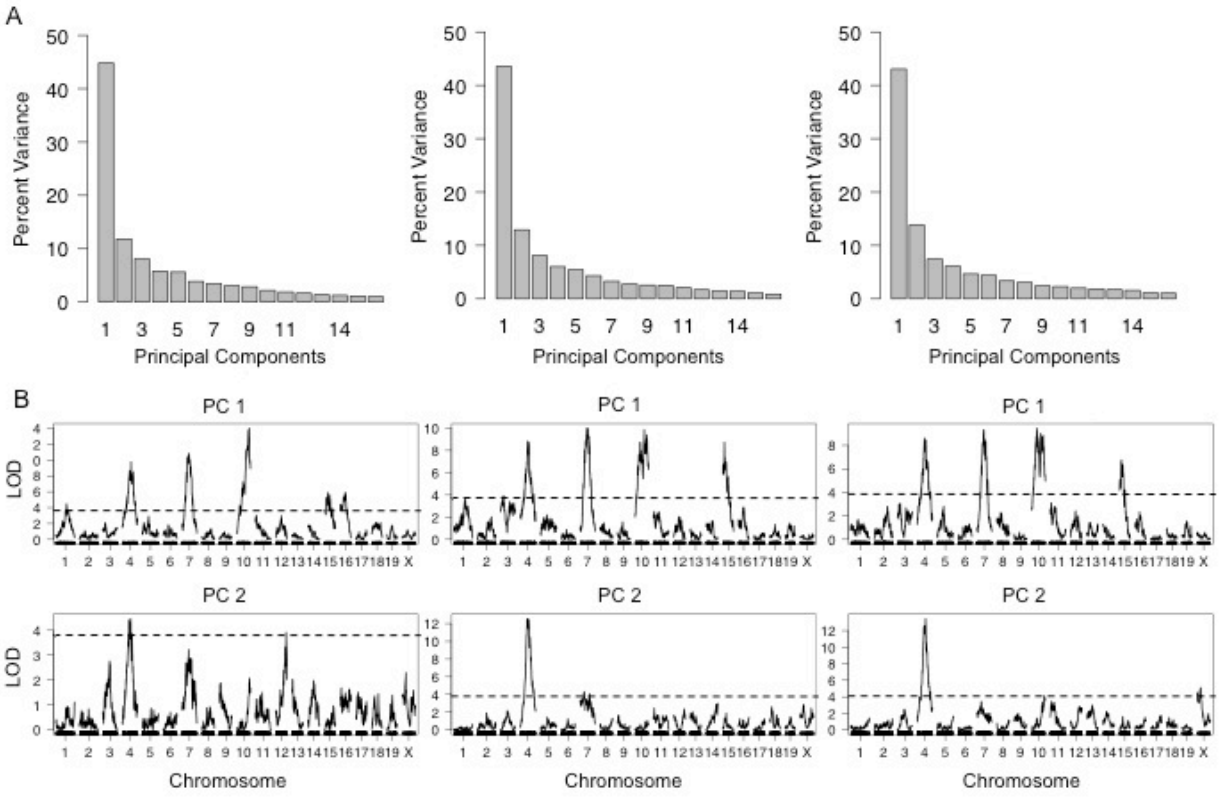

Table S2.1 Phenotypic means and standard deviations of GI and WSB at 5, 10 and 16 weeks

	5 weeks							10 weeks							16 weeks						
	WSB/EiJ			Gough (GI)				WSB/EiJ			Gough (GI)				WSB/EiJ			Gough (GI)			
Trait	N	Mean	SD	N	Mean	SD	p-value	N	Mean	SD	N	Mean	SD	p-value	N	Mean	SD	N	Mean	SD	p-value
SL	16	18.96	0.36	20	21.75	0.53	<2.2e-16	12	19.85	0.37	20	22.69	0.52	<2.2e-16	7	19.36	0.78	15	22.88	0.63	<2.2e-16
SW	16	9.41	0.13	20	9.95	0.21	1.70E-13	12	9.44	0.11	20	10.01	0.21	5.30E-12	7	9.46	0.14	15	9.92	0.1	5.20E-06
ZW	16	10.57	0.18	20	11.34	0.2	7.20E-13	12	10.91	0.15	20	11.69	0.23	2.80E-11	7	11.07	0.33	15	11.76	0.27	7.30E-05
ZL	16	7.42	0.18	20	8.59	0.3	<2.2e-16	12	7.88	0.17	20	9.13	0.33	<2.2e-16	7	8.24	0.24	15	9.28	0.24	7.80E-09
HCV	16	7.76	0.35	20	8.23	0.23	1.90E-04	12	7.7	0.34	20	8.17	0.24	1.30E-04	7	8	0.26	15	8.27	0.22	4.10E-01
HL	16	7.61	0.59	20	9.32	0.63	5.60E-14	12	8.33	0.66	20	10.17	0.69	1.00E-10	7	9.29	0.73	15	11.55	0.27	1.60E-07
HMD	16	0.87	0.04	20	1.08	0.05	2.20E-16	12	0.87	0.06	20	1.09	0.07	1.40E-12	7	0.86	0.07	15	1.03	0.06	7.70E-05
UL	16	9.87	0.38	20	11.25	0.45	4.40E-15	12	10.68	0.48	20	12.35	0.46	1.10E-15	7	10.28	0.19	15	12.17	0.35	8.40E-11
PGL	16	12.14	0.35	20	15.06	0.55	<2.2e-16	12	13.87	0.63	20	16.91	0.58	<2.2e-16	7	13.89	0.7	15	17.18	0.3	5.30E-14
SVL	16	7.93	0.28	20	10	0.39	<2.2e-16	12	8.75	0.28	20	10.81	0.38	<2.2e-16	7	8.99	0.39	15	10.9	0.27	1.90E-12
FL	16	11.02	0.3	20	13.21	0.39	<2.2e-16	12	12.22	0.41	20	14.91	0.36	<2.2e-16	7	12.84	0.46	15	15.63	0.19	7.30E-14
FMD	16	0.89	0.04	20	1.07	0.04	<2.2e-16	12	0.92	0.04	20	1.1	0.05	8.40E-16	7	0.91	0.07	15	1.07	0.06	1.60E-04
TL	16	13.06	0.36	20	15.46	0.31	<2.2e-16	12	14.35	0.35	20	16.78	0.37	<2.2e-16	7	14.53	0.37	15	16.93	0.16	<2.2e-16
TMD	16	0.77	0.05	20	0.98	0.06	<2.2e-16	12	0.8	0.05	20	1	0.08	8.00E-11	7	0.79	0.07	15	0.92	0.08	6.00E-03
PTW	16	2.27	0.11	20	2.71	0.11	<2.2e-16	12	2.41	0.09	20	2.83	0.11	<2.2e-16	7	2.38	0.13	15	2.9	0.07	3.90E-12
MC	16	10.76	0.29	20	12.3	0.39	<2.2e-16	12	10.87	0.34	20	12.48	0.41	<2.2e-16	7	10.68	0.25	15	12.1	0.16	1.20E-10

N is the number of individuals measured for each trait at a given time point and $\bar{x}$ is the mean. P-values are for two-trailed T-tests and are significant if $p < 0.05$.

Table S2.2 P-values of two-tailed T-tests performed for 16 skeletal traits between each time point within GI and within WSB.

Trait	GI 5 to 10 week	GI 10 to 16 week	WSB 5 TO 10 week	WSB 10 TO 16 week
SL	<0.001	0.869	<0.001	0.154
SW	0.396	0.002	0.423	0.763
ZW	<0.001	0.686	<0.001	0.264
ZL	<0.001	0.689	<0.001	0.005
HCV	0.564	0.558	0.691	0.047
HL	<0.001	<0.001	0.007	0.027
HMD	0.631	<0.001	0.814	0.705
UL	<0.001	0.01	0.001	0.052
PGL	<0.001	0.702	<0.001	0.945
SVL	<0.001	0.061	<0.001	0.195
FL	<0.001	<0.001	<0.001	0.013
FMD	0.073	<0.001	0.284	0.832
TL	<0.001	0.506	<0.001	0.329
TMD	0.33	<0.001	0.344	0.986
PTW	0.001	0.125	0.001	0.675
MC	0.195	<0.001	0.362	0.175

Table S2.3 Genomic positions of single-trait QTL

	5 week					10 week					16 week				
Trait	chr	Pos (Mb)	LOD	Lower CI	Upper CI	chr	Pos (Mb)	LOD	Lower CI	Upper CI	chr	Pos (Mb)	LOD	Lower CI	Upper CI
SL	1	159.6	4.8	76	181.5	4	93.6	8.1	68.1	150.8	2	43	4.5	24.7	55
	4	59.2	4.3	36.7	129.1	7	105.2	9	68.2	124.6	4	127	4.7	57.7	155.6
	6	75.5	4.8	7.6	80.6	10	110.4	14.2	67.5	111.9	7	118.9	6.2	68.2	125.4
	7	76.3	6.2	65.6	126.9	11	12.7	4.8	3.3	63	10	67.1	9.4	59.5	122.5
	10	123.4	22.4	119.2	125	15	30.6	10.3	8.1	47.8	11	16.2	4.3	3.3	72.8
	15	71.6	5.2	6.1	100.9						15	46.5	7.3	30.2	58.1
SW	3	58.3	8.9	44	101.7	3	100.5	12.8	52	102.4	3	59.6	10.8	44	65.4
	8	123.9	4.3	120	131.2	10	107.4	20.3	101.9	113.9	10	121.2	19.6	113.7	121.8
	10	121.2	18.8	114.8	122.9	15	9.2	4.7	6.1	68.4	15	12.6	4.7	6.1	50.9
	16	29.7	4.8	8.6	91.1	17	47.4	6.2	43.4	67.5	17	48.1	6.5	43.4	52.8
	17	48.1	6.5	32.9	53.8						19	15.1	4.3	3.2	35.9
ZW	3	128.9	4.6	52.3	137.5	3	133.9	10.9	100.7	137.5	3	133.9	6.6	125.2	137.5
	7	81.3	6.5	65.6	97.3	7	81.3	6.7	68.2	105.8	6	15.4	4.3	3.4	139.1
	10	119.5	20.5	114.4	122.9	10	110.3	10.6	45	116.1	7	81.3	5.4	62.1	121.8
	15	11.3	5.4	6.1	72.6	12	27.7	4.4	16.1	47.7	10	113.5	10.1	45.6	120.8
	16	76.3	6.1	37.5	84.9	15	24.9	4.5	6.1	71.6	12	27.7	5.6	3.6	29.7
											15	24.9	4.7	6.1	38
ZL	4	93.9	9.3	53.7	103.4	3	121.2	5.3	3.2	142.7	4	88.2	9.2	74.8	108.5
	10	123.8	6.4	113.7	125.9	4	93.9	9	85.2	105.1	10	76.7	9.6	64.1	116.1
						10	115.6	7.7	68	125	15	34.3	4.4	20.6	50.9
						15	30.6	6.1	6.8	45.1					
						16	48.2	4.9	4	64.8					
HCV	10	31.3	5.1	24.8	121.2	3	21.2	6.6	16	109.8	3	59.6	4.7	28.9	119.1
	15	41.5	4.8	28.8	102.1	10	63.2	8.6	45.7	69.3	10	57.1	5	23	91.2

	17	60.3	5.3	46.2	82.1	15	94.9	6.7	93.6	99.5	15	71.8	4.7	42.3	95.6
HL	7	95.4	4.7	30.5	109.4	4	94.4	4.3	75.7	100.3	10	58.6	5.2	46.4	69.4
	10	36.6	4.9	24.7	41.7	11	63.6	4.6	11.6	68.6					
HMD	15	99.5	6.4	48.5	101.8	5	127.5	5.1	69.9	132.5	7	135.1	5.1	79	137.3
						10	31.6	5	22.5	51.2	13	58.7	4.8	3.9	75.9
						13	58.7	4.9	47.7	73	15	53.2	5.5	29.3	76.2
						15	54.9	6.3	48.5	98.5					
UL	1	78.1	4.4	67.3	129.8	1	145.9	5.2	128.8	181.5	4	104.1	10.3	65.4	119
	4	86.1	9.2	57.7	94.9	4	75.6	11.7	66.8	98.7	7	87.9	7.3	81.2	127.1
	7	131.4	4.2	73.5	143.6	7	133.3	4.6	81.2	152.4	15	11.2	5	6.1	76.5
	15	75.6	5.1	56.9	87.8	15	30.6	4.6	7.2	55.4					
PGL	1	80.4	11	76	128.6	1	82.8	4.5	76	148.9	4	93.9	10.9	83.2	108.5
	4	94.1	6.6	69.2	131	4	95.1	7.5	88.2	108.5	7	87.9	7	73.4	126.1
	7	118.6	9.2	81.6	124.6	7	124.1	9.1	89.8	136.1	8	31.2	5	12.2	71.5
	10	119.5	12.9	119.2	125	10	65.8	6.8	33.9	71	10	65.8	5.1	39.3	129.8
	11	12.2	4.4	3.3	19.8	11	16.2	4.5	3.3	18.5	11	12.2	5.6	3.3	18.2
						15	30.7	4.4	8.1	38.9					
SVL	1	135.5	8.3	94.2	148.9	1	137.3	5.7	94.2	172.2	1	162.2	4.7	117.6	180
	4	94.1	5.4	55.6	129.1	4	94.1	10.6	68.1	107.3	4	94	7.2	68.1	130.5
	7	97	7.3	70.3	120.9	7	97	6.1	81.8	126.9	7	87.9	4.6	62.1	124.1
	10	123.4	11.5	119.2	125	10	121.2	6.6	110.2	125.6	8	128.5	4.2	89	130.8
	11	16.2	5.1	3.3	44.2	11	12.2	5	3.3	34.6	10	119.5	6.9	118.6	125
	16	4.8	5.9	3.5	40						11	16.2	6	3.3	60.8
											12	70.1	4.5	62.1	99.5
											15	30.7	4.3	26.6	66.5
FL	1	145.4	5.8	122.1	165	2	149.7	4.4	102.8	160.1	2	117.9	6.1	94.4	154.4
	4	94.1	10.5	87.6	103.4	4	98.7	17.7	85	107.3	4	104.1	15.8	91	108.6
	7	90.8	15.2	86.5	99.3	7	125.2	14	87.6	126.9	7	91.2	14.7	85.4	124.6

	10	123.4	6.1	119.2	125.9	11	12.7	4.7	3.3	54.7	11	51.8	4.8	11.8	66.1
	11	12.9	5.1	7.1	16.8	15	44.3	9.5	7.6	55.4	15	46.5	5.7	7.6	59.4
	12	92.6	4.8	68.3	113.4										
	15	72.3	6.6	6.1	76										
	16	4.9	4.5	3.5	64.8										
FMD	4	133.1	5.3	124.1	144.6	7	63.1	4.5	53.6	143.6	2	161	4.9	124.6	168.4
	8	29.1	5.3	4.9	34.6	8	60.1	5.3	37.4	109.6	7	71	4.3	57.3	134.4
	11	85	7	81	102	12	44.9	4.5	9.5	84.1	X	48.1	8	35.4	57.8
	14	32.6	5.6	8.7	47	14	10.8	4.4	8.7	46.5					
						X	48.1	6.1	33.9	56.8					
TL	1	145.4	8.5	95.6	162.2	1	145.9	6.5	121.8	165	4	93.9	16.2	88.6	108.6
	4	106.9	12.7	91	111.4	4	94.1	17.1	88.6	108.5	7	125.2	5.1	82.2	126.9
	7	98.1	10.9	75.2	122.6	7	125.2	10.2	87.6	126.9	10	123.4	5.4	39.3	129.8
	10	119.5	9.6	119.2	125.6	10	45.7	4.6	19	129.8	12	70.8	5	59.1	93.9
	11	82.1	4.3	68.3	102	12	79.8	4.7	68.3	98.8	14	46.2	4.6	34.4	52.7
	12	76.4	5.7	60.6	92.7	14	71.6	5	30.6	87.7					
	14	45.6	7.5	30.6	48.6	15	30.6	6.2	6.9	76					
	15	74.2	4.6	6.9	84.7										
	16	4.9	5.4	3.5	51.6										
TMD	11	66.1	5.1	62.7	109.5	3	115.5	5.2	96.7	148.1	3	116.4	4.9	101.4	150.1
	15	75.6	4.6	38	86.8	11	109	5.7	94.3	119	6	35.7	4.4	17.7	53.5
						15	70.6	5.3	6.1	86.8					
PTW	10	116.7	7.6	102.9	123.4	4	62.3	5.5	43	108.5	5	129.3	4.9	72.7	140
						10	119.6	10.7	119	125.6	10	119.3	8.6	108.8	125.6
						15	30.6	4.5	6.1	78.8	15	50.9	4.3	6.9	76
						18	58.6	5.8	50.3	62.5	18	21	4.4	3.2	60.8
MC	1	128.4	8.3	121.8	139.8	1	137.9	7.6	121.8	154	1	139.4	6.7	121.8	153.9

4	106.9	17.2	88.2	118.7	4	88.6	12.9	87.6	107.3	4	94.1	13.9	87.6	108.5
7	86.2	6.1	68.2	119.9	7	90.6	6.2	75.2	122.6	10	122.5	10.7	119.2	125
10	119.4	10.1	118.3	125.6	10	122.9	10.7	119.2	125	11	12.2	5.2	5.3	35.2
11	12.2	4.9	4.7	46.4	11	34.2	4.4	8.9	61.5					
14	45.6	5.7	30.6	52.7	14	45.6	5.4	33.5	59.2					

Table S2.4 Summary of size-corrected QTL.

5 week					10 week					16 week				
Chr	Trait	QTL original	QTL BW covariate	QTL shape ratios	Chr	Trait	QTL original	QTL BW covariate	QTL shape ratios	Chr	Trait	QTL original	QTL BW covariate	QTL shape ratios
4	UL	X	X	X	4	UL	X	X	X	4	UL	X	X	X
4	PGL	X	X	X	4	PGL	X	X	X	4	PGL	X	X	X
4	SVL	X	X	X	4	MC	X	X	X	4	SVL	X	X	X
4	FL	X	X	X	14	FMD	X	X	X	4	FL	X	X	X
4	FMD	X	X	X	14	TL	X	X	X	4	TL	X	X	X
4	TL	X	X	X	14	MC	X	X	X	4	MC	X	X	X
4	MC	X	X	X	5	HMD	X	X	X	12	ZW	X	X	X
14	FMD	X	X	X	12	FMD	X	X	X	12	SVL	X	X	X
14	TL	X	X	X	X	FMD	X	X	X	1	SVL	X	X	X
14	MC	X	X	X	1	SVL	X	X		4	ZL	X	X	X
11	FMD	X	X	X	1	TL	X	X		6	TMD	X	X	X
4	SL	X	X		1	MC	X	X		7	FL	X	X	X
4	ZL	X	X		3	SW	X	X		14	TL	X	X	X
8	FMD	X	X		3	ZW	X	X		X	FMD	X	X	X
8	SW	X	X		3	ZL	X	X		3	SW	X	X	
10	SL	X	X		3	HCV	X	X		3	ZW	X	X	
10	SW	X	X		4	SL	X	X		10	SL	X	X	
10	ZW	X	X		4	ZL	X	X		10	SW	X	X	
10	PGL	X	X		7	SL	X	X		10	ZW	X	X	
15	FL	X	X		7	PGL	X	X		10	ZL	X	X	
15	HMD	X	X		7	TL	X	X		10	PTW	X	X	
15	UL	X	X		10	SL	X	X		10	MC	X	X	
16	SW	X	X		10	SW	X	X		1	MC	X	X	
16	ZW	X	X		10	ZW	X	X		2	SL	X	X	

17	SW	X	X		10	ZL	X	X		4	SL	X	X						
17	HCV	X	X		10	HCV	X	X		7	UL	X	X						
1	PGL	X	X		10	PTW	X	X		12	TL	X	X						
3	SW	X	X		10	MC	X	X		13	HMD	X	X						
11	TL	X	X		12	ZW	X	X		15	SL	X	X						
12	TL	X	X		12	TL	X	X		17	SW	X	X						
7	SL	X		X	15	SL	X	X		18	PTW	X	X						
7	ZW	X		X	15	HCV	X	X		7	ZW	X		X					
1	SL	X			15	HMD	X	X		15	HMD	X		X					
1	UL	X			15	FL	X	X		2	FL	X							
1	SVL	X			16	ZL	X	X		2	FMD	X							
1	FL	X			17	SW	X	X		15	FL	X							
1	TL	X			18	PTW	X	X		7	SL	X							
1	MC	X			4	SVL	X	X	X	7	HMD	X							
7	HL	X			4	FL	X	X	X	7	PGL	X							
7	UL	X			4	TL	X	X	X	7	SVL	X							
7	PGL	X			7	FL	X	X	X	7	FMD	X							
7	SVL	X			1	UL	X			7	TL	X							
7	FL	X			1	PGL	X			8	PGL	X							
7	TL	X			4	HL	X			8	SVL	X							
7	MC	X			4	PTW	X			10	HCV	X							
10	ZL	X			7	ZW	X			10	HL	X							
10	HCV	X			7	UL	X			10	PGL	X							
10	HL	X			7	SVL	X			10	SVL	X							
10	SVL	X			7	FMD	X			10	TL	X							
10	FL	X			7	MC	X			11	SL	X							
10	TL	X			10	HMD	X			15	ZW	X							
10	PTW	X			10	PGL	X			11	PGL	X							
10	MC	X			10	SVL	X			11	SVL	X							

11	PGL	X		
11	SVL	X		
11	FL	X		
11	TMD	X		
11	MC	X		
15	SL	X		
15	ZW	X		
15	HCV	X		
15	TL	X		
15	TMD	X		
16	SVL	X		
16	FL	X		
16	TL	X		
3	ZW	X		
6	SL	X		
12	FL	X		
14	PTW		X	X
14	PGL		X	X
14	SVL		X	X
14	FL		X	X
1	ZW		X	X
9	PGL		X	X
X	FMD		X	X
2	ZW		X	
2	FL		X	
9	SVL		X	
9	FL		X	
9	MC		X	
12	ZW		X	

10	TL	X		
11	SL	X		
11	HL	X		
11	PGL	X		
11	SVL	X		
11	TMD	X		
11	MC	X		
15	SW	X		
15	ZW	X		
15	ZL	X		
15	UL	X		
15	PGL	X		
15	TL	X		
15	TMD	X		
15	PTW	X		
2	FL	X		
3	TMD	X		
8	FMD	X		
13	HMD	X		
1	ZW		X	X
1	ZL		X	X
11	FMD		X	X
11	TL		X	X
14	PGL		X	X
14	PTW		X	X
14	SVL		X	X
X	HMD		X	X
X	FL		X	X
2	ZW		X	X

11	FL	X		
11	MC	X		
15	SW	X		
15	ZL	X		
15	HCV	X		
15	UL	X		
15	SVL	X		
15	PTW	X		
3	TMD	X		
5	PTW	X		
6	ZW	X		
19	SW	X		
14	PGL		X	X
14	FMD		X	X
14	MC		X	X
1	ZW		X	X
2	ZW		X	X
3	FL		X	X
6	HMD		X	X
X	HL		X	X
3	HCV		X	
6	SW		X	
12	SL		X	
X	SW		X	
8	SW			X
8	UL			X
11	ZW			X
11	ZL			X
11	FMD			X

12	FMD		X			12	SVL		X	X		11	TL			X			
6	SW		X			5	ZW		X			1	ZL			X			
11	ZW		X			8	SW			X		6	SVL			X			
17	ZW		X			8	UL			X		7	SW			X			
X	FL		X			9	SVL			X		10	UL			X			
7	SW			X		9	TL			X		14	SVL			X			
7	ZL			X		9	MC			X									
7	PTW			X		11	ZW			X									
1	ZL			X		11	ZL			X									
10	UL			X		X	MC			X									
						X	ZL			X									
						1	SW			X									
						2	SW			X									
						3	MC			X									
						6	HMD			X									
						7	SW			X									
						13	TL			X									
						14	ZL			X									

Presence of QTL for original single-trait scans (original) and after size correction, including when body weight is used as an additive covariate (QTL BW covariate) and utilizing shape ratios (skeletal trait/body weight0.33) instead of raw skeletal measurements (QTL shape ratios). An "X" indicates the presence of a statistically significant QTL.

Table S2.5 Phenotypic correlations among time points for each of the 16 skeletal traits.

Trait	5 and 10 weeks	10 and 16 weeks	5 and 16 weeks
SL	0.65	0.65	0.56
SW	0.81	0.8	0.76
ZW	0.79	0.8	0.75
ZL	0.54	0.56	0.52
HL	0.76	0.71	0.66
HMD	0.57	0.74	0.53
UL	0.66	0.72	0.64
PGL	0.7	0.78	0.61
SVL	0.8	0.82	0.73
FL	0.75	0.82	0.71
FMD	0.62	0.74	0.57
TL	0.8	0.8	0.68
TMD	0.6	0.79	0.55
PTW	0.54	0.58	0.5
MC	0.81	0.8	0.76

Values represent the Pearson Product Moment.

Table S2.6 Evidence for modularity among GI skeletal traits using MINT analyses

	Traits	Modules	Description	γ*	Jack knife	Rank	γ*	Jack knife	Rank	γ*	Jack knife	Rank
Whole Skeleton				5 week				10 week		16 week		
H_0	[SL] [SW] [ZW] [ZL] [HL] [HMD] [UL] [PGL] [SVL] [FL] [FMD] [TL] [TMD] [PTW] [MC] [HCV]	[$trait_1$] [$trait_2$] … [$trait_n$]	No modularity	0	100	2	0	95	2	0	100	3
H_1	**[SL,SW,ZW,ZL, PGL,SVL, HCV] [HL,HMD,UL] [FL,FMD,TL,TMD, PTW,MC]**	**[skull,pelvis] [forelimb] [hindlimb]**	**Developmental timing - skull and pelvis begin to develop first at E9, followed by forelimb at E10 and hindlimb at E11**	**-0.01**	**100**	**1**	**-0.02**	**100**	**1**	**-0.01**	**100**	**2**
H_2	[SL,ZW,ZL] [SW,HL,HMD,UL, PGL,SVL,FL,FMD, TL,TMD,PTW,MC, HCV]	[some skull] [some skull, remaining traits]	Mesoderm vs CNC-derived - most of the skeleton is derived from mesoderm, except for CNC-derived skull bones	0.08	100	4	0.02	81	3	0.06	83	4
H_3	**[SL,SW,ZW,ZL, SVL, HCV] [HL,HMD,UL,FL, FMD,TL,TMD,PTW ,MC, PGL]**	**[skull, sacral vertebrae] [limb, pelvic girdle]**	**axial vs appendicular skeleton**	0.03	89	3	0.02	69	4	**-0.01**	**100**	**1**
Limb				5 week				10 week		16 week		

H_0	[H] [HMD] [UL] [FL] [FMD] [TL] [TMD] [PTW] [MC]	[$trait_1$] [$trait_2$] … [$trait_n$]	no modularity	0	100	3	0	100	3	0	100	3
H_1	[HL,HMD,UL,FL, FMD,TL,TMD,PTW ,MC]	[all limb traits]	All limb traits as one module	0	100	4	0	100	4	0	100	4
H_2	[HL,HMD,UL] [FL,FMD,TL,TMD, PTW,MC]	[forelimb] [hindlimb]	Forelimb: Tbx5, Hox9 Hindlimb: Tbx4, Islet1	0.08	100	5	0.05	100	5	0.02	100	5
H_3	[HL,HMD,FL,FMD] [UL,TL,TMD,PTW] [MC]	[stylopod] [zeugopod [autopod]	Limb progression during development - stylopod: Hox9; zeugopod: Hox11; autopod: Hox13	0.13	100	6	0.13	100	6	0.12	100	6
H_4	**[HL,UL,FL,TL,MC] [HMD,FMD,TMD]**	**[limb lengths] [limb diameters]**	**limb length vs width - functional load**	**-0.28**	**100**	**1**	**-0.43**	**100**	**1**	**-0.53**	**100**	**1**
H_5	[HL,UL] [HMD] [FL,TL,MC] [FMD,TMD]	[forelimb lengths] [forelimb diameters] [hindlimb lengths] [hindlimb diameters]	forelimb to hindlimb developmental timing and functional load	-0.1	100	2	-0.2	100	2	-0.26	100	2

Each model is composed of non-overlapping sets of skeletal traits partitioned into hypothesized modules. The best fitting model (in bold-face) has the lowest goodness of fit statistic (γ*) based on similarity between expected and observed covariance matrices. Models are ranked based on their γ* value and jackknife values provide support for model rankings.

Table S2.7 Genomic positions of multi-trait QTL

5 Week

Chr	Traits	Pos (cM)	LOD	Lower CI	Upper CI
1	SL,UL,PGL,SVL,FL,TL,MC	57	15.8	45.5	61.3
3	SW,ZW	27.7	9.5	23.8	36.6
4	SL,ZL,UL,PGL,SVL,FL,FMD,TL,MC	32	25.9	26.8	43.8
7	SL,ZW,HL,UL,PGL,SVL,FL,TL,MC	37.1	17.2	34.5	40
10P	HCV,HL,	14.4	8.3	0	53.5
10D	SL,SW,ZW,ZL,HCV,PGL,SVL,FL,TL,PTW,MC	60.7	36	55.7	62.7
11P	PGL,SVL,FL,MC	4.1	11.8	0	21
11D	FMD,TL,TMD	43.3	16.2	39.4	53.4
12	FL,TL	23.2	6.2	20.9	29.8
14	FMD,TL,MC	15	10.2	10.4	29.7
15	SL,ZW,HCV,HMD,UL,FL,TL,TMD	26.7	13.1	12.7	29.3
16	SW,ZW,SVL,FL,TL	0.3	8.7	0	3.2
17	SW,HCV	0.7	9	0	53.8

10 Week

Chr	Traits	Pos (cM)	LOD	Lower CI	Upper CI
1	UL,PGL,SVL,TL,MC	57	13.1	41.1	69.6
3	SW,ZW,ZL,HCV,TMD	13.8	15.9	10.4	36.7
4	SL,ZL,HL,UL,PGL,SVL,FL,TL,PTW,MC	38.8	32	31.7	42.2
7	SL,ZW,UL,PGL,SVL,FL,FMD,TL,MC	47.3	18	37	48.6
10	SL,SW,ZW,ZL,HCV,HMD,PGL,SVL,TL,PTW,MC	13.1	31.2	0	52.9
11	SL,HL,PGL,SVL,FL,MC	36.1	8.7	33.1	54.2
12	ZW,FMD,TL	9.6	6.7	3.8	13.9
14	FMD,TL,MC	6.8	7.3	0	15.4
15	SL,SW,ZW,ZL,HCV,HMD,UL,PGL,FL,TL,TMD,PTW	7.4	19.3	0.2	17.6

16 Week

Chr	Traits	Pos (cM)	LOD	Lower CI	Upper CI
1	SVL,MC	47.3	8	0	90.6
2	FL,FMD	65.6	7.1	53.5	80.5
3	SW,HCV	35.7	12.3	27.7	46.9
4	SL,ZL,UL,PGL,SVL,FL,TL,MC	43.6	31.4	31.7	44.2
6	ZW,TMD	9.3	9.1	6.8	68.8
7	SL,ZW,HMD,UL,PGL,SVL,FL,FMD,TL	37.7	18.8	33.9	48.6
10	SL,SW,ZW,ZL,HCV,HL,PGL,SVL,TL,PTW,MC	26.1	33	15.9	60.7
11	SL,PGL,SVL,FL,MC	34.4	10.7	31	39.5
12	SVL,TL	11.8	5.9	8.3	16.8
15	SL,SW,ZW,ZL,HCV,HMD,UL,SVL,FL,PTW	16.3	16	6.9	22.3

Table S2.8 Genomic positions of multi-trait QTL for skeletal modules.

Whole skeleton											
Time	Model	Module	Traits	Chr.	pos (cM)	pos (Mb)	LOD	lower CI (cM)	lower CI (Mb)	upper CI (cM)	upper CI (Mb)
5	H1	[skull, pelvis]	[SL,SW,ZW,ZL,HCV, PGL,SVL]	1	40.7	89.1	20.1	36	76	48.5	123.6
				3	30	83.4	11.3	15.5	51.4	35	101.2
				4	43.9	106.9	24.7	33.5	84.4	45	110
				5	32.9	73.8	9.9	27.5	66.2	38	87.2
				6	30.1	82	9.5	26	72	34.5	93.9
				7	34.5	82	12.1	25.5	66.6	48	126.6
				8	59.4	128.8	10.3	51	120	60.5	129.2
				10	60	123.4	28.4	55	119	61.5	125
				11	55.4	103.6	13.2	49.5	94.8	57	105.8
				13	49.7	113.7	9.6	31	84.9	54.5	119.4
				16	17	37.7	10.1	4	11.3	35.5	77
				17	16.2	47.8	11.7	13.5	43.4	19.5	51.9
		[Forelimb]	[HL,HMD,UL]	1	53.8	136.2	6.9	36.5	76.7	67.5	169.5
				4	35.4	88.2	10.1	23	57.7	48.5	118.9
				5	31.8	72.3	6.9	29	66.9	37	84.3
				7	34.9	85	10.5	28.5	75.2	40.5	103.1
				10	14.4	35.2	7.1	4.5	17.6	60.5	123.8
				15	28	74.7	7.7	15.5	51.5	41	93.6
				16	24.8	51	6.4	15	34.2	34	74.4
		[Hindlimb]	[FL,FMD,TL,TMD,PTW, MC]	1	54.2	137.1	9	47.5	121.3	59	153
				3	47	126.8	9.9	33.5	96.7	51.5	130.8
				4	35.4	88.2	19.6	32.5	83.3	44.5	108.5

				7	37.1	90.8	15.2	31	78.6	40.5	103.1
				8	9.2	29.1	9.9	0	4.9	27	77.6
				10	60.7	123.8	17.9	52.5	116.9	62.5	125.3
				11	42.8	81.6	23.4	40	77.7	51	97.1
				12	22	63.5	9.8	20	58.6	29.5	81.8
				13	6	30.4	8.9	0	3.9	9	37.8
				14	15	45.7	9.4	0	8.7	31	77
				15	9	36.3	10.3	6.5	28	27.5	73.9
				16	1	6.1	8.8	0	3.5	25	51.6
				19	0.9	7.1	8.7	0	3.2	2.5	11.2
Time	Model	Module	Traits	Chrom	pos (cM)	pos (Mb)	LOD	lower CI (cM)	lower CI (Mb)	upper CI (cM)	upper CI (Mb)
10	H1	[skull, pelvis]	[SL,SW,ZW,ZL,HCV, PGL,SVL]	1	40.7	89.1	11.3	31	67.3	48	122.6
				3	13.5	47.2	17.2	3	21.2	35	101.2
				4	42.1	104	23.6	38.5	98.2	44.5	108.5
				7	53.7	135.1	13.9	44	118.9	55.5	137.1
				10	45.4	110.5	23.3	42	102.9	56.5	119.4
				11	47.7	91.6	10.4	3	11.4	56	104.2
				13	47.9	112.4	9.2	16	51.4	51	116
				15	45.5	95.9	11.8	6.5	28	49.5	99
				17	15.1	44.8	10	11.5	32.9	18.5	50.2
		[Forelimb]	[HL,HMD,UL]	1	57.8	146.7	6.6	32.5	70.4	65.5	165.3
				4	32.5	83.3	14.5	28.5	69.2	37.5	95.4
				7	37.1	90.8	8.1	15.5	48.2	41	104.7
				10	13.6	31.5	8.3	9.5	24.7	15	36.1
				15	17	54.9	10.2	7	30.2	18.5	57.3

		[Hindlimb]	[FL,FMD,TL,TMD,PTW, MC]	1	57.5	144.2	7.8	28	60.3	67.5	169.5
				2	56	127.8	8.6	44.5	89.2	67.5	154.2
				3	48.4	129.1	12.2	10.5	38.1	55	137.5
				4	38.5	98.2	26.5	32.5	83.3	42.5	104.4
				5	28.2	66.9	7.6	15	40	32	72.7
				6	46.2	117.5	7	39	99.7	50	125.9
				7	34.9	85	15.2	30	76.9	48	126.6
				8	39.4	106.2	11	30.5	85	41	110.2
				9	18.2	49.8	6.5	6	29.3	36	89.2
				10	58.5	122.9	14.3	55	119	62.5	125.3
				11	36.1	67.2	20.8	33.5	63.1	42	81.1
				12	10.1	30.9	12.3	4	15.9	16	47.7
				14	17.1	47.6	11	0	8.7	26	69.1
				15	7.5	30.7	15.1	6	27.1	13.5	47.8
				18	23	55.1	9.9	11.5	30.1	26.5	58.9

Time	Model	Module	Traits	Chrom	pos (cM)	pos (Mb)	LOD	lower CI (cM)	lower CI (Mb)	upper CI (cM)	upper CI (Mb)
16	H3	[axial]	[SL,SW,ZW,ZL,HCV, SVL]	1	68.9	170.1	11.8	36	76	74	177.5
				3	16.5	52.3	12.2	1.5	15.1	21.5	61.7
				4	42.4	104.4	18.4	38.5	98.2	50	122.6
				6	30.1	82	9.9	28	77.7	51.5	129.8
				7	44	118.9	10.4	41.5	105.2	64.5	145.6
				10	56.7	119.4	22.1	52	116.7	60.5	123.8
				11	50	95.5	10.6	2.5	10.4	56	104.2
				15	13.1	45.1	10.5	8	34.1	27	72.6

		[appendicular]	[HL,HMD,UL,PGL,FL, FMD,TL,TMD,PTW,MC]	1	53.8	136.2	12.1	2.5	12.6	58.5	148.9
				2	65.6	149.7	14.3	55	124.6	72	162.2
				3	47.3	127.8	16.2	35	101.2	54	135.8
				4	43.9	106.9	31.5	33.5	84.4	44.5	108.5
				5	31	69.9	15.2	27.5	66.2	32.5	73.4
				6	15.5	46.7	14	10.5	35.7	18.5	51.9
				7	48	126.6	20.4	32.5	81.2	49.5	129.4
				10	58.5	122.9	17.3	56	119.3	62.5	125.3
				11	36.5	68	18.1	32.5	62.7	41	80.5
				12	12	35.6	14.3	9	29.7	17	52.6
				15	16.3	52.1	14.9	0.5	8.1	18.5	57.3
				18	20.1	47.7	13.9	0	3.2	23.5	55.3

Limb

Time	Model	Module	Traits	Chrom	pos (cM)	pos (Mb)	LOD	lower CI (cM)	lower CI (Mb)	upper CI (cM)	upper CI (Mb)
5	H4	[limb lengths]	[HL,UL,FL,TL,MC]	1	53.8	136.2	10.5	47.5	121.3	59	153
				4	36.2	90.8	19	33.5	84.4	44.5	108.5
				7	37.1	90.8	14.8	33	81.3	40.5	103.1
				8	26	71	8.6	21.5	52.2	39	106.2
				10	56.7	119.4	12.7	46	111.3	63	125.9
				11	42	81.1	19.4	36	67.2	43.5	83.2
				12	22	63.5	9.1	20	58.6	29.5	81.8
				15	9	36.3	9	0	6.1	29.5	76.2
				16	21	42.1	10	15	34.2	27.5	59.3
		[limb diameters]	[HMD,FMD,TMD,PTW]	5	31.8	72.3	7.4	24.5	54.4	37.5	85.9

				7	34.5	82	7.6	28.5	75.2	38	91.6
				8	9.2	29.1	7.4	0	4.9	13.5	35.3
				10	53	118	12.4	49	113.6	63.5	125.9
				11	43.6	83.2	17.6	39	72.6	54	102
Time	Model	Module	Traits	Chrom	pos (cM)	pos (Mb)	LOD	lower CI (cM)	lower CI (Mb)	upper CI (cM)	upper CI (Mb)
10	H4	[limb lengths]	[HL,UL,FL,TL,MC]	1	57.5	144.2	9	52.5	134.6	65.5	165.3
				4	38.5	98.2	22.5	34.5	87	44.5	108.5
				7	37.1	90.8	13.6	30.5	77.6	48.5	126.9
				8	31.8	89	9.5	29	81.3	35	95.3
				10	58.5	122.9	13.4	55	119	63	125.9
				11	36.1	67.2	16.6	32.5	62.7	41	80.5
				12	28.6	79.8	7.5	9.5	30.4	48.5	109.9
				14	15	45.7	7	0	8.7	36	87.7
				15	8.2	34.1	11.7	0.5	8.1	20.5	61
		[limb diameters]	[HMD,FMD,TMD,PTW]	4	24.4	59.7	7.6	14	40.4	36.5	92.1
				5	45.2	106.6	9.7	21	49.5	48.5	114.6
				8	39.4	106.4	7.2	30.5	85	41.5	111.1
				10	11.9	28.6	10.8	9.5	24.7	62	125.3
				11	49.4	94.8	16	47.5	91.6	55.5	103.6
				12	9.5	30.4	9.6	4	15.9	15	45.5
				14	24.8	67.8	7.7	0.5	10	32.5	78.5
				15	7.5	30.7	8.5	5.5	26.6	24.5	68.7
				18	25	58.2	7.7	20	47.7	27.5	60.7
Time	Model	Module	Traits	Chr	pos	pos	LOD	lower	lower	upper	upper

				om	(cM)	(Mb)		CI (cM)	CI (Mb)	CI (cM)	CI (Mb)
16	H4	[limb lengths]	[HL,UL,FL,TL,MC]	1	54.2	137.1	8.9	2.5	12.6	58.5	148.9
				2	65.6	149.7	9.4	55	124.6	90	179
				4	43.9	106.9	22.6	35	88.2	45	110
				7	38.3	91.6	17.3	32.5	81.2	48.5	126.9
				10	58.5	122.9	13.6	57	120.8	62.5	125.3
				11	34.4	64.9	11.6	24	45.9	38	70.4
				12	12	35.6	8.4	9	29.7	17	52.6
				14	17.1	47.6	8	13.5	37.5	19.5	56.2
				15	1.3	11.3	9.1	0	6.1	16.5	52.5
				18	31.8	65.5	7.8	0	3.2	34.5	68.7
		[limb diameters]	[HMD,FMD,TMD,PTW]	2	70.9	161.3	7.6	56	127.8	76	166.5
				5	31	69.9	11.2	25.5	59.9	35	78.2
				7	34.5	82.2	7.2	32	80.1	53.5	134.4
				10	33.5	87.7	8.6	11	27.7	59.5	123.4
				11	39.5	74.9	8.5	32.5	62.7	44	85.8
				12	14.5	41.8	7.1	8.5	29.2	18	55.2
				15	16.5	52.5	8.3	6.5	28	19.5	58.6
				18	11.1	29.3	8.3	4.5	15.9	23.5	55.3

Genomic positions (in cM and Mb), chromosomal locations, LOD scores, and lower and upper confidence intervals (CI) in cM and Mb of skeletal modules of best-fitting models from MINT analyses at 5, 10, and 16 weeks of age. Confidence intervals are the 1.5 LOD interval.

Table S2.9 Tests for pleiotropy of skeletal modules

Whole skeleton											
Time	Model	Module	Traits	Chr	LOD	P/L	P-val	QTL 1 pos (cM)	QTL 1 traits	QTL 2 pos (cM)	QTL 2 traits
5	H1	[skull, pelvis]	[SL,SW,ZW,ZL,HCV, PGL, SVL]	1	19.3	P	0.41	37.9			
				3	9.3	P	0.88	30			
				4	25.9	P	0.7	36.4			
				5	9.6	P	0.86	32.9			
				6	8.3	P	0.13	30.1			
				7	12.2	P	0.2	62.5			
				8	9.9	P	0.13	59.4			
				10	24.6	P	0.47	60.7			
				11	19.2	L	0	8.5	SL, PGL, SVL	55.4	SW, ZW, ZL, HCV
				13	9.6	P	0.35	49.1			
				16	9.1	P	0.86	7.4			
				17	10.1	P	0.21	17.8			
		[Forelimb]	[HL, HMD, UL]	1	6.8	P	0.16	62.4			
				4	9.8	P	0.12	35.4			
				5	6	P	0.31	31.2			
				7	10.6	P	0.78	34.9			
				10	6.6	P	0.23	14.4			
				15	7.6	P	0.33	28.1			
				16	5.7	P	0.3	29.1			
		[Hindlimb]	[FL, FMD, TL, TMD, PTW, MC]	1	7.2	P	0.05	47.5			

				3	13.3	L	0.03	8.04	TL	48.84	FL, FMD, TMD, PTW, MC
				4	22.1	L	0.01	35.36	FL, TL, PTW, MC	57.81	FMD, TMD
				7	13.9	P	0.09	32.3			
				8	14.1	L	0	9.2	FMD, TMD	25.7	FL, TL, PTW, MC
				10	17.1	P	0.67	60.7			
				11	27.7	L	0	18.9	FL, MC	53	FMD, TL, TMD, PTW
				12	9.5	P	0.1	23.2			
				13	8	P	0.39	6			
				14	9.2	P	0.18	17.1			
				15	9.7	P	0.71	9.4			
				16	7.5	P	0.06	1.1			
				19	8.7	P	0.14	1.1			
Time	Model	Module	Traits	Chr	LOD	P/L	P-val	QTL 1 pos (cM)	Traits under QTL 1	QTL 2 pos (cM)	Traits under QTL 2
10	H1	[skull, pelvis]	[SL, SW, ZW, ZL, HCV, PGL, SVL]	1	11.3	P	0.23	37.9			
				3	14.4	P	0.55	13.6			
				4	27.1	L	0	36.4	ZW, HCV	61	SL, SW, ZL, PGL, SVL
				7	13.7	P	0.95	53.7			
				10	20.6	P	0.54	45.4			
				11	16.9	L	0	8.5	SL, PGL, SVL	50.1	SW, ZW, ZL, HCV
				13	9.8	P	0.19	47.9			
				15	11.3	P	0.1	7.5			
				17	8.9	P	0.16	15.1			

		[Forelimb]	[HL, HMD, UL]	1	4.9	P	0.53	62.4			
				4	13.1	P	0.12	30			
				7	6.9	P	0.24	22.5			
				10	7.1	P	0.28	13.6			
				15	9.3	P	0.36	16.7			
		[Hindlimb]	[FL, FMD, TL, TMD, PTW, MC]	1	6.8	P	0.45	64.7			
				2	9.8	P	0.62	56			
				3	13.5	P	0.12	51.8			
				4	27.3	P	0.12	35.1			
				5	6.2	P	0.21	23.8			
				6	6.6	P	0.2	46.2			
				7	13.1	P	0.83	47.3			
				8	10.7	P	0.22	31.3			
				9	6.1	P	0.07	6.6			
				10	15	P	0.09	56.8			
				11	23.7	L	0	36.3	FL, FMD, TL, PTW, MC	53	TMD
				12	11.5	P	0.69	9.6			
				14	12	P	0.15	8.5			
				15	14.6	P	0.67	7.5			
				18	9.7	P	0.15	22.9			

Time	Model	Module	Traits	Chr	LOD	P/L	P-val	QTL 1 pos (cM)	Traits under QTL 1	QTL 2 pos (cM)	Traits under QTL 2
16	H3	[axial]	[SL, SW, ZW, ZL, HCV, SVL]	1	14.1	L	0.03	30.4	SL, SW, ZW, ZL	68.3	HCV, SVL

		3	8.3	P	0.22	13.4			
		4	13.4	P	0.07	42.2			
		6	8.8	P	0.62	30.1			
		7	11.3	P	0.99	62.5			
		10	18.4	P	0.98	57.1			
		11	15.6	L	0	5.6	SL, SVL	50.1	SW, ZW, ZL, HCV
		15	10.4	P	0.48	12.3			
[appendicular]	[HL, HMD, UL, PGL, FL, FMD, TL, TMD, PTW, MC]	1	13.7	L	0.03	38.2	PGL, FMD	53.2	HL, HMD, UL, FL, TL, TMD, PTW, MC
		2	18.7	P	0.08	45.5			
		3	16.4	P	0.34	47.7			
		4	32.7	P	0.06	42.6			
		5	13.2	P	0.25	29.8			
		6	18.4	L	0	15.5	HMD, UL, TMD, PTW, MC	68.8	HL, PGL, FL, FMD, TL
		7	18.9	P	0.34	35.2			
		10	21.4	L	0	33.5	HMD, UL, FMD	58.5	HL, PGL, FL, TL, TMD, PTW, MC
		11	21.1	L	0.01	36.3	HL, HMD, UL, PGL, FL, FMD, TL, PTW, MC	65.4	TMD
		12	13.6	P	0.22	12			
		15	15.3	P	0.54	16.3			
		18	14.1	P	0.06	0			

Limb

Time	Model	Module	Traits	Ch	LOD	P/L	P-val	QTL 1 pos (cM)	Traits under QTL 1	QTL 2 pos (cM)	Traits under QTL 2
5	H4	[limb lengths]	[HL, UL, FL, TL, MC]	1	8.6	P	0.93	53.2			
				4	16.5	P	0.09	35.4			
				7	13.5	P	0.89	38.4			
				8	8	P	0.14	25.7			
				10	10.7	L	0	1.9	UL	53.9	HL, FL, TL, MC
				11	19.5	P	0.06	42.1			
				12	8.5	P	0.45	26.9			
				15	9.2	L	0	8.8	UL, FL, TL, MC	38.5	HL
				16	8.2	P	0.16	20.3			
		[limb diameters]	[HMD, FMD, TMD, PTW]	5	7	P	0.66	31.2			
				7	6.9	P	0.42	32			
				8	6.6	P	0.14	9.2			
				10	12.2	P	0.12	53			
				11	21.1	L	0	43.6	HMD, FMD	56.3	TMD, PTW

Time	Model	Module	Traits	Chr	LOD	P/L	P-val	QTL 1 pos (cM)	Traits under QTL 1	QTL 2 pos (cM)	Traits under QTL 2
10	H4	[limb lengths]	[HL, UL, FL, TL, MC]	1	7	P	0.43	61.6			
				4	19.8	P	0.12	41.8			
				7	12.6	P	0.96	47.8			
				8	7.3	P	0.62	32.6			
				10	12.7	P	0.2	58.5			

				11	15.3	L	0.02	33.8	HL, FL, TL, MC	65.5	UL
				12	6.9	P	0.12	47.6			
				14	7.3	P	0.52	34.2			
				15	11.3	P	0.09	9.4			
		[limb diameters]	[HMD, FMD, TMD, PTW]	4	7.7	P	0.45	32.9			
				5	8.2	P	0.28	22.4			
				8	6.8	P	0.73	36.5			
				10	16.7	L	0	11.9	HMD, FMD, TMD	56.3	PTW
				11	15	P	0.61	50.1			
				12	9.6	P	0.59	9.3			
				14	10	L	0.01	8.6	FMD, TMD	31.9	HMD, PTW
				15	7.9	P	0.34	10.6			
				18	7.6	P	0.95	25			

Time	Model	Module	Traits	Chrom	LOD	P/L	P-Value	QTL 1 pos (cM)	Traits under QTL 1	QTL 2 pos (cM)	Traits under QTL 2
16	H4	[limb lengths]	[HL, UL, FL, TL, MC]	1	7	P	0.17	53.2			
				2	19.3	L	0.01	45.5	HL, UL, FL, MC	81.9	TL
				4	20.4	P	0.85	42.6			
				7	15.8	P	0.18	38.3			
				10	15.1	L	0.02	21.3	HL, FL, TL, MC	58.3	UL
				11	10.7	P	0.58	34.3			
				12	7.2	P	0.26	11.8			
				14	7.3	P	0.23	17.1			
				15	9.4	P	0.99	1.3			

		18	10.1	L	0	0	HL, UL, FL, TL	31.8	MC
[limb diameters]	[HMD, FMD, TMD, PTW]	2	4.6	P	0.58	73.5			
		5	9.7	P	0.39	31			
		7	4.4	P	0.26	0.6			
		10	8.6	L	0.04	33.5	HMD, FMD, TMD	58.5	PTW
		11	7.6	L	0	36.6	HMD, FMD, PTW	65.4	TMD
		12	7.6	P	0.24	14.6			
		15	8.6	P	0.81	16.3			
		18	7.9	P	0.6	6.6			

Support for pleiotropy (P) and linkage (L) for sets of QTL for skeletal modules of best-fitting models from MINT analyses. QTL positions (in cM), LOD scores, and p-values are provided for each set of QTL. A large p-value indicates that the data are consistent with the pleiotropic model (H0). If Linkage is supported, QTL 1 and QTL 2 positions, along with the partitioning of traits affected by each of the two linked QTL, are listed.

Appendix B

Supplementary Material from Chapter 3

Figure S3.1 Plot of CV2 and CV3 scores for GI and WSB mandible specimens based on Procrustes coordinate data. CV scores are color-coded based strain and sex: GI = red; WSB = blue, females = orange; males = light blue.

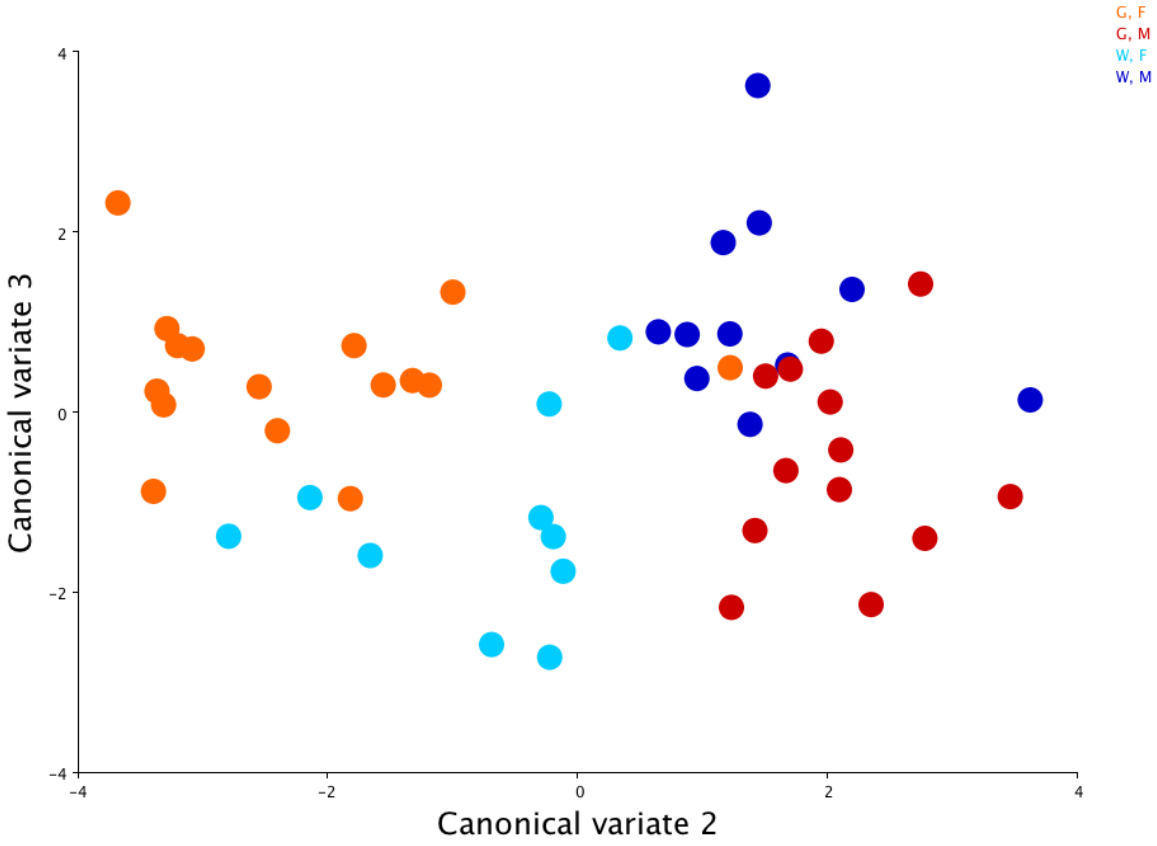

Figure S3.2 (A) Principal Components Analysis of Procrustes coordinates for F2 mandible specimens. (B) The positions of the top 4 landmarks contributing most to shape variation underlying principal components (PC) 1-5 are highlighted with yellow circles. Mandible diagram adapted from The Anatomy of the Laboratory Mouse (Cook 1965).

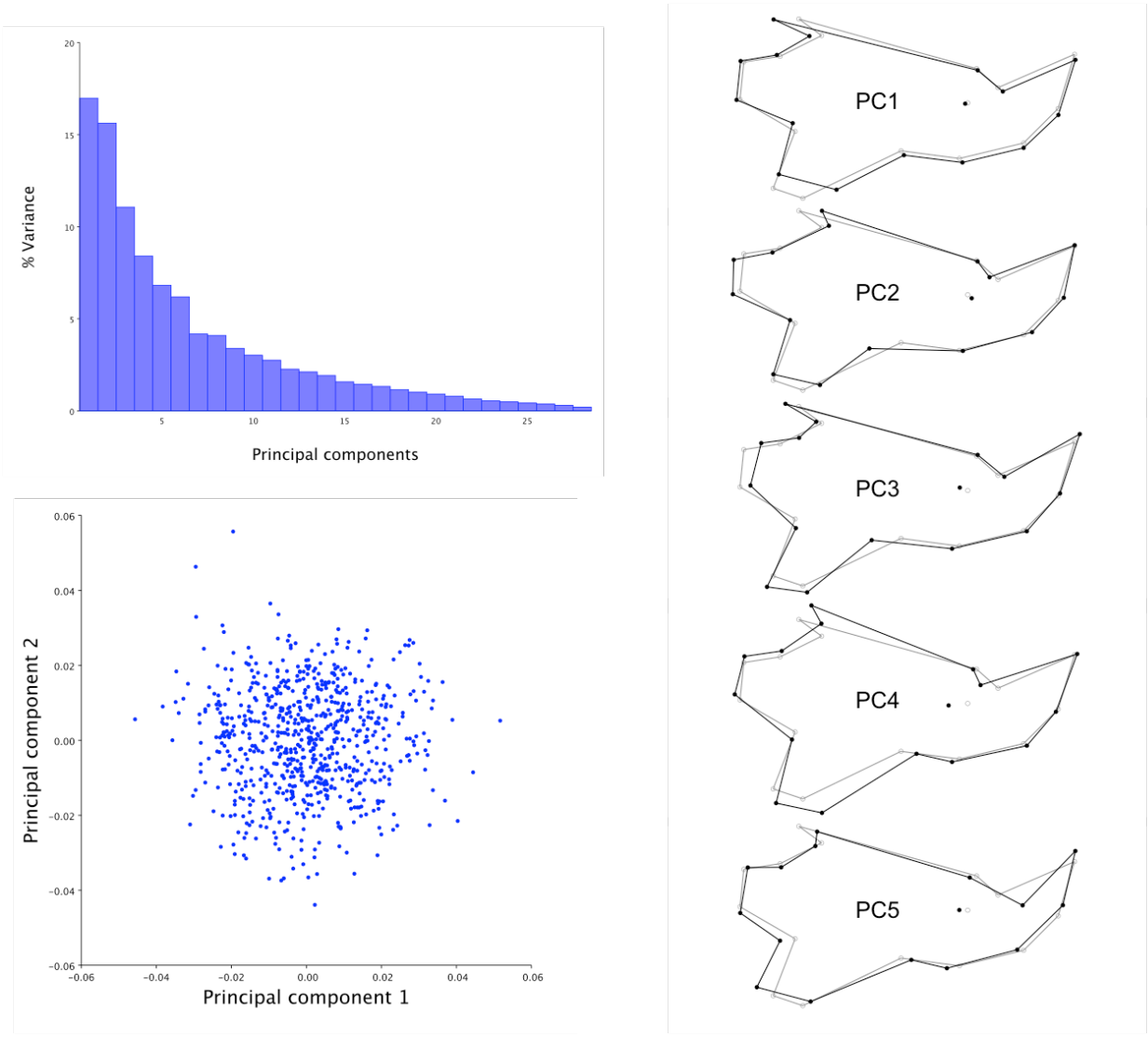

Figure S3.3 Dominance effects for QTL identified for (A) absolute Euclidean distances, (B) Euclidean distances adjusted for body weight, and (C) Euclidean distances with body weight as an additive covariate in the QTL model.

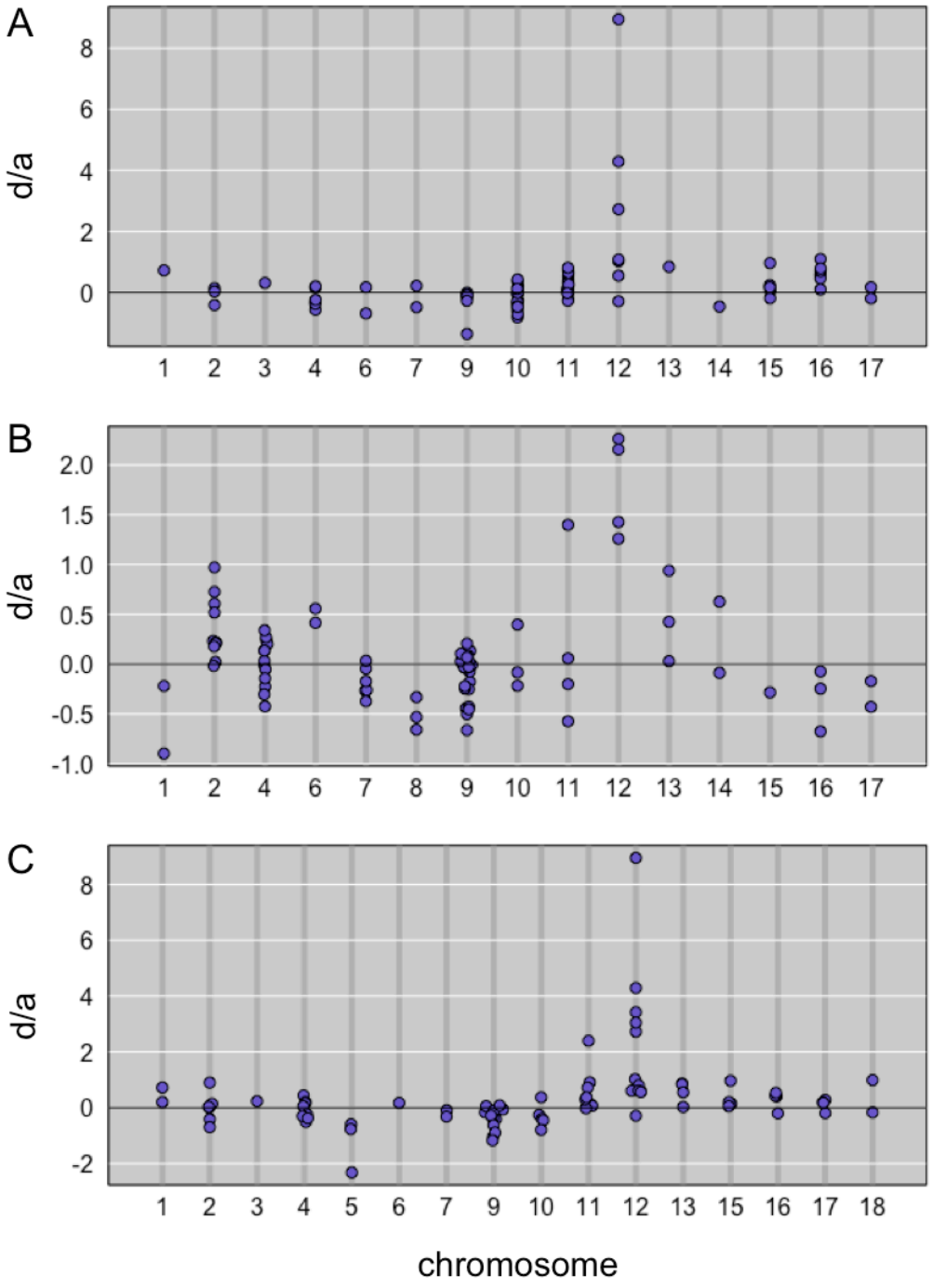

Figure S3.4 Mandible locations and QTL identified for Euclidean distances predicted to affect (A) leverage, (B) load resistance, (C) and movement of the mandible.

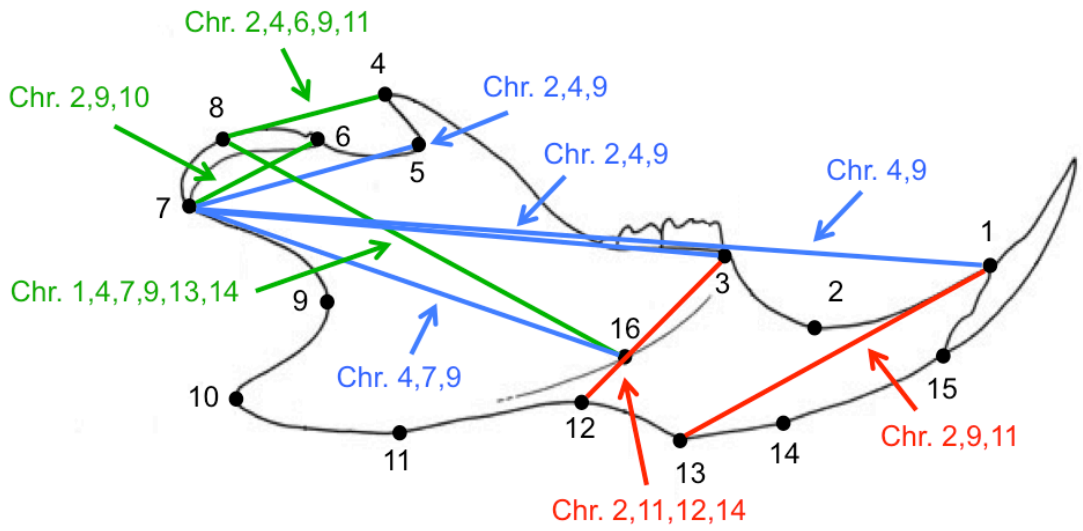

Table S3.1 Phenotypic means and standard deviations of all pairwise Euclidean distances measured between 16 landmarks for GI and WSB mandibles at age = 16 weeks.

Trait	GI F Average	GI F SD	WSB F Average	WSB F SD	P-Value	GI M Average	GI M SD	WSB M Average	WSB M SD	P-Value
1_2	3.46	0.21	2.98	0.16	0.000001	3.37	0.22	2.82	0.12	0.000000
1_3	4.09	0.21	3.40	0.25	0.000000	3.97	0.26	3.21	0.18	0.000000
1_4	11.39	0.44	9.75	0.67	0.000000	10.79	0.49	9.13	0.54	0.000000
1_5	10.37	0.36	8.77	0.49	0.000000	10.00	0.46	8.29	0.48	0.000000
1_6	11.86	0.36	10.15	0.62	0.000000	11.54	0.45	9.75	0.64	0.000000
1_7	13.65	0.47	11.47	0.48	0.000000	13.20	0.49	10.98	0.63	0.000000
1_8	13.24	0.39	11.52	0.65	0.000000	12.85	0.47	10.98	0.71	0.000000
1_9	11.58	0.43	9.93	0.43	0.000000	11.28	0.42	9.53	0.44	0.000000
1_10	13.24	0.47	11.33	0.52	0.000000	12.95	0.50	10.92	0.51	0.000000
1_11	12.57	0.50	10.33	0.55	0.000000	12.20	0.51	10.04	0.42	0.000000
1_12	7.61	0.33	6.79	0.37	0.000002	7.57	0.38	6.58	0.31	0.000001
1_13	6.18	0.27	5.53	0.27	0.000001	6.03	0.29	5.32	0.24	0.000002
1_14	4.24	0.27	3.75	0.28	0.000101	4.13	0.32	3.48	0.29	0.000044
1_15	2.36	0.48	1.88	0.18	0.003403	2.25	0.16	1.83	0.11	0.000000
1_16	4.76	0.25	4.18	0.26	0.000003	4.63	0.31	4.03	0.16	0.000007
2_3	1.22	0.15	0.94	0.16	0.000190	1.15	0.20	0.82	0.14	0.000173
2_4	8.58	0.36	7.40	0.63	0.000002	8.03	0.42	6.88	0.47	0.000002
2_5	7.45	0.28	6.33	0.44	0.000000	7.14	0.40	5.96	0.41	0.000001
2_6	8.78	0.29	7.54	0.57	0.000000	8.52	0.36	7.25	0.57	0.000002
2_7	7.35	0.38	5.93	0.45	0.000000	7.07	0.50	6.11	1.58	0.050125
2_8	10.09	0.32	8.89	0.59	0.000000	9.77	0.38	8.45	0.64	0.000004
2_9	8.16	0.29	7.01	0.34	0.000000	7.94	0.28	6.74	0.35	0.000000
2_10	9.79	0.34	8.36	0.40	0.000000	9.59	0.35	8.10	0.41	0.000000
2_11	9.12	0.38	7.34	0.47	0.000000	8.85	0.35	7.23	0.34	0.000000
2_12	4.19	0.21	3.85	0.23	0.000682	4.24	0.27	3.78	0.24	0.000244
2_13	3.10	0.15	2.86	0.11	0.000127	3.06	0.13	2.78	0.15	0.000063
2_14	2.49	0.10	2.18	0.07	0.000000	2.47	0.09	2.08	0.11	0.000000
2_15	2.63	0.29	2.28	0.12	0.001195	2.65	0.16	2.18	0.13	0.000000
2_16	1.30	0.10	1.22	0.11	0.086796	1.26	0.19	1.21	0.10	0.412483
3_4	7.50	0.32	6.59	0.52	0.000017	7.01	0.26	6.15	0.36	0.000001
3_5	6.40	0.23	5.54	0.30	0.000000	6.15	0.25	5.24	0.30	0.000000
3_6	7.82	0.24	6.84	0.46	0.000000	7.62	0.27	6.60	0.46	0.000001
3_7	9.57	0.36	8.12	0.30	0.000000	9.23	0.32	7.77	0.45	0.000000
3_8	9.17	0.30	8.22	0.47	0.000001	8.91	0.29	7.82	0.53	0.000003
3_9	7.56	0.28	6.61	0.22	0.000000	7.38	0.24	6.34	0.29	0.000000
3_10	9.43	0.34	8.13	0.35	0.000000	9.26	0.33	7.85	0.37	0.000000
3_11	8.88	0.37	7.24	0.47	0.000000	8.62	0.34	7.07	0.31	0.000000
3_12	4.14	0.19	3.84	0.17	0.000669	4.15	0.23	3.72	0.22	0.000118
3_13	3.65	0.16	3.29	0.13	0.000005	3.57	0.21	3.10	0.20	0.000015

3_14	3.65	0.17	3.09	0.19	0.000000	3.55	0.23	2.86	0.19	0.000000
3_15	3.76	0.29	3.14	0.16	0.000005	3.72	0.26	2.93	0.23	0.000000
3_16	1.42	0.12	1.34	0.08	0.086129	1.38	0.16	1.27	0.10	0.065398
4_5	1.18	0.10	1.15	0.25	0.591244	0.98	0.11	0.99	0.14	0.834701
4_6	1.52	0.21	1.34	0.13	0.022387	1.66	0.16	1.44	0.13	0.001926
4_7	3.94	0.29	3.17	0.11	0.000000	3.99	0.32	3.21	0.22	0.000001
4_8	2.65	0.30	2.24	0.17	0.000619	2.82	0.24	2.37	0.23	0.000188
4_9	4.54	0.22	3.90	0.16	0.000000	4.47	0.27	3.87	0.23	0.000009
4_10	6.99	0.30	5.85	0.27	0.000000	6.96	0.43	5.78	0.28	0.000000
4_11	7.34	0.26	6.23	0.31	0.000000	7.17	0.38	6.06	0.23	0.000000
4_12	6.95	0.25	6.04	0.40	0.000000	6.43	0.27	5.61	0.34	0.000001
4_13	8.65	0.35	7.51	0.53	0.000001	8.20	0.39	6.98	0.45	0.000000
4_14	10.42	0.37	9.03	0.56	0.000000	9.88	0.39	8.47	0.46	0.000000
4_15	11.17	0.52	9.69	0.61	0.000001	10.68	0.48	9.06	0.57	0.000000
4_16	7.67	0.33	6.67	0.43	0.000000	7.19	0.32	6.16	0.46	0.000002
5_6	1.68	0.26	1.56	0.28	0.256096	1.75	0.22	1.63	0.16	0.160002
5_7	4.10	0.30	3.37	0.12	0.000000	4.02	0.28	3.31	0.21	0.000002
5_8	3.11	0.29	4.18	4.28	0.307830	3.11	0.21	2.83	0.24	0.007567
5_9	3.95	0.23	4.66	4.14	0.486962	3.91	0.26	3.38	0.22	0.000038
5_10	6.51	0.31	6.70	4.11	0.846556	6.47	0.40	5.36	0.24	0.000000
5_11	6.71	0.27	6.78	3.84	0.939184	6.56	0.36	5.47	0.20	0.000000
5_12	5.80	0.19	5.93	3.19	0.868362	5.47	0.24	4.69	0.30	0.000001
5_13	7.48	0.30	7.17	2.56	0.618626	7.22	0.37	6.00	0.40	0.000000
5_14	9.25	0.30	8.42	1.72	0.061558	8.93	0.38	7.49	0.42	0.000000
5_15	10.04	0.49	8.96	1.11	0.001489	9.78	0.46	8.13	0.52	0.000000
5_16	6.52	0.26	6.23	2.28	0.614968	6.26	0.32	5.18	0.42	0.000001
6_7	2.50	0.27	1.89	0.22	0.000001	2.36	0.29	1.77	0.10	0.000004
6_8	1.44	0.14	1.38	0.15	0.338712	1.37	0.13	1.24	0.10	0.000004
6_9	3.23	0.17	2.74	0.19	0.000000	3.14	0.24	2.67	0.22	0.018191
6_10	5.57	0.29	4.58	0.27	0.000000	5.48	0.41	4.43	0.23	0.000084
6_11	6.00	0.22	5.08	0.29	0.000000	5.81	0.34	4.87	0.26	0.000000
6_12	6.43	0.21	5.48	0.37	0.000000	6.08	0.27	5.20	0.43	0.000000
6_13	8.32	0.28	7.14	0.49	0.000000	8.08	0.32	6.77	0.55	0.000007
6_14	10.34	0.31	8.91	0.53	0.000000	10.05	0.34	8.55	0.57	0.000000
6_15	11.34	0.53	9.83	0.57	0.000000	11.13	0.42	9.41	0.68	0.000000
6_16	7.72	0.28	6.64	0.43	0.000000	7.51	0.34	6.32	0.58	0.000000
7_8	1.47	0.17	1.36	0.14	0.070709	1.40	0.19	1.21	0.11	0.010386
7_9	2.71	0.16	2.21	0.15	0.000000	2.57	0.22	2.14	0.21	0.000109
7_10	4.00	0.27	3.32	0.21	0.000000	3.93	0.40	3.23	0.20	0.000026
7_11	4.77	0.18	4.24	0.27	0.000001	4.61	0.27	4.03	0.29	0.000042
7_12	7.15	0.34	5.87	0.32	0.000000	6.67	0.36	5.52	0.43	0.000000
7_13	9.18	0.34	7.68	0.36	0.000000	8.84	0.29	7.27	0.50	0.000000
7_14	11.48	0.43	9.70	0.36	0.000000	11.08	0.36	9.32	0.53	0.000000

7_15	12.90	0.48	10.91	0.47	0.000000	12.45	0.47	10.41	0.65	0.000000
7_16	9.16	0.39	7.63	0.28	0.000000	8.82	0.40	7.26	0.55	0.000000
8_9	3.44	0.13	3.24	0.23	0.007307	3.32	0.21	3.07	0.28	0.025732
8_10	5.28	0.27	4.63	0.27	0.000001	5.19	0.38	4.41	0.26	0.000018
8_11	5.93	0.19	5.45	0.34	0.000058	5.75	0.31	5.13	0.34	0.000178
8_12	7.39	0.27	6.56	0.40	0.000001	6.97	0.31	6.15	0.51	0.000093
8_13	9.36	0.29	8.30	0.51	0.000000	9.07	0.31	7.79	0.60	0.000002
8_14	11.51	0.35	10.17	0.53	0.000000	11.16	0.36	9.67	0.62	0.000000
8_15	12.62	0.57	11.17	0.60	0.000001	12.35	0.44	10.60	0.75	0.000001
8_16	8.98	0.32	7.95	0.42	0.000000	8.70	0.36	7.49	0.64	0.000011
9_10	2.58	0.12	2.08	0.20	0.000000	2.57	0.24	2.01	0.17	0.000002
9_11	2.81	0.12	2.38	0.22	0.000000	2.71	0.16	2.23	0.17	0.000000
9_12	4.56	0.22	3.77	0.28	0.000000	4.24	0.21	3.51	0.28	0.000000
9_13	6.59	0.24	5.60	0.29	0.000000	6.41	0.15	5.28	0.30	0.000000
9_14	8.98	0.34	7.73	0.28	0.000000	8.74	0.28	7.44	0.33	0.000000
9_15	10.44	0.61	9.12	0.40	0.000001	10.27	0.38	8.71	0.46	0.000000
9_16	6.89	0.29	5.86	0.19	0.000000	6.72	0.32	5.59	0.36	0.000000
10_11	1.02	0.17	1.35	0.34	0.002108	1.03	0.33	1.21	0.31	0.166583
10_12	5.70	0.28	4.65	0.25	0.000000	5.42	0.29	4.43	0.32	0.000000
10_13	7.54	0.28	6.35	0.34	0.000000	7.37	0.22	6.08	0.34	0.000000
10_14	10.03	0.39	8.62	0.35	0.000000	9.80	0.33	8.37	0.38	0.000000
10_15	11.76	0.70	10.26	0.48	0.000001	11.60	0.46	9.85	0.52	0.000000
10_16	8.49	0.35	7.15	0.30	0.000000	8.33	0.37	6.90	0.42	0.000000
11_12	4.96	0.33	3.56	0.46	0.000000	4.63	0.42	3.47	0.36	0.000000
11_13	6.71	0.33	5.15	0.46	0.000000	6.48	0.32	5.01	0.34	0.000000
11_14	9.19	0.43	7.42	0.49	0.000000	8.91	0.37	7.31	0.33	0.000000
11_15	10.98	0.71	9.14	0.58	0.000000	10.75	0.51	8.86	0.42	0.000000
11_16	7.84	0.40	6.16	0.45	0.000000	7.60	0.41	6.02	0.33	0.000000
12_13	2.04	0.24	1.83	0.23	0.025726	2.17	0.23	1.77	0.25	0.000481
12_14	4.45	0.23	4.02	0.24	0.000054	4.53	0.23	3.99	0.35	0.000193
12_15	6.08	0.58	5.62	0.31	0.022730	6.21	0.37	5.43	0.32	0.000018
12_16	2.93	0.20	2.64	0.16	0.000588	3.00	0.21	2.59	0.28	0.000417
13_14	2.49	0.21	2.27	0.09	0.003388	2.43	0.17	2.30	0.17	0.064000
13_15	4.31	0.59	4.08	0.26	0.221833	4.30	0.28	3.90	0.22	0.000850
13_16	2.24	0.15	1.96	0.14	0.000038	2.21	0.14	1.86	0.15	0.000005
14_15	2.05	0.39	1.99	0.29	0.658780	2.04	0.31	1.77	0.27	0.033283
14_16	2.81	0.12	2.40	0.16	0.000000	2.74	0.14	2.32	0.11	0.000000
15_16	3.66	0.43	3.28	0.22	0.013156	3.65	0.27	3.15	0.14	0.000011

Table S3.2 One-way ANOVA table comparing the effects of strain and sex on maximum bite force and maximum passive gape between GI and WSB.

Trait	ANOVA				
Maximum Bite Force	Df	Sum Sq	Mean Sq	F	P
Strain	1	23.798	23.798	33.205	9.42e-07 ***
Sex	1	2.694	2.694	3.759	0.0594
Strain x Sex	1	0.057	0.057	0.08	0.7788
Residuals	41	29.385	0.717		
Relative Max Bite Force	Df	Sum Sq	Mean Sq	F	P
Strain	1	0.8685	0.8685	11.748	0.0014 **
Sex	1	0.1564	0.1564	2.116	0.1534
Strain x Sex	1	0.0068	0.0068	0.092	0.7631
Residuals	41	3.031	0.0739		
Maximum Gape	Df	Sum Sq	Mean Sq	F	P
Strain	1	22.184	22.184	34.837	4.7e-07 ***
Sex	1	0.199	0.199	0.313	0.579
Strain x Sex	1	0.298	0.298	0.469	0.497
Residuals	44	28.019	0.637		
Relative Maximum Gape	Df	Sum Sq	Mean Sq	F	P
Strain	1	0.113	0.11319	1.384	0.246
Sex	1	0.07	0.07024	0.859	0.359
Strain x Sex	1	0.008	0.0078	0.095	0.759
Residuals	44	3.598	0.08177		

Table S3.3 Genomic positions, LOD scores, and effect sizes of QTL identified for absolute and relative Euclidean distances, Euclidean distances with body weight as a covariate, principal components (PC) from PCA, and centroid size (CS).

Trait	Treatment	Marker	Chr	Pos	LOD	Low CI	High CI	GG	GW	WW	a	d	d/a	N	SD	a/SD
L1-7	ABS	UNC18746398	10	47.8	9.6	43.7	61.7	12.18	12.00	11.89	0.14	-0.04	-0.26	744	0.42	0.34
L1-7	ABS	UNC19597461	11	26.3	6.1	23.5	39.1	12.11	12.02	11.88	0.12	0.02	0.17	744	0.42	0.28
L9-12	ABS	UNC8349017	4	64.6	9.9	58.7	66.1	3.74	3.85	3.91	-0.09	0.03	-0.30	753	0.27	-0.33
L9-12	ABS	UNC16310877	9	17.1	4.7	2.7	32.6	3.75	3.87	3.85	-0.05	0.07	-1.36	753	0.27	-0.18
L9-12	ABS	UNC20343150	11	58.6	4.7	5.6	61.9	3.89	3.85	3.75	0.07	0.03	0.40	753	0.27	0.25
L7-10	ABS	JAX00651832	7	45.1	6.3	42.9	62.4	3.46	3.37	3.34	0.06	-0.03	-0.48	752	0.22	0.26
L7-10	ABS	UNC18906603	10	60.1	5.2	50.6	67.0	3.44	3.39	3.33	0.06	0.00	0.00	752	0.22	0.26
L7-10	ABS	UNC25202762	15	4.2	13.2	0.0	8.2	3.47	3.39	3.30	0.08	0.00	0.06	752	0.22	0.39
L7-10	ABS	JAX00076212	17	16.2	4.6	3.7	22.2	3.34	3.38	3.44	-0.05	-0.01	0.17	752	0.22	-0.24
L7-13	ABS	UNC030456578	3	18.8	5.0	11.7	36.6	8.14	8.09	7.99	0.08	0.02	0.32	757	0.34	0.23
L7-13	ABS	UNC18750788	10	47.8	6.0	33.3	65.3	8.20	8.06	8.02	0.09	-0.05	-0.59	757	0.34	0.26
L7-13	ABS	UNC19780488	11	33.6	6.4	23.5	35.5	8.17	8.08	7.99	0.09	0.00	-0.02	757	0.34	0.27
L7-13	ABS	UNC21390243	12	25.4	4.3	22.6	47.6	8.04	8.13	8.01	0.01	0.11	8.95	757	0.34	0.04
L11-15	ABS	UNC20507933	11	73.9	4.4	27.5	77.0	9.71	9.66	9.51	0.10	0.05	0.54	748	0.44	0.22
L11-15	ABS	UNC21399053	12	26.9	4.1	15.6	39.5	9.71	9.66	9.51	0.10	0.05	0.55	748	0.44	0.23
L8-4	ABS	UNC3474714	2	44.4	5.1	38.9	81.9	2.57	2.51	2.43	0.07	0.01	0.14	744	0.26	0.27
L8-4	ABS	UNC6852444	4	6.0	4.3	1.6	46.6	2.44	2.49	2.56	-0.06	-0.01	0.16	744	0.26	-0.23
L8-4	ABS	JAX00698977	9	31.0	9.9	24.5	37.7	2.41	2.49	2.57	-0.08	0.00	-0.01	744	0.26	-0.31
L8-4	ABS	UNC26231186	15	51.8	4.0	47.1	53.3	2.55	2.50	2.43	0.06	0.01	0.15	744	0.26	0.23
L8-16	ABS	UNC18750788	10	47.8	5.0	43.4	57.8	8.22	8.07	8.05	0.08	-0.07	-0.81	756	0.37	0.22
L8-16	ABS	UNC19667803	11	28.9	4.3	17.6	34.9	8.18	8.10	8.01	0.09	0.01	0.13	756	0.37	0.23
L8-16	ABS	UNC22472068	13	10.3	4.4	2.8	2.9	8.14	8.13	7.98	0.08	0.07	0.84	756	0.37	0.21
L3-7	ABS	JAX00299656	10	50.9	7.8	43.7	55.7	8.60	8.47	8.41	0.09	-0.03	-0.34	747	0.31	0.31
L3-7	ABS	UNC19667803	11	28.9	7.1	23.5	35.5	8.57	8.49	8.39	0.09	0.01	0.11	747	0.31	0.29
L3-7	ABS	UNC21435638	12	28.1	4.1	22.6	47.6	8.46	8.53	8.42	0.02	0.09	4.29	747	0.31	0.07
L7-16	ABS	UNC18796530	10	51.1	5.1	41.8	60.7	8.22	8.07	8.05	0.09	-0.06	-0.71	749	0.37	0.23
L7-16	ABS	UNC19667803	11	28.9	5.6	23.0	36.2	8.20	8.10	8.00	0.10	0.00	0.05	749	0.37	0.26
L7-16	ABS	UNC21390243	12	25.4	4.7	21.3	29.8	8.09	8.16	8.01	0.04	0.11	2.73	749	0.37	0.11
L5-7	ABS	UNC16706423	9	31.8	8.7	26.6	47.6	3.62	3.70	3.75	-0.07	0.01	-0.16	724	0.20	-0.32

L5-7	ABS	UNC18831913	10	54.9	6.4	47.4	63.5	3.75	3.69	3.63	0.06	0.00	-0.04	724	0.20	0.29
L5-7	ABS	UNC19667803	11	28.9	6.8	16.0	39.1	3.75	3.69	3.63	0.06	0.00	0.04	724	0.20	0.29
L5-7	ABS	364959	16	0.3	4.0	0.0	14.6	3.72	3.70	3.64	0.04	0.02	0.58	724	0.20	0.20
L3-12	ABS	UNC8335888	4	62.0	6.2	53.4	76.5	4.03	3.98	3.92	0.06	0.01	0.20	751	0.20	0.27
L3-12	ABS	UNC21390243	12	25.4	5.2	20.3	29.8	4.00	4.00	3.91	0.04	0.04	1.02	751	0.20	0.21
L1-13	ABS	UNC3371968	2	43.6	5.4	36.9	46.3	5.62	5.53	5.49	0.06	-0.03	-0.41	751	0.22	0.30
L1-13	ABS	JAX00301197	10	58.5	4.1	43.7	64.7	5.58	5.54	5.48	0.05	0.01	0.22	751	0.22	0.24
L1-13	ABS	UNC150107299	15	8.2	4.6	0.0	15.3	5.58	5.54	5.48	0.05	0.01	0.24	751	0.22	0.23
L6-7	ABS	UNC17559025	10	7.0	9.6	3.5	24.2	2.14	2.11	2.04	0.05	0.02	0.37	747	0.16	0.31
L6-7	ABS	UNC20482098	11	71.4	6.2	61.5	77.0	2.12	2.11	2.04	0.04	0.03	0.72	747	0.16	0.25
L6-7	ABS	UNC26301227	16	2.6	5.1	0.0	53.3	2.13	2.11	2.06	0.04	0.02	0.46	747	0.16	0.23
L11-12	ABS	UNC110175963	11	60.5	5.8	54.7	63.1	3.97	3.90	3.77	0.10	0.03	0.32	753	0.38	0.27
L11-13	ABS	UNC19780488	11	33.6	4.8	27.5	36.5	5.84	5.74	5.67	0.08	-0.02	-0.23	753	0.35	0.24
L11-13	ABS	JAX00069042	16	22.4	4.6	15.8	44.2	5.78	5.79	5.66	0.06	0.07	1.09	753	0.35	0.17
L1-15	ABS	JAX00254507	1	33.2	5.6	27.8	36.6	2.04	2.03	1.98	0.03	0.02	0.73	753	0.13	0.23
L1-15	ABS	UNC12159294	6	54.7	9.8	46.6	59.1	2.06	2.03	1.97	0.05	0.01	0.17	753	0.13	0.34
L1-15	ABS	JAX00637356	7	17.3	5.1	8.7	61.2	2.05	2.03	1.99	0.03	0.01	0.22	753	0.13	0.25
L9-10	ABS	UNC18966502	10	65.9	4.3	49.4	67.0	2.22	2.17	2.15	0.04	-0.01	-0.29	752	0.17	0.22
L9-10	ABS	JAX00316240	11	41.2	6.1	24.1	47.8	2.23	2.17	2.14	0.04	-0.01	-0.27	752	0.17	0.25
L9-10	ABS	UNC24065075	14	21.4	4.5	1.0	25.6	2.14	2.19	2.21	-0.03	0.02	-0.46	752	0.17	-0.21
L9-10	ABS	JAX00061684	15	13.7	4.3	0.0	20.1	2.22	2.18	2.15	0.04	-0.01	-0.19	752	0.17	0.23
L3-15	ABS	UNC8081790	4	48.6	7.1	43.3	65.0	3.18	3.25	3.26	-0.04	0.02	-0.57	753	0.15	-0.27
L3-15	ABS	UNC18746398	10	47.8	8.4	43.7	52.4	3.29	3.22	3.20	0.05	-0.02	-0.45	753	0.15	0.31
L3-15	ABS	UNC21392101	12	25.5	6.2	22.6	29.1	3.25	3.25	3.18	0.03	0.04	1.08	753	0.15	0.22
L3-15	ABS	UNC160190867	16	0.3	4.2	0.0	7.4	3.27	3.24	3.20	0.03	0.00	0.10	753	0.15	0.21
L4-7	ABS	UNC3776734	2	51.9	8.3	40.0	57.9	3.64	3.57	3.49	0.08	0.00	0.04	745	0.22	0.34
L4-7	ABS	JAX00173604	9	33.6	13.1	27.6	37.7	3.47	3.56	3.64	-0.09	0.01	-0.06	745	0.22	-0.39
L4-7	ABS	JAX00412482	16	0.0	4.4	0.0	8.1	3.58	3.57	3.49	0.05	0.03	0.70	745	0.22	0.20
L11-14	ABS	JAX00301340	10	60.7	4.5	25.0	67.0	8.20	8.11	8.00	0.10	0.01	0.15	750	0.39	0.25
L11-14	ABS	UNC19782007	11	33.8	5.6	25.7	44.7	8.20	8.11	7.99	0.10	0.01	0.10	750	0.39	0.27
L11-14	ABS	JAX00418890	16	20.8	4.0	0.0	41.9	8.15	8.13	8.00	0.07	0.06	0.79	750	0.39	0.19
L10-12	ABS	UNC8349017	4	64.6	8.1	58.7	66.1	4.64	4.77	4.83	-0.09	0.04	-0.37	752	0.31	-0.30
L10-12	ABS	UNC10731520	6	6.7	5.6	0.0	7.8	4.83	4.72	4.70	0.07	-0.05	-0.69	752	0.31	0.22

L10-12	ABS	UNC20343150	11	58.6	8.8	56.8	62.8	4.84	4.76	4.63	0.10	0.03	0.26	752	0.31	0.33
L6-10	ABS	UNC18906603	10	60.1	7.0	51.1	67.0	4.79	4.71	4.64	0.07	0.00	0.00	751	0.25	0.30
L6-10	ABS	UNC20484054	11	71.4	4.4	66.5	77.0	4.75	4.73	4.64	0.05	0.03	0.64	751	0.25	0.22
L6-10	ABS	UNC25242917	15	6.0	6.9	0.0	8.7	4.78	4.72	4.64	0.07	0.01	0.17	751	0.25	0.27
L1-3	ABS	UNC16618912	9	28.1	4.2	16.2	38.1	3.49	3.53	3.56	-0.03	0.00	-0.09	753	0.16	-0.20
L1-3	ABS	UNC18905760	10	60.0	7.2	40.7	64.7	3.56	3.54	3.47	0.05	0.02	0.43	753	0.16	0.29
L1-3	ABS	UNC27696615	17	8.4	4.7	4.9	31.4	3.57	3.52	3.49	0.04	-0.01	-0.19	753	0.16	0.23
L7-12	ABS	UNC8349017	4	64.6	7.1	58.1	67.7	5.91	6.03	6.10	-0.09	0.02	-0.24	756	0.33	-0.28
L7-12	ABS	UNC16675236	9	31.1	5.4	9.3	34.9	5.92	6.03	6.09	-0.09	0.02	-0.27	756	0.33	-0.26
L7-12	ABS	UNC19667803	11	29.0	4.6	6.3	59.6	6.09	6.01	5.94	0.08	0.00	-0.02	756	0.33	0.23
L7-9	ABS	JAX00299656	10	50.9	6.2	41.8	57.8	2.33	2.26	2.24	0.04	-0.02	-0.47	754	0.16	0.27
L7-9	ABS	UNC20799452	12	9.3	4.1	5.9	21.1	2.31	2.27	2.24	0.04	-0.01	-0.29	754	0.16	0.22
L7-9	ABS	UNC24994731	15	0.5	5.9	0.0	8.8	2.29	2.29	2.22	0.04	0.03	0.97	754	0.16	0.22
L1-11	ABS	JAX00301340	10	60.7	4.8	50.7	67.0	11.06	10.96	10.83	0.11	0.01	0.12	748	0.45	0.26
L1-11	ABS	UNC20534356	11	76.4	4.1	25.7	77.0	11.00	10.98	10.83	0.09	0.07	0.81	748	0.45	0.20
L1-7	REL	UNC3985525	2	57.6	4.8	44.2	59.0	4.38	4.36	4.27	0.05	0.03	0.61	719	0.25	0.22
L1-7	REL	UNC6866651	4	6.2	4.6	0.0	18.3	4.29	4.33	4.39	-0.05	-0.01	0.24	719	0.25	-0.20
L1-7	REL	UNC16479547	9	24.5	6.8	15.9	39.9	4.26	4.34	4.40	-0.07	0.01	-0.18	719	0.25	-0.27
L9-12	REL	UNC8349017	4	64.6	7.6	58.1	69.8	1.35	1.39	1.41	-0.03	0.01	-0.23	728	0.13	-0.25
L9-12	REL	UNC080272713	8	27.5	5.7	24.6	31.3	1.34	1.40	1.41	-0.03	0.02	-0.66	728	0.13	-0.25
L9-12	REL	JAX00695211	9	22.4	7.2	5.1	33.2	1.34	1.39	1.41	-0.04	0.02	-0.44	728	0.13	-0.28
L9-12	REL	UNC18515876	10	39.7	4.0	0.0	46.8	1.36	1.39	1.41	-0.03	0.00	-0.08	728	0.13	-0.21
L7-10	REL	UNC16561779	9	26.0	5.6	22.4	34.1	1.20	1.22	1.25	-0.02	0.00	-0.07	727	0.09	-0.28
L7-10	REL	UNC25199618	15	4.2	8.3	0.0	6.0	1.25	1.22	1.20	0.03	-0.01	-0.28	727	0.09	0.31
L7-10	REL	UNC27950488	17	16.2	5.5	6.9	21.6	1.20	1.22	1.24	-0.02	0.00	-0.17	727	0.09	-0.24
L7-13	REL	JAX00222885	4	7.2	5.0	0.0	13.5	2.88	2.92	2.96	-0.04	0.00	-0.01	732	0.19	-0.21
L7-13	REL	UNC16686479	9	31.4	6.0	5.6	40.5	2.86	2.92	2.97	-0.06	0.00	-0.03	732	0.19	-0.29
L11-15	REL	UNC13134657	7	32.8	5.0	28.5	53.7	3.43	3.48	3.52	-0.04	0.00	-0.05	723	0.19	-0.23
L11-15	REL	UNC16619894	9	28.7	5.2	13.0	55.2	3.42	3.48	3.53	-0.05	0.00	-0.01	723	0.19	-0.28
L11-15	REL	UNC21428926	12	27.9	4.8	11.1	36.5	3.48	3.49	3.43	0.03	0.04	1.43	723	0.19	0.13
L8-4	REL	JAX00502246	2	55.2	6.4	43.2	66.7	0.93	0.90	0.87	0.03	0.00	0.02	721	0.10	0.31
L8-4	REL	UNC6866651	4	6.2	7.0	4.1	18.3	0.87	0.90	0.93	-0.03	-0.01	0.20	721	0.10	-0.30
L8-4	REL	UNC10992143	6	14.5	4.9	9.1	22.7	0.88	0.89	0.93	-0.02	-0.01	0.56	721	0.10	-0.23

L8-4	REL	UNC16642471	9	29.5	12.4	24.5	37.7	0.86	0.90	0.94	-0.04	0.00	0.03	721	0.10	-0.40
L8-4	REL	JAX00321431	11	58.8	4.4	49.7	77.0	0.87	0.90	0.92	-0.02	0.00	-0.20	721	0.10	-0.23
L8-16	REL	JAX00247992	1	18.9	5.3	4.7	23.4	2.88	2.93	2.96	-0.04	0.01	-0.22	731	0.19	-0.21
L8-16	REL	JAX00222885	4	7.2	4.5	0.0	18.3	2.89	2.92	2.97	-0.04	-0.01	0.14	731	0.19	-0.21
L8-16	REL	UNC13659934	7	44.9	5.3	37.1	55.5	2.88	2.93	2.96	-0.04	0.01	-0.26	731	0.19	-0.22
L8-16	REL	UNC16561779	9	26.0	5.2	10.3	40.5	2.87	2.93	2.97	-0.05	0.01	-0.25	731	0.19	-0.26
L8-16	REL	UNC22472068	13	10.3	3.9	8.2	21.5	2.94	2.94	2.88	0.03	0.03	0.94	731	0.19	0.15
L8-16	REL	UNC24849100	14	51.8	4.4	48.0	58.5	2.95	2.93	2.88	0.03	0.02	0.63	731	0.19	0.16
L3-7	REL	UNC6866651	4	6.2	4.9	0.0	11.5	3.03	3.06	3.11	-0.04	-0.01	0.27	722	0.19	-0.21
L3-7	REL	UNC16699990	9	31.6	4.9	9.3	53.2	3.01	3.07	3.11	-0.05	0.00	-0.04	722	0.19	-0.26
L7-16	REL	JAX00222885	4	7.2	4.2	0.0	18.3	2.89	2.93	2.97	-0.04	0.00	0.03	724	0.19	-0.20
L7-16	REL	UNC13659934	7	44.9	4.4	36.6	55.5	2.88	2.93	2.96	-0.04	0.01	-0.26	724	0.19	-0.19
L7-16	REL	UNC16751553	9	32.8	6.2	16.2	40.5	2.86	2.93	2.98	-0.06	0.01	-0.24	724	0.19	-0.29
L5-7	REL	UNC3528819	2	45.5	5.8	42.9	57.9	1.35	1.34	1.31	0.02	0.01	0.52	704	0.10	0.22
L5-7	REL	JAX00546540	4	6.2	7.8	0.1	18.3	1.31	1.33	1.36	-0.03	-0.01	0.34	704	0.10	-0.27
L5-7	REL	UNC16699990	9	31.6	14.3	23.9	37.0	1.29	1.33	1.37	-0.04	0.00	0.03	704	0.10	-0.41
L3-12	REL	JAX00101874	2	67.2	5.8	57.4	70.9	1.47	1.44	1.41	0.03	0.00	-0.02	726	0.11	0.25
L3-12	REL	UNC20343150	11	58.6	6.8	56.8	62.8	1.41	1.43	1.47	-0.03	0.00	0.06	726	0.11	-0.28
L3-12	REL	UNC21390243	12	25.4	4.3	15.1	32.6	1.43	1.45	1.41	0.01	0.02	2.26	726	0.11	0.09
L3-12	REL	UNC24611047	14	41.9	4.6	33.9	58.5	1.45	1.44	1.42	0.02	0.00	-0.09	726	0.11	0.16
L1-13	REL	UNC020446908	2	45.5	6.8	43.0	58.0	2.02	2.00	1.97	0.03	0.01	0.23	726	0.11	0.25
L1-13	REL	UNC16502816	9	24.7	4.9	21.4	38.1	1.97	1.99	2.02	-0.03	0.00	0.07	726	0.11	-0.25
L1-13	REL	JAX00314237	11	36.1	4.7	17.9	50.1	1.97	2.00	2.01	-0.02	0.01	-0.57	726	0.11	-0.18
L6-7	REL	UNC3811386	2	53.4	6.9	47.3	61.6	0.77	0.77	0.74	0.02	0.01	0.73	722	0.07	0.25
L6-7	REL	UNC16757890	9	33.2	5.8	21.8	55.2	0.74	0.76	0.78	-0.02	0.00	0.00	722	0.07	-0.29
L6-7	REL	UNC17559025	10	7.0	6.4	3.5	11.2	0.77	0.76	0.74	0.02	0.01	0.40	722	0.07	0.22
L11-12	REL	UNC17199210	9	53.2	5.0	28.1	59.3	1.36	1.41	1.44	-0.04	0.01	-0.22	728	0.13	-0.27
L11-13	REL	UNC16757890	9	33.2	4.2	5.7	58.6	2.04	2.07	2.11	-0.04	0.00	0.13	728	0.14	-0.26
L11-13	REL	JAX00370019	13	45.7	4.5	35.4	50.9	2.10	2.08	2.04	0.03	0.01	0.43	728	0.14	0.20
L11-13	REL	UNC27329052	16	41.2	5.1	31.2	45.0	2.11	2.07	2.04	0.04	0.00	-0.07	728	0.14	0.27
L1-15	REL	UNC12154012	6	54.7	7.2	47.1	63.2	0.74	0.73	0.71	0.02	0.01	0.41	728	0.06	0.27
L11-16	REL	UNC13448875	7	41.2	6.1	32.5	48.0	2.40	2.46	2.48	-0.04	0.01	-0.37	728	0.15	-0.27
L11-16	REL	UNC17199210	9	53.2	4.7	23.3	58.6	2.40	2.46	2.48	-0.04	0.02	-0.43	728	0.15	-0.26

L11-16	REL	UNC21363333	12	24.6	4.4	11.1	36.0	2.46	2.46	2.42	0.02	0.03	1.26	728	0.15	0.14
L3-15	REL	UNC3985525	2	57.6	4.2	53.1	67.9	1.18	1.17	1.15	0.02	0.00	0.22	728	0.07	0.22
L3-15	REL	JAX00563463	4	47.4	8.5	16.4	50.5	1.14	1.17	1.18	-0.02	0.01	-0.42	728	0.07	-0.29
L3-15	REL	UNC16751553	9	32.8	5.7	9.3	39.4	1.15	1.17	1.19	-0.02	0.00	-0.03	728	0.07	-0.29
L3-15	REL	UNC21392101	12	25.5	5.9	16.4	29.8	1.17	1.18	1.15	0.01	0.02	2.15	728	0.07	0.11
L4-7	REL	UNC3985525	2	57.6	11.0	44.4	58.4	1.32	1.29	1.25	0.04	0.01	0.21	722	0.10	0.37
L4-7	REL	UNC6882525	4	6.4	8.1	4.1	20.2	1.26	1.28	1.31	-0.03	0.00	0.13	722	0.10	-0.29
L4-7	REL	JAX00173035	9	30.9	17.7	26.0	37.7	1.24	1.28	1.33	-0.05	0.00	0.03	722	0.10	-0.48
L2-11	REL	UNC13641136	7	44.5	4.7	28.6	47.2	2.85	2.88	2.92	-0.04	0.00	0.03	728	0.16	-0.22
L2-11	REL	UNC17199210	9	53.2	4.2	10.6	57.7	2.84	2.89	2.91	-0.04	0.02	-0.50	728	0.16	-0.23
L11-14	REL	UNC13659934	7	44.9	6.0	32.5	53.5	2.88	2.93	2.96	-0.04	0.01	-0.17	725	0.17	-0.25
L11-14	REL	UNC23377569	13	47.9	4.1	34.1	52.8	2.95	2.92	2.89	0.03	0.00	0.03	725	0.17	0.18
L11-14	REL	JAX00427019	16	40.4	4.7	29.1	47.2	2.98	2.91	2.90	0.04	-0.03	-0.68	725	0.17	0.24
L10-12	REL	UNC8349017	4	64.6	8.0	58.2	69.8	1.67	1.72	1.74	-0.03	0.01	-0.30	727	0.12	-0.27
L10-12	REL	UNC15064184	8	28.8	5.9	19.8	39.4	1.67	1.72	1.74	-0.03	0.01	-0.33	727	0.12	-0.28
L10-12	REL	UNC16143584	9	10.1	6.2	5.1	33.6	1.67	1.72	1.73	-0.03	0.02	-0.66	727	0.12	-0.23
L10-12	REL	UNC18515876	10	39.7	5.6	23.1	45.4	1.68	1.72	1.74	-0.03	0.01	-0.22	727	0.12	-0.26
L10-12	REL	UNC20336483	11	58.4	4.4	54.3	61.5	1.72	1.73	1.68	0.02	0.03	1.40	727	0.12	0.16
L6-10	REL	UNC16757890	9	33.2	4.4	10.3	47.9	1.68	1.70	1.73	-0.03	0.00	0.08	726	0.10	-0.27
L6-10	REL	UNC27928059	17	15.6	4.2	6.9	20.0	1.68	1.70	1.71	-0.02	0.01	-0.43	726	0.10	-0.21
L3-11	REL	UNC17199210	9	53.2	4.5	25.8	58.6	2.74	2.80	2.82	-0.04	0.02	-0.45	729	0.15	-0.25
L1-3	REL	UNC301459	1	11.9	5.0	8.9	21.0	1.25	1.28	1.28	-0.01	0.01	-0.90	728	0.08	-0.19
L1-3	REL	UNC3985525	2	57.6	6.3	53.5	59.3	1.29	1.28	1.25	0.02	0.00	0.18	728	0.08	0.27
L1-3	REL	JAX00563463	4	47.4	4.5	16.4	52.9	1.25	1.27	1.29	-0.02	0.00	-0.05	728	0.08	-0.22
L1-3	REL	UNC16642471	9	29.5	9.6	21.8	33.8	1.25	1.27	1.30	-0.03	0.00	0.11	728	0.08	-0.35
L1-3	REL	JAX00071271	16	34.3	4.1	26.1	36.9	1.29	1.27	1.26	0.02	0.00	-0.25	728	0.08	0.22
L7-12	REL	UNC8349017	4	64.6	5.4	47.9	76.2	2.14	2.18	2.20	-0.03	0.00	-0.14	731	0.16	-0.19
L7-12	REL	UNC15064184	8	28.8	4.6	4.9	50.1	2.13	2.18	2.20	-0.04	0.02	-0.53	731	0.16	-0.23
L7-12	REL	JAX00699093	9	31.2	9.5	20.2	33.8	2.11	2.17	2.23	-0.06	0.00	-0.03	731	0.16	-0.36
L7-9	REL	JAX00173035	9	30.9	6.0	21.8	55.2	0.80	0.82	0.84	-0.02	0.00	0.21	729	0.07	-0.30
L1-11	REL	JAX00496435	2	45.5	4.2	43.2	58.4	3.97	3.97	3.91	0.03	0.03	0.97	723	0.21	0.15
L1-11	REL	UNC16646037	9	29.9	6.3	21.8	39.4	3.89	3.95	4.01	-0.06	0.00	0.07	723	0.21	-0.30
L1-7	BW	UNC16706423	9	31.8	5.8	21.8	37.0	11.93	12.03	12.07	-0.07	0.03	-0.41	744	0.42	-0.17

L1-7	BW	UNC18750788	10	47.8	5.5	32.6	61.7	12.18	12.00	11.89	0.14	-0.04	-0.26	744	0.42	0.34
L1-7	BW	UNC21390243	12	25.4	5.5	21.3	44.8	11.99	12.07	11.92	0.03	0.12	3.42	744	0.42	0.08
L3-7	BW	UNC18750788	10	47.8	4.6	31.7	55.7	8.60	8.47	8.42	0.09	-0.04	-0.39	747	0.31	0.30
L3-7	BW	UNC19667803	11	28.9	4.3	16.0	37.0	8.57	8.49	8.39	0.09	0.01	0.11	747	0.31	0.29
L3-7	BW	UNC21442090	12	28.1	5.2	22.6	29.8	8.46	8.53	8.42	0.02	0.09	4.29	747	0.31	0.07
L7-16	BW	UNC16699990	9	31.6	4.8	21.8	48.7	8.02	8.13	8.13	-0.06	0.06	-1.04	749	0.37	-0.15
L7-16	BW	UNC21390243	12	25.4	5.5	22.6	29.1	8.09	8.16	8.01	0.04	0.11	2.73	749	0.37	0.11
L7-16	BW	JAX00356294	13	11.9	4.5	8.5	19.2	8.14	8.13	8.00	0.07	0.06	0.87	749	0.37	0.18
L5-7	BW	UNC3517270	2	44.8	4.9	37.8	50.7	3.74	3.70	3.65	0.05	0.00	0.01	724	0.20	0.22
L5-7	BW	JAX00116686	4	6.2	4.9	0.1	18.3	3.66	3.68	3.74	-0.04	-0.02	0.44	724	0.20	-0.19
L5-7	BW	UNC16706423	9	31.8	12.7	27.2	35.3	3.62	3.70	3.75	-0.07	0.01	-0.16	724	0.20	-0.32
L5-7	BW	UNC19595363	11	26.2	4.7	4.4	39.9	3.75	3.69	3.63	0.06	0.00	0.07	724	0.20	0.29
L3-12	BW	UNC8335888	4	62.0	6.2	55.2	76.5	4.03	3.98	3.92	0.06	0.01	0.20	751	0.20	0.27
L3-12	BW	UNC20337194	11	58.4	4.2	53.4	61.9	3.96	3.96	4.03	-0.04	-0.03	0.91	751	0.20	-0.18
L3-12	BW	UNC21390243	12	25.4	5.2	20.3	29.8	4.00	4.00	3.91	0.04	0.04	1.02	751	0.20	0.21
L3-12	BW	UNC29659434	18	41.8	4.1	23.8	52.1	3.94	3.98	4.01	-0.04	0.01	-0.17	751	0.20	-0.19
L1-13	BW	UNC3371968	2	43.6	8.1	40.5	49.2	5.62	5.53	5.49	0.06	-0.03	-0.41	751	0.22	0.30
L1-13	BW	UNC9530593	5	35.2	4.2	28.2	61.2	5.47	5.54	5.56	-0.04	0.03	-0.59	751	0.22	-0.20
L1-13	BW	UNC21245532	12	22.0	4.2	9.6	29.8	5.56	5.54	5.48	0.04	0.02	0.59	751	0.22	0.18
L1-13	BW	UNC29549056	18	36.6	4.0	29.0	43.3	5.52	5.52	5.58	-0.03	-0.03	0.99	751	0.22	-0.14
L6-7	BW	UNC3811386	2	53.4	6.0	47.3	62.0	2.12	2.11	2.06	0.03	0.03	0.90	747	0.16	0.18
L6-7	BW	UNC17087279	9	47.0	4.9	27.6	55.2	2.06	2.10	2.12	-0.03	0.01	-0.37	747	0.16	-0.20
L6-7	BW	UNC17559025	10	7.0	9.2	3.9	9.1	2.14	2.11	2.04	0.05	0.02	0.37	747	0.16	0.31
L6-7	BW	UNC20482098	11	71.4	4.9	61.0	77.0	2.12	2.11	2.04	0.04	0.03	0.72	747	0.16	0.25
L6-7	BW	UNC26299295	16	2.5	4.4	0.0	8.1	2.13	2.11	2.06	0.04	0.01	0.40	747	0.16	0.23
L8-4	BW	UNC3474714	2	44.4	5.6	39.3	80.5	2.57	2.51	2.43	0.07	0.01	0.14	744	0.26	0.27
L8-4	BW	UNC6852444	4	6.0	4.6	1.6	46.6	2.44	2.49	2.56	-0.06	-0.01	0.16	744	0.26	-0.23
L8-4	BW	UNC16673344	9	31.0	10.4	25.5	37.7	2.41	2.49	2.57	-0.08	0.00	-0.01	744	0.26	-0.31
L8-4	BW	UNC26231186	15	51.8	4.0	39.6	53.3	2.55	2.50	2.43	0.06	0.01	0.15	744	0.26	0.23
L8-16	BW	UNC21390243	12	25.4	4.0	22.6	45.4	8.08	8.15	8.02	0.03	0.10	3.05	756	0.37	0.09
L8-16	BW	UNC22472068	13	10.3	5.7	8.5	18.0	8.14	8.13	7.98	0.08	0.07	0.84	756	0.37	0.21
L1-3	BW	UNC3985525	2	57.6	4.6	40.8	61.6	3.57	3.52	3.51	0.03	-0.02	-0.69	753	0.16	0.17
L1-3	BW	UNC10042402	5	52.1	4.3	47.8	60.1	3.49	3.54	3.52	-0.02	0.04	-2.32	753	0.16	-0.10

L1-3	BW	JAX00699093	9	31.2	7.4	21.8	35.3	3.49	3.52	3.56	-0.03	0.00	0.06	753	0.16	-0.20
L1-3	BW	UNC26906114	16	27.3	4.2	21.2	36.5	3.55	3.53	3.49	0.03	0.01	0.43	753	0.16	0.19
L1-3	BW	UNC27695833	17	8.4	5.0	3.3	20.0	3.57	3.52	3.49	0.04	-0.01	-0.19	753	0.16	0.23
L1-11	BW	UNC16757890	9	33.2	5.1	23.3	53.3	10.90	10.95	11.00	-0.05	0.00	-0.03	748	0.45	-0.11
L1-11	BW	UNC21435638	12	28.1	4.7	16.4	29.8	10.99	10.98	10.84	0.08	0.06	0.81	748	0.45	0.17
L1-15	BW	JAX00254507	1	33.2	4.6	25.1	54.2	2.04	2.03	1.98	0.03	0.02	0.73	753	0.13	0.23
L1-15	BW	UNC12159294	6	54.7	10.5	47.1	58.1	2.06	2.03	1.97	0.05	0.01	0.17	753	0.13	0.34
L3-11	BW	UNC21428926	12	27.9	4.8	17.3	29.8	7.77	7.74	7.64	0.07	0.04	0.61	748	0.35	0.19
L3-15	BW	UNC510223	1	19.7	6.5	17.8	22.0	3.21	3.23	3.27	-0.03	-0.01	0.20	753	0.15	-0.21
L3-15	BW	JAX00563463	4	47.4	9.3	39.1	52.7	3.18	3.25	3.27	-0.04	0.02	-0.51	753	0.15	-0.27
L3-15	BW	UNC9601838	5	37.1	4.5	31.2	60.1	3.19	3.24	3.25	-0.03	0.02	-0.77	753	0.15	-0.19
L3-15	BW	UNC18746398	10	47.8	5.1	26.9	51.7	3.29	3.22	3.20	0.05	-0.02	-0.45	753	0.15	0.31
L3-15	BW	UNC27695833	17	8.4	4.3	0.0	38.4	3.26	3.24	3.20	0.03	0.01	0.28	753	0.15	0.21
L4-7	BW	UNC3776734	2	51.9	10.4	43.9	57.9	3.64	3.57	3.49	0.08	0.00	0.04	745	0.22	0.34
L4-7	BW	UNC6882525	4	6.4	5.3	1.6	48.5	3.51	3.55	3.60	-0.05	0.00	0.06	745	0.22	-0.21
L4-7	BW	UNC16757890	9	33.2	16.2	27.6	37.7	3.47	3.56	3.64	-0.09	0.01	-0.06	745	0.22	-0.39
L6-10	BW	UNC25241266	15	5.9	5.9	0.0	8.7	4.77	4.72	4.64	0.07	0.01	0.20	751	0.25	0.27
L6-10	BW	UNC27928059	17	15.6	4.4	5.8	20.7	4.67	4.71	4.76	-0.05	-0.01	0.20	751	0.25	-0.18
L7-9	BW	UNC17086614	9	47.0	4.9	29.5	55.2	2.24	2.27	2.30	-0.03	0.00	-0.09	754	0.16	-0.20
L7-9	BW	UNC18750788	10	47.8	4.0	0.0	56.3	2.33	2.26	2.25	0.04	-0.03	-0.79	754	0.16	0.24
L7-9	BW	UNC20799452	12	9.3	4.3	5.8	22.6	2.31	2.27	2.24	0.04	-0.01	-0.29	754	0.16	0.22
L7-9	BW	UNC24994731	15	0.5	4.5	0.0	12.3	2.29	2.29	2.22	0.04	0.03	0.97	754	0.16	0.22
L7-10	BW	UNC13945176	7	62.2	4.5	43.8	73.4	3.44	3.38	3.33	0.06	0.00	-0.09	752	0.22	0.25
L7-10	BW	UNC25199618	15	4.2	12.4	0.0	7.4	3.47	3.39	3.30	0.08	0.00	0.06	752	0.22	0.39
L7-10	BW	JAX00076212	17	16.2	5.7	6.9	20.7	3.34	3.38	3.44	-0.05	-0.01	0.17	752	0.22	-0.24
L7-12	BW	UNC8349017	4	64.6	7.4	58.7	67.6	5.91	6.03	6.10	-0.09	0.02	-0.24	756	0.33	-0.28
L7-12	BW	JAX00699093	9	31.2	7.7	20.2	35.1	5.92	6.03	6.09	-0.09	0.02	-0.28	756	0.33	-0.26
L7-13	BW	UNC5382306	3	21.5	4.8	14.6	36.6	8.15	8.09	7.99	0.08	0.02	0.23	757	0.34	0.23
L7-13	BW	UNC16684648	9	31.4	4.4	8.6	37.7	8.00	8.10	8.12	-0.06	0.04	-0.63	757	0.34	-0.17
L7-13	BW	UNC19780488	11	33.6	4.1	16.5	36.2	8.17	8.08	7.99	0.09	0.00	-0.02	757	0.34	0.27
L7-13	BW	UNC21390243	12	25.4	4.9	22.6	47.4	8.04	8.13	8.01	0.01	0.11	8.95	757	0.34	0.04
L9-12	BW	UNC8349017	4	63.7	9.7	58.7	66.1	3.74	3.85	3.91	-0.09	0.03	-0.30	753	0.27	-0.33
L9-12	BW	JAX00695211	9	22.4	5.6	3.5	33.2	3.75	3.86	3.87	-0.06	0.05	-0.88	753	0.27	-0.21

L9-12	BW	UNC19186816	11	7.2	4.1	4.0	61.5	3.83	3.87	3.78	0.03	0.06	2.40	753	0.27	0.09
L10-12	BW	UNC8349017	4	63.7	9.3	58.9	66.1	4.64	4.77	4.83	-0.09	0.04	-0.37	752	0.31	-0.30
L10-12	BW	UNC16145215	9	10.1	4.8	4.4	47.0	4.68	4.77	4.77	-0.05	0.05	-1.17	752	0.31	-0.14
L10-12	BW	UNC20337194	11	58.4	6.7	54.5	61.5	4.83	4.76	4.63	0.10	0.03	0.30	752	0.31	0.32
L11-12	BW	UNC17199210	9	53.2	4.4	29.5	60.5	3.83	3.89	3.95	-0.06	-0.01	0.09	753	0.38	-0.16
L11-12	BW	UNC20343150	11	58.6	4.5	54.3	63.1	3.97	3.91	3.77	0.10	0.04	0.37	753	0.38	0.26
L11-13	BW	UNC23348239	13	46.7	4.9	41.5	49.7	5.80	5.77	5.67	0.06	0.04	0.55	753	0.35	0.18
L11-13	BW	UNC27329404	16	41.2	5.0	25.2	45.0	5.80	5.77	5.66	0.07	0.04	0.53	753	0.35	0.20
L11-14	BW	UNC23377569	13	47.9	4.4	34.8	52.8	8.18	8.11	8.04	0.07	0.00	0.03	750	0.39	0.18
L11-14	BW	UNC27123531	16	34.1	4.9	25.2	47.2	8.19	8.10	8.04	0.08	-0.02	-0.20	750	0.39	0.19
L11-15	BW	UNC21390243	12	25.4	6.1	17.3	29.8	9.70	9.66	9.51	0.09	0.06	0.62	748	0.44	0.21
L11-16	BW	UNC13456165	7	41.8	4.2	32.3	53.7	6.73	6.79	6.82	-0.05	0.01	-0.32	748	0.39	-0.12
L11-16	BW	UNC21363333	12	24.6	4.7	16.4	29.8	6.84	6.81	6.69	0.08	0.04	0.56	748	0.39	0.19
PC1		UNC15185	1	0.0	6.6	0.0	20.2	0.00	0.00	0.00	0.00	0.00	-0.40	714	0.01	-0.29
PC1		UNC13176880	7	34.8	4.7	5.1	40.1	0.00	0.00	0.00	0.00	0.00	0.39	714	0.01	0.22
PC1		UNC17154932	9	50.6	8.4	33.8	56.1	0.00	0.00	0.00	0.00	0.00	0.32	714	0.01	0.26
PC1		UNC21637767	12	35.0	5.5	30.6	45.8	0.00	0.00	0.00	0.00	0.00	-0.23	714	0.01	-0.28
PC2		JAX00101732	2	66.4	4.9	44.4	85.5	0.00	0.00	0.00	0.00	0.00	-0.14	714	0.01	0.26
PC2		UNC6960118	4	7.2	5.5	1.6	14.5	0.00	0.00	0.00	0.00	0.00	0.00	714	0.01	-0.27
PC2		JAX00141068	6	19.7	4.6	3.2	39.8	0.00	0.00	0.00	0.00	0.00	0.45	714	0.01	-0.22
PC2		JAX00321431	11	58.8	5.5	54.3	62.8	0.00	0.00	0.00	0.00	0.00	0.41	714	0.01	-0.26
PC3		UNC8325771	4	61.4	4.0	39.9	70.1	0.00	0.00	0.00	0.00	0.00	0.00	714	0.01	0.22
PC3		UNC16467939	9	23.9	6.3	4.4	33.2	0.00	0.00	0.00	0.00	0.00	-0.49	714	0.01	0.27
PC3		UNC23233661	13	40.2	4.4	30.2	47.9	0.00	0.00	0.00	0.00	0.00	0.27	714	0.01	-0.23
PC4		UNC8419972	4	67.4	4.6	55.8	76.5	0.00	0.00	0.00	0.00	0.00	0.28	714	0.01	-0.24
PC4		UNC13568970	7	42.9	7.9	40.0	52.0	0.00	0.00	0.00	0.00	0.00	-0.23	714	0.01	0.32
PC4		UNC16716563	9	32.2	6.9	23.3	39.1	0.00	0.00	0.00	0.00	0.00	0.55	714	0.01	-0.27
PC4		JAX00369870	13	45.2	6.3	32.6	47.0	0.00	0.00	0.00	0.00	0.00	0.67	714	0.01	-0.25
PC4		backupUNC150422514	15	0.4	6.1	0.0	16.7	0.00	0.00	0.00	0.00	0.00	-0.32	714	0.01	0.27
PC5		UNC7764002	4	36.9	4.4	22.8	46.8	0.00	0.00	0.00	0.00	0.00	-0.55	714	0.01	-0.20
PC5		UNC17467989	10	3.3	6.1	0.0	45.8	0.00	0.00	0.00	0.00	0.00	0.11	714	0.01	-0.26
PC6		UNC13201239	7	35.5	4.2	32.5	47.2	0.00	0.00	0.00	0.00	0.00	-1.06	714	0.01	0.19

PC6	UNC23194768	13	38.2	6.2	35.9	47.9	0.00	0.00	0.00	0.00	0.00	-0.74	714	0.01	-0.25
PC6	UNC25457590	15	12.1	4.3	2.0	17.6	0.00	0.00	0.00	0.00	0.00	-0.52	714	0.01	0.22
PC8	JAX00668294	6	21.0	4.7	9.7	35.9	0.00	0.00	0.00	0.00	0.00	2.62	714	0.01	-0.03
PC8	JAX00290261	10	22.6	6.8	18.1	52.5	0.00	0.00	0.00	0.00	0.00	0.17	714	0.01	0.29
PC8	UNC21424756	12	27.6	5.0	19.4	33.4	0.00	0.00	0.00	0.00	0.00	0.01	714	0.01	-0.26
PC8	UNC27427399	16	47.8	5.6	31.2	53.1	0.00	0.00	0.00	0.00	0.00	-0.74	714	0.01	0.24
PC8	UNC27501759	17	0.1	4.5	0.0	19.2	0.00	0.00	0.00	0.00	0.00	0.63	714	0.01	-0.22
PC9	UNC070679160	7	40.9	5.9	36.7	59.8	0.00	0.00	0.00	0.00	0.00	-0.38	714	0.01	-0.27
PC9	UNC24040936	14	19.3	9.4	6.8	26.3	0.00	0.00	0.00	0.00	0.00	0.08	714	0.01	-0.33
PC9	UNC28031943	17	20.7	4.9	6.0	26.0	0.00	0.00	0.00	0.00	0.00	0.08	714	0.01	-0.25
PC10	UNC1401095	1	46.1	4.8	25.1	50.6	0.00	0.00	0.00	0.00	0.00	0.47	714	0.01	-0.21
PC10	UNC12162881	6	55.2	6.0	40.6	58.1	0.00	0.00	0.00	0.00	0.00	-0.11	714	0.01	-0.26
PC10	backupUNC101 411698	10	50.7	4.6	16.4	55.1	0.00	0.00	0.00	0.00	0.00	-0.87	714	0.01	0.22
PC10	UNC19751074	11	31.9	4.2	26.3	40.2	0.00	0.00	0.00	0.00	0.00	-0.95	714	0.01	-0.18
PC10	UNC26244567	15	53.3	4.1	40.4	53.3	0.00	0.00	0.00	0.00	0.00	0.01	714	0.01	-0.21
PC10	UNC27793465	17	12.0	6.4	3.7	24.8	0.00	0.00	0.00	0.00	0.00	-0.45	714	0.01	-0.28
PC10	UNC29345742	18	25.7	9.6	18.6	37.8	0.00	0.00	0.00	0.00	0.00	0.17	714	0.01	-0.33
PC10	UNC30477146	19	36.5	4.2	20.3	45.3	0.00	0.00	0.00	0.00	0.00	1.18	714	0.01	-0.15
PC11	JAX00216253	2	20.8	4.6	14.0	88.6	0.00	0.00	0.00	0.00	0.00	-0.11	714	0.01	0.25
PC11	UNC20388460	11	62.1	4.3	4.1	73.0	0.00	0.00	0.00	0.00	0.00	-0.29	714	0.01	0.23
PC12	UNC3954508	2	56.9	8.1	52.7	59.9	0.00	0.00	0.00	0.00	0.00	0.01	714	0.01	-0.35
PC12	UNC6225534	3	48.8	6.5	44.0	55.6	0.00	0.00	0.00	0.00	0.00	0.44	714	0.01	-0.25
PC12	UNC28501792	17	43.4	4.6	40.1	52.5	0.00	0.00	0.00	0.00	0.00	2.86	714	0.01	-0.09
PC13	UNC3380410	2	43.9	5.5	40.9	56.0	0.00	0.00	0.00	0.00	0.00	-0.29	714	0.01	0.31
PC13	UNC7613365	4	32.0	5.7	29.1	60.9	0.00	0.00	0.00	0.00	0.00	-0.26	714	0.01	0.24
PC13	UNC9779259	5	42.4	4.2	40.8	66.6	0.00	0.00	0.00	0.00	0.00	1.28	714	0.01	-0.17
PC13	backupJAX0028 6389	10	12.5	9.3	9.3	55.7	0.00	0.00	0.00	0.00	0.00	0.10	714	0.01	-0.35
PC13	UNC19924383	11	39.5	6.2	33.6	44.3	0.00	0.00	0.00	0.00	0.00	-0.24	714	0.01	-0.27
PC14	UNC1408936	1	46.1	5.6	23.5	61.4	0.00	0.00	0.00	0.00	0.00	-0.22	714	0.00	0.26
PC14	UNC6226186	3	48.8	10.3	29.8	61.5	0.00	0.00	0.00	0.00	0.00	0.22	714	0.00	-0.36
PC14	UNC8136843	4	51.0	6.4	45.2	58.4	0.00	0.00	0.00	0.00	0.00	-0.19	714	0.00	0.27
PC15	JAX00501685	2	54.1	9.4	52.0	62.2	0.00	0.00	0.00	0.00	0.00	-0.23	714	0.00	-0.38

PC15	UNC12422348	7	1.4	4.8	0.0	18.0	0.00	0.00	0.00	0.00	0.00	0.16	714	0.00	-0.25
PC15	UNC15745127	8	62.3	4.5	1.3	62.8	0.00	0.00	0.00	0.00	0.00	0.59	714	0.00	0.21
PC16	JAX00367408	13	35.9	6.5	20.7	54.7	0.00	0.00	0.00	0.00	0.00	-0.42	714	0.00	-0.29
PC16	UNC25286720	15	7.1	5.1	0.0	28.9	0.00	0.00	0.00	0.00	0.00	-0.93	714	0.00	-0.21
PC16	JAX00071378	16	35.6	6.5	13.4	40.0	0.00	0.00	0.00	0.00	0.00	-0.15	714	0.00	-0.28
PC17	UNC3115467	2	29.4	5.3	19.2	35.3	0.00	0.00	0.00	0.00	0.00	-0.07	714	0.00	0.27
PC17	backupUNC050328531	5	12.2	5.5	4.3	26.8	0.00	0.00	0.00	0.00	0.00	-0.32	714	0.00	0.28
PC17	UNC14142175	8	1.3	4.3	0.0	17.0	0.00	0.00	0.00	0.00	0.00	-0.20	714	0.00	-0.24
PC17	UNC17586853	10	8.7	4.9	0.0	41.3	0.00	0.00	0.00	0.00	0.00	0.11	714	0.00	-0.23
PC17	UNC20799452	12	9.3	4.2	0.0	16.3	0.00	0.00	0.00	0.00	0.00	-0.29	714	0.00	-0.25
PC17	JAX00045238	13	20.5	6.5	13.9	29.2	0.00	0.00	0.00	0.00	0.00	0.17	714	0.00	0.28
PC17	UNC26156200	15	44.6	4.6	38.7	53.3	0.00	0.00	0.00	0.00	0.00	-0.53	714	0.00	-0.24
PC17	UNC28181651	17	26.3	5.7	4.4	33.3	0.00	0.00	0.00	0.00	0.00	-0.39	714	0.00	-0.26
PC18	UNC24065075	14	21.4	5.9	16.3	31.9	0.00	0.00	0.00	0.00	0.00	-0.12	714	0.00	0.27
PC18	JAX00070066	16	27.6	6.8	18.8	33.7	0.00	0.00	0.00	0.00	0.00	0.17	714	0.00	0.28
PC19	UNC10260053	5	63.5	5.2	47.1	66.5	0.00	0.00	0.00	0.00	0.00	-0.73	714	0.00	-0.23
PC19	UNC23453339	13	52.8	4.1	35.4	55.2	0.00	0.00	0.00	0.00	0.00	1.78	714	0.00	0.14
PC19	UNC27127119	16	34.3	5.2	5.7	48.9	0.00	0.00	0.00	0.00	0.00	0.19	714	0.00	-0.26
PC20	UNC6092111	3	43.1	5.0	21.0	53.5	0.00	0.00	0.00	0.00	0.00	0.33	714	0.00	-0.23
PC22	UNC268995	1	10.2	4.6	0.0	40.7	0.00	0.00	0.00	0.00	0.00	-0.95	714	0.00	0.20
PC22	UNC16670332	9	31.0	4.2	26.0	41.3	0.00	0.00	0.00	0.00	0.00	2.35	714	0.00	0.12
PC22	UNC25636612	15	17.6	5.5	0.4	29.8	0.00	0.00	0.00	0.00	0.00	0.41	714	0.00	-0.25
PC23	UNC19991777	11	41.7	4.2	38.6	63.5	0.00	0.00	0.00	0.00	0.00	1.40	714	0.00	-0.16
PC23	UNC22908684	13	28.2	5.5	22.6	41.5	0.00	0.00	0.00	0.00	0.00	0.05	714	0.00	0.26
PC24	UNC5906887	3	36.6	4.4	24.6	36.6	0.00	0.00	0.00	0.00	0.00	-1.68	714	0.00	-0.14
PC24	UNC8396212	4	66.7	12.7	62.9	69.8	0.00	0.00	0.00	0.00	0.00	0.17	714	0.00	0.39
PC25	UNC28885691	18	8.4	6.0	5.7	11.8	0.00	0.00	0.00	0.00	0.00	0.39	714	0.00	0.27
PC26	JAX00326709	12	4.0	5.7	0.0	38.1	0.00	0.00	0.00	0.00	0.00	-0.11	714	0.00	0.27
PC27	UNC6639515	4	0.0	4.9	0.0	2.1	0.00	0.00	0.00	0.00	0.00	0.06	714	0.00	-0.25
PC28	JAX00675505	8	33.3	5.7	0.0	41.3	0.00	0.00	0.00	0.00	0.00	-0.32	714	0.00	-0.27
Centroid Size	JAX00300565	10	56.9	9.9	46.3	61.7	1535	1516	1502	16.2	-2.72	-0.17	748	43.0	0.38
Centroid Size	UNC19667803	11	29.0	7.9	17.5	33.6	1531	1516	1503	14.0	-0.87	-0.06	748	43.0	0.33